FUNCTIONAL MONOMERS GRAFTED POLYOLEFINS AND THEIR APPLICATIONS IN THE COMPATIBILIZATION OF POLYMER BLENDS

By

LI YAO

A DISSERTATION PRESENTED TO THE GRADUATE SCHOOL
OF THE UNIVERSITY OF FLORIDA IN PARTIAL FULFILLMENT
OF THE REQUIREMENTS FOR THE DEGREE OF
DOCTOR OF PHILOSOPHY

UNIVERSITY OF FLORIDA

1996

ACKNOWLEDGEMENTS

I would like to express my gratitude to my advisor and supervisory committee chairman Dr Charles L Beatty, for his guidance, encouragement, generous support, and assistance during this research.

My gratitude extends to Dr Chris Batich, Dr James Adair, Dr Arthur Fricke, and Dr Stanley Bates for their participation in the doctoral committee

My sincere thanks must go to my friends and colleagues, Mr David Bennett, Mr Shugang Yang, Mr Thomas Joseph, Ms Jeanne Hampton and Mr James Rhods for their help in some technical issues and in the correction of my dissertation In addition, I would like to thank all other students for their friendship and cooperation.

I would also like to thank my parents, my brother, and my parents-in-law for their support and encouragement

I am grateful to my wife, Qing Pan, for her great love, support, patience, which have brought me to the completion of this work.

TABLE OF CONTENTS

Abstract of Dissertation Presented to the Graduate School
of the University of Florida in Partial Fulfillment of the
Requirements for the Degree of Doctor of Philosophy

FUNCTIONAL MONOMERS GRAFTED POLYOLEFINS AND THEIR APPLICATIONS IN THE COMPATIBILIZATION OF POLYMER BLENDS

By

LI YAO

December 1996

Chairperson: Dr. Charles L. Beatty
Major Department: Materials Science and Engineering

Plastics today form a sizable fraction of solid wastes and recycling these waste plastics would be an attractive solution to one of the ever-increasing environmental problems. However, most of the polymers are thermodynamically immiscible with each other. Processing of the mixtures of polymer wastes is not likely to yield products with excellent mechanical properties. Since the separation of waste plastics is not yet economically feasible, compatibilization is the potentially practical route to explore in the high value applications of recycled plastics. Besides the traditional compatibilization by block or graft copolymers, recently an *in situ* compatibilization technique has been developed in which the compatibilizers are formed during the compounding of polymer blends with functional polymers as precursors.

This research was devoted to the synthesis, characterization and applications of functional monomers grafted polyolefins. The functional monomers, including maleic

anhydride (MA), glycidyl methacrylate (GMA), and 2-isopropenyl-2-oxazoline (IPOZ), were utilized and compared in this investigation. Three major grafting techniques: solid-state, melt, and solution grafting, were studied. Meanwhile, the reactivities of the grafted polyolefins with other functional groups were compared. The thermal degradation of polypropylene caused by the peroxide during grafting was also rheologically studied. A novel crosslinking method by multifunctional monomer was employed to compensate for the chain scission by the peroxide and to restore the mechanical and rheological properties of the grafted polypropylene.

Due to their high reactivities, GMA melt grafted polyolefins were used in the reactive compatibilization of HDPE/PET, polyolefin/PVC, and PP/ABS blends. The differences between reactive and nonreactive blends in terms of processability, morphologies, mechanical and thermal properties have been investigated. The compatibilization mechanisms were also analyzed by FTIR detecting, torque measurements, and lap shear adhesion measurements. It was found that GMA grafted polyolefins can effectively form interfacial bonds with other phases by interfacial reaction during melt processing. The high compatibilizing efficiency of the GMA grafted polyolefins was manifested by the dramatically improved mechanical and morphological properties of the compatibilized blends with the addition of a small amount of the GMA grafted polyolefins.

CHAPTER 1
GENERAL INTRODUCTION

1.1 Background

There is intense commercial interest in multiphase polymer blends or alloys, because of the potential opportunities for combining the attractive features of several materials into one, or for improving deficient characteristics of particular materials [1-5]. In the polymer recycling area, it is usually commercially infeasible to separate all kinds of recycled polymers, many of them are polymer blends. As a result, the studies of polymer blends are critical to both polymer modification and polymer recycling.

Few polymers form truly miscible blends. Examples include the binary blends of poly(phenylene ether) (PPE)/polystyrene (PS), polyvinylchloride (PVC)/nitrile butadiene rubber (NBR), PVC/polymethylmethacrylate (PMMA), and PVC/polymeric plasticizers. The mechanical blending of miscible polymers results in a homogeneous morphology that exhibits a single glass transition [1]. Miscibility in these systems is attributed to the presence of specific interactions between the blend components (hydrogen bonding, ionic, dispersion, etc.) [3].

Also, some polymers are immiscible but mechanically compatible, such as polycarbonate (PC) with acrylonitrile-butadiene styrene (ABS), which give a multiphase morphology with efficient dispersion of the minor component and good interfacial adhesion between the two unmodified components.

However, most polymers are not mixable during processing and as a result, a sharp interface may occur between the multiphases. Their overall performances are related to the size and morphology of the dispersed phase and its stability to coalescence or gross segregation [2] and their mechanical properties are usually lower than those of the constituents. Immiscibility in most polymer blends is related to the disparity between the polarities of components and the existence of a large interfacial tension in the melt, which makes it difficult to properly disperse the components during low stress or quiescent conditions. It also leads to poor interfacial adhesion in the solid state which causes easy mechanical failure via these weak defects between phases [2,6]. Remedying these problems can be carried out by using compatibilizers to improve the interfacial interaction.

The importance of the interface interaction in multiphase polymer systems has been long recognized. Physical and chemical interactions across the phase boundaries are known to control the overall performances of both the immiscible polymer blends and polymer composites [1]. Strong interactions brought in by compatibilizers could result in good adhesion and efficient stress transfer from the continuous to the dispersed polymer phase in blends.

1.2 The Classification of Compatibilizers

1.2.1 Block, or Graft Copolymers (Preformed Compatibilizers)

Over the last two decades, block and graft copolymers have been used as interfacial agents to upgrade the bulk properties of polymer blends. These copolymers have segments capable of specific interactions with each of the blend components and their miscibility

depends on their closely matched solubility parameter. For example, di- or tri- block copolymers of styrene and butadiene (SBR) and hydrogenated butadiene of isoprene are effective compatibilizers for most polyolefin/PS blends [7-11]. Also, PP/PE could be compatibilized with poly(ethylene-co-propylene) elastomer [12]. Further, EPDM (poly(ethylene-co-propylene-co-diene))/PMMA with EPDM-g-MMA as compatibilizer [11], PS/nylon 6 (PA-6) or EPDM with PS/PA-6 block copolymers or styrene-ethylene/butylene-styrene triblock copolymer as compatibilizer [13,14], and PVC/PS with PMMA/PS block copolymer as compatibilizer [15] are all effective blending systems.

However, compatibilization by preformed block or graft copolymers has not been used as extensively as the potential utility might suggest. A primary reason for this is the lack of economically viable and industrially practical routes for synthesis of such copolymers as additives for systems of interest.

1.2.2 Copolymers Formed *In Situ* (by Precursors of the Compatibilizers)

In this case, graft or block copolymers acting as compatibilizers are formed during the compounding of polymer blends. There are two types of *in situ* reaction, free radical, and non-free radical. High impact polystyrene (HIPS)/ABS blends are the classical examples of systems compatibilized by block or graft copolymer formed through free radical reactions *in situ* [1,2]. Recently, a PS/PE system was also compatibilized by styrene/ethylene graft copolymers formed *in situ* by free radical reactions [16]. Also, EPDM and MMA was extruded in a twin-screw extruder with peroxide as the initiator. This system yields a mixture of EPDM and PMMA in which EPDM g-MMA acts as a compatibilizer [10].

Non-free radical type of *in situ* compatibilization was first proposed by Ide *et al* [17] in the compatibilization of maleic anhydride (MA) grafted PP (PP g-MA) and PA-6 through the reaction of the anhydride with the terminal $-NH_2$ groups of PA-6. Since then, more and more attention has been paid to exploring functional polymers as precursors of compatibilizers. Polyamides or polyesters have begun to be blended with elastomers containing carboxyl, maleic anhydride or epoxy groups, in which the interchain copolymers are formed between the end groups of polyamide or polyester and the reactive group of elastomers *in situ* [18-22]. Usually, the functional polymers could be graft polymers or random copolymers containing functional groups. The most widely used functional polymers are MA or acrylic acid (AA) grafted or random copolymerized polyolefin copolymers. Generally, the functional polymers have A-co-C or A-g-C (C represents the reactive unit) structure. it can compatibilize the immiscible polymer A and B if C is capable of a chemical reaction with B. The majority of the blends employ polyamide as one component and copolymers containing anhydride or carboxyl functionality as functional polymers. For example, PE or PP can also be compatibilized with PA-6 by carboxyl functionalized PE copolymer or PP-g-AA [23]. PS can be compatibilized with PA-6 by anhydride functionalized PS [24]. ABS/PA-6 can be compatibilized by SAN-co-MA copolymer, and PA-6,6/acrylate rubber can be compatibilized by SMA or EPDM-g-MA copolymer [26]. Besides nylon family, poly(ethylene terephthalate) (PET) and poly(butylene terephthalate) (PBT) are compatibilized with functional rubbers with epoxy group [27,28]. Recently, a dual-functional-polymer compatibilization model has been developed in our research group. In this case, two functional polymers, for example, are A-co-C (or A-g-C) and B-co-D (or B-g-D) (C and D represent the reactive units or groups, and they are reactive with each other). When

the two functional polymers contact each other during the compatibilization of A/B blends, a copolymer A-B is formed by the reaction of C and D groups. This compatibilization model has been successfully applied in the compatibilization of PE/PP blends in our research group. By adding a small amount of PE-g-epoxy and PP-g-MA to the uncompatibilized PE/PP blends, the two functionalized polymers form PE-g-PP copolymer by the interfacial reaction of epoxy and MA groups, which functions as the compatibilizer. The other two examples of this compatibilization models are the compatibilizations of polyolefins/PVC and PP/ABS blends which will be discussed in detail in this dissertation.

Figure (1-1) shows the reported examples of common compatibilizing reactions between functionalized blend constituents based on the most recent literature survey.

1.3 The Synthesis of Functional Polymers

Inserting the reactive monomer into the backbone of polymers during polymerization is the most widely used method to synthesize the functional polymers. However, the foreign units inserted may disturb the molecular backbone of the original polymer and change its physical properties. The good examples for these functional copolymers are poly (ethylene-co AA) (Zeeland Chemicals), poly(styrene-co-MA) (Arco Chemical), poly(styrene-co-oxazoline) (Dow Chemical), poly(styrene-co acrylonitrile co MA) (Dow Chemical), and poly(ethylene-co-glycidyl methacrylate) (Nippon Shokubai Co.). These copolymers contain the reactive monomer from 1% up to 50% (wt. %). They keep most of the physical properties of the homopolymers, but they have certain changes in thermal and mechanical properties.

Grafting of preformed polymers is another important method for the preparation of polymers with a functional group. Since the grafting does not disturb the backbone structure, grafted polymer keeps most of physical properties of the original polymer. The traditional grafting technique is solution grafting, which needs to dissolve the polymer in organic solvent and then introduce initiator and monomers in the solution. At the same time, the reaction should be protected by nitrogen and kept at high temperature. Several hours of reaction is usually required to achieve a high graft ratio. The high cost and high toxicity of the organic solvent used for the grafting make this processing economically and ecologically impractical. Recently, melt grafting and solid-state grafting have been developed to remedy the problems of low productivity and high solvent cost of the traditional solution grafting. Both solid state and melt grafting are carried out without any solvent. Also, both solid state and melt grafting are usually carried out via continuous twin-screw extrusion which have much higher productivity than solution grafting. However, neither melt grafting nor solid state grafting could reach as high of a graft ratio as solution grafting.

1.4 The Acidic Monomers and Basic Monomers Functionalized Polymers

Most of the commercially available functional polymers contain only acidic reactive groups such as carboxylic acid, acrylic acid, or maleic anhydride, which can only be used to compatibilize with polymers containing basic reactive groups, like nylon with amine end groups. Basic groups functionalized polymers have also been developed recently. The most widely used one is polyetheramine (Jeffamine Series, Huntsman Chemical Co.), which has been used with PP g-MA to improve the surface paintability and flexibility of PP [39]. Another kind of newly published functional polymer is LDPE grafted with 2-(dimethylamino)

ethyl methacrylate (DMAEMA) [40, 41]. This kind of grafted LDPE can form ionic bonds or polar interactions with polymers containing carboxylic acid or maleic anhydride groups. However, the low reactivity of tertiary amines makes the compatibilizing efficiency of this functionalized polymer low [41]. Recently, Dow Chemicals developed oxazoline functionalized PS based on the copolymerization of styrene and a small amount of oxazoline monomer. Since its availability, it has been used to compatibilize PS/LDPE or PS/EP rubber blends along with PE-g-MA or EP-g-MA [42, 43]. Besides these, it has also been successfully used with carboxylated nitrile rubber (XNBR) to compatibilize NBR/PS blends [44]. The reaction mechanism of oxazoline with other groups are shown in Figure (1-1) (reaction 6-8).

1.5 The Epoxy Functionalized Polymers

Recently, *in situ* compatibilized polymer blends based on copolymers containing glycidyl methacrylate (GMA) monomer have attracted great attention because of potentially broad applications. The unique property of the epoxy group of GMA is its extremely high reactivities with both basic groups (primary amine or secondary amine groups) and acidic groups (hydroxyl, carboxylic anhydride) which means the GMA functionalized polymers compatible with both nylon (amine end group) based and polyester (hydroxyl and carboxylic end groups) based polymers. The mechanisms of these reactions are shown in Figure (1-1) above (reaction 2 to 5). Chung and Carter [29] used styrene-acrylonitrile-glycidyl methacrylate copolymer to compatibilize PET/ABS blends which have extremely high low-temperature impact properties. Akkapeddi *et al.* [30-31] reported using ethylene-g-GMA (EGMA) as a reactive compatibilizer in the blends of PET with PC and with various polyolefins. Lee and Chang investigated a series of reactive compatibilized blends based on

GMA-containing copolymers including the following polymer pairs PS/nylon [32], PS/PET [28], HIPS/PET [34], ABS/phenoxy [34], ABS/nylon[35], ABS/polyacetal [36], polyphenylene oxide (PPO)/PBT [37], and PMMA/PET [38] However, most of the epoxy functionalized polymers mentioned here are synthesized by solution copolymerization or solution grafting which is still economically costly for wide application.

1.6 About the Study of This Dissertation

The studies of this dissertation are divided into two parts The first part describes synthesizing the MA, GMA, and oxazoline monomer grafted polyolefins and compares the reactivities of them with various other reactive groups (Chapter 2 – 5) The second part demonstrates the applications of GMA grafted polyolefins in the compatibilization of three polymer blends, HDPE/PET, PVC/polyolefin, and PP/ABS which are major components of recycled plastics (Chapter 6 – 8) The purpose of developing functional monomers functionalized polyolefins is to find a versatile, economical, and highly reactive functional polymer which can achieve compatibilization efficiently for various polyolefin blends

In Chapter 2, several grafting techniques including solution, melt and solid-state grafting are applied to synthesize the epoxy group functionalized polyolefin by using GMA as monomer Two other commonly used monomers, maleic anhydride (MA) and 2-isopropenyl 2-oxazoline (IPOZ), are also grafted on polyolefin and compared with the grafting of GMA monomer Since epoxy and oxazoline groups possess high reactivities with various chemical groups, a separate chapter (Chapter 4) studies and compares the reactivities of the GMA grafted and oxazoline grafted polyolefin with other functional groups for example, carboxylic acid, hydroxyl, and amine groups in the melt. In Chapter 5, a twin-screw

extruder is applied to carry out the grafting continuously and the grafting is optimized by changing the operation parameters, extrusion procedures, and using comonomer technique. In order to compensate for the loss of mechanical properties of PP caused by thermal degradation during melt grafting, a novel recouping technique is studied in Chapter 6.

The applications of the synthesized GMA grafted polyolefin in the compatibilization of three major binary blends of recycled plastics: HDPE/PET, PVC/polyolefin, and ABS/PP are described in Chapter 6, 7, and 8. For HDPE/PET blend, the compatibilization mechanism is based on the interfacial reaction between the grafted epoxy groups and the carboxylic acid end groups or hydroxyl groups of PET. For both PVC/polyolefin and ABS/PP blends, dual-functional polymer model is employed for the compatibilization. Besides GMA grafted polyolefin, another functional polymer is carboxylated nitrile rubber (XNBR) for PVC/polyolefin compatibilization, and poly(styrene-co-maleic anhydride) (SMA) for ABS/PP compatibilization. The selection of these two functional polymers is based on the facts that XNBR and SMA are miscible with PVC and ABS matrix, respectively.

Methods to characterize the grafted polyolefin include solvent extraction for the purification and gel amount measurement for crosslinking density; elemental analysis, FTIR, and ^{1}H-NMR for graft ratio measurement. Double-plate rotational rheometer, melt flow index, and torque measurements are used as major tools for the rheology, interfacial reaction, and processability studies of the blends. Scanning electron microscopy (SEM) is used to analyze the morphologies of blends. The thermal characterization is carried out by differential scanning calorimeter (DSC). The mechanical properties are characterized by detecting tensile properties and Izod impact strength. Lap shear adhesion measurement is also employed to study the interfacial interaction between different phases.

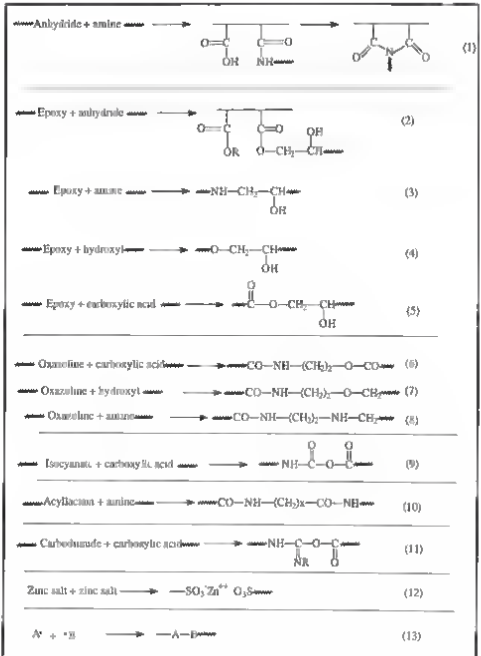

Figure (1-1) Examples of interfacial reactions between functional blending constituents

PART I THE GRAFTING OF POLYOLEFINS WITH FUNCTIONAL MONOMERS

CHAPTER 2 - CHAPTER 5

CHAPTER 2
THE GRAFTING OF POLYETHYLENE BY SOLID-STATE, MELT AND SOLUTION GRAFTING

2.1 Introduction

Polyethylene is an apolar and chemically inert polymer, but its polarity or chemical reactivity can be modified by means of grafting various functional monomers onto its backbone without substantial loss of its physical properties. The grafting processing may be carried out in the solution-state [44, 45] molten-state [46, 47] or solid-state [48-50]. The grafted polyethylene has various applications, especially as a precursor of a compatibilizer for polymer blends as illustrated in Chapter 1.

Solid-State grafting was recently proposed to graft maleic anhydride (MA) onto polypropylene (PP) [48-50]. This grafting technique allows for the reactive monomer to be grafted onto the surface of PP particles below the melting temperature of PP. The grafted MA unit can form interphase linkage between a polymer and fillers (like $CaCO_3$) or a polymer and a polymer in polymer blends. As the grafting is carried out at low temperatures (below T_m of polyolefins), the toxic fume which is usually formed during melt grafting can be avoided. Also, unlike solution grafting, no solvent is needed for this process which makes this process economically attractive.

The grafting of polyolefins in the melt is becoming an increasingly important industrial process. The MA grafting onto polyolefin backbone via the twin screw extrusion process has

been widely used in industry [51-54]. Various other monomers like acrylic acid, hydroxy ethyl methacrylate (HEMA) and 2-(dimethylamino) ethyl methacrylate (DMAEMA) [40, 41, 55, 56] have also been successfully grafted onto polyolefin according to recent publications.

Solution grafting is a traditional grafting technique. Its greatest advantage is being able to achieve a high graft ratio via a long grafting time. Unfortunately, a toxic and expensive solvent is needed for this process and the disposal of the waste solvent is an ecological problem. The high cost of the solvent makes the grafted polymers produced by this technique extremely expensive.

In this study, these three grafting methods are studied and compared in the grafting of high density polyethylene (HDPE) with three types of frequently used functional monomers: maleic anhydride (MA), glycidyl methacrylate (GMA), and 2-isopropenyl-2-oxazoline (IPOZ). As illustrated in Chapter 1, MA monomer is only reactive to basic groups, while IPOZ and GMA are reactive with both acidic and basic groups.

2.2 Experiment

2.2.1 Materials

Pelletized HDPE was supplied from Eastman Chemical Products(Tenite PLS H6001-A). Maleic anhydride (99%) was bought from Fisher Scientific and used as received. Glycidyl methacrylate was bought from Aldrich Chemical Co. and purified by column chromatography before application. The 2,5-dimethyl-2,5-di(t-butylperoxyl)hexane was supplied by Lucidol Division, Pennwalt Corp. and used as an initiator for the grafting. 2-isopropenyl-2-oxazoline (boiling point: 50.5-51.5°C/17 torr) was synthesized according to Appendix A. 1-2

dichlorobenzene (DCB) was bought from Fischer Scientific and used as a high temperature solvent for the solution grafting. The chemical structures of the three monomers are shown in Figure (2.1).

2.2.2 Grafting Procedures

2.2.2.1 Solid state grafting

Solid-state grafting was carried out in a Brabender twin-roller mixer with the temperature below the T_m of HDPE (80°C and 100°C). HDPE had been cryogenically ground to powder (~ 100 μm). The ground HDPE was mixed with a monomer/initiator solution, then put in the running mixer at 100 rpm. The processing was protected in inert atmosphere (N_2 gas protection). The mixing was stopped after a determined time.

2.2.2.2 Melt grafting

The melt grafting of HDPE was performed on the same batch mixer as used in solid state grafting. The polymer, monomer and initiator were premixed and charged into the mixer, which is operating at 70 rpm and at a set temperature between 160-180°C for MA and GMA monomer, had between 150-170°C for oxazoline monomer.

2.2.2.3 Solution grafting

The solution grafting reaction was carried out in a three-neck flask equipped with a stirrer and a thermometer. The temperature in the flask, which was heated in a heating mantle with voltage controls, was maintained with a precision of ± 1°C. HDPE was dissolved in the DCB at about 120°C, the temperature was raised to the desired temperature and the monomers which had been mixed with the desired amount of peroxide was added. After determined grafting time, the reaction was stopped and the reaction product was poured into

5-10 volumes of acetone with constant stirring. The precipitated product was filtered, washed twice with acetone, and subsequently dried overnight at 50°C in a vacuum oven.

2.2.3 Analysis

The raw graft products from solid-state grafting and melt grafting were vacuum dried at 100°C for 2 days to remove the unreacted residue monomer. FTIR was used to detect the wt % of converted monomer (grafted and homopolymerized monomer) in the sample. The FTIR samples were prepared by compression molding at 160°C for 1 min to a transparent thin film. The wt.% of converted monomer is calculated by comparing the ratio of the absorbance of the characteristic groups of the monomers (carbonyl for MA (1706 cm^{-1}) and GMA (1738 cm^{-1}), oxazoline ring for IPOZ (1637 cm^{-1})) to the methyl group of PE (1376 cm^{-1}). The absolute converted monomer (wt.%) can be determined by oxygen elemental analysis. Combining the results of element analysis and FTIR absorbance ratio constructs the calibration curves so that the converted monomer (wt%) can be calculated by measuring the height of the characteristic peak. The calibration curves for the three monomers grafted HDPE by the above method is illustrated in Appendix B and Chapter 4. After the wt % of grafted and homopolymerized monomer was determined, the sample was dissolved in refluxing toluene then the dissolved polymer was precipitated in methanol. The homopolymer

$$Graftratio(GR) = \frac{Mass\ of\ monomer\ grafted\ on\ polymer}{Mass\ of\ polymer} \times 100\%$$

$$Graftefficiency(GE) = \frac{Mass\ of\ monomer\ grafted}{Total\ monomer\ converted} \times 100\%$$

$$Conversion = \frac{Total\ monomer\ converted}{Total\ monomer} \times 100\%$$

of monomers would be dissolved in methanol solvent. The precipitated polymer was dried in a vacuum dryer at 50°C for 1 day. Since the remaining monomer structure is all from grafted monomer, the determined amount of monomer by FTIR should be the wt.% of grafted monomer. The calculation of graft ratio, graft efficiency, and conversion are based on the formula shown above. The total amount of monomer used for the calculation of conversion above can be calculated by:

$$\frac{P_1}{P} \times M$$

P1 : mass of detected polymer; P : mass of blended polymer; M : mass of blended monomer. The FTIR spectra of the purified grafted HDPE by the three grafting methods are shown in Figure (2-2) to (2-4).

2.3 Results and Analysis

2.3.1 Grafting Mechanism

The exact mechanism of the grafting process is very complicated and controversial. Basically, there are at least three reactions that coexist and compete with each other: grafting of monomer onto PE backbone, homopolymerization of monomer; and crosslinking of PE

macroradicals (as shown in Figure (2-5)). After the decomposition of the peroxide, the free radical RO• abstracts hydrogen from PE and generates macroradical PE•. All of these three reactions mentioned above compete for the free radicals or PE macroradicals. The overall graft ratio should be affected by the competitions between the three reactions. However, the homopolymerization of monomer could be suppressed by the high processing temperature. If the processing temperature is above the ceiling temperature of the homopolymer, depolymerization (Figure (2-5), step 4) will occur which will favor the grafting.

2.3.2 Solid-State Grafting

Figure (2-6) shows the changes in the graft ratios (GR) of the three monomers processed by this technique along with the processing time. Maleic anhydride has a much higher graft ratio than the other two monomers. However, the overall conversions of the three monomers are quite close according to Table (2-2). It seems that the relatively low graft ratios of both GMA and IPOZ could be attributed to the competition between monomer grafting and homopolymerization. This was further confirmed by Figure (2-7) in which the graft efficiency of GMA and IPOZ are much lower than that of MA. This kind of difference in the graft efficiency can be due to the different molecular structures and polarities of these three monomers (Figure (2-1) and Table (2-1)). From the structures point of view, MA is reluctant to homopolymerization because of the strong steric hindrance due to the di-substitution of the two adjacent carbonyl groups at the 1 and 2 positions of the double bond. Also, due to the electron-attracting nature of the two carbonyl groups, the electrons around the double bond are deficient making it insensitive to the attack of free radicals. From the Q-e value [57, 58] comparison, the polarities sequences of these three monomers is MA >> IPOZ

>GMA (according to the e Values), which means that the electron density of the vinyl group of MA is extremely low Besides, the symmetry of the double bond and the electron cloud is the another reason for the reluctance of MA to the homopolymerization. Comparatively the chemical structures of both GMA and IPOZ lack steric hindrance factor For GMA, only one carbonyl group demonstrates the electron-attracting affect, while for IPOZ, this kind of effect caused by the oxazoline ring is also trivial.

From the above structure analysis both GMA and IPOZ tend to homopolymerize in addition to grafting, while for MA, the possibility of homopolymerization under the conditions employed in the solid-state grafting is low However, Table (2-3) indicates that the detected graft efficiency (GE) of MA is lower than 100%, which means that MA grafting still accompanies the homopolymerization. According to reference [59 60]..poly(MA) can only be formed under low temperatures (around 60°C) for a long period of reaction time In the solid-state grafting, the processing temperature is low (80°C or 100°C) and the reaction time is long (35 min), it is quite possible that the homopolymerization of MA still exists

From the standpoint of monomer dispersion in a polymer matrix, monomers are coated outside polyolefin particles as a thin layer during grafting. As the polyolefin matrix is still in the solid state, it is impossible for a monomer to disperse in a polymer on a molecular scale The coalescent state of the monomer droplet facilitates the formation of homopolymer which makes the graft ratio (GR) of both GMA and IPOZ low Figure (2-6) also gives us some information about the grafting rate The graft ratio keeps increasing even after 35 min, which means the grafting rate is extremely low Thus is because of the low concentration of PE macroradicals under the low processing temperature, which makes monomer has no reactive site to be grafted onto

The effects of monomer concentration on the graft ratio and the graft efficiency were also studied (Figure (2-8)). For all three monomers, there is no obvious change in the graft ratios with the increasing monomer wt.% especially for GMA and IPOZ. The domination of homopolymerization caused by monomer coalescence can be the explanation for this phenomena. Obviously, increasing the amount of monomer is not an effective way to increase the graft ratio and graft efficiency simultaneously for the solid-state grafting of these three monomers.

Very low crosslinking densities were recorded for all of these three solid-state grafted HDPE by the melt flow index (MFI) value measurement (Table (2-3)). According to the reaction mechanism illustrated in Figure (2-5), the low temperature makes it difficult for peroxide to abstract the hydrogen from the PE backbone (Figure (2-5), step (1)) and consequently, only a small amount of PE macroradicals can be generated. The low concentration of PE macroradicals could result in both crosslinking and low grafting ratio as illustrated before (Figure (2-5), step (2) and (5)).

Table (2-3) also shows the effects of temperature and initiator concentration on the graft ratio, graft efficiency, and conversion. The increment of peroxide does result in high conversion for all of the monomers, but the graft efficiencies are reduced for GMA and IPOZ, and also has no obvious improvement on the graft ratio of them. As explained above, the low processing temperature generates low concentration of PE radicals even the concentration of peroxide is high. However, the high concentration of peroxide does facilitate the homopolymerization which makes the graft efficiency lower.

2.3.3 Melt Grafting

Compared with the solid state grafting illustrated previously the melt grafting process is carried out above the melting point of polyolefins The molten state makes it easier to dissolve the monomer into the melts, which can deter the homopolymerization and increase the graft ratio When the melt grafting is carried out under temperature close to the ceiling temperature of homopolymerization, the depolymerization reaction (Figure (2-5), step (4)) begins to play an important role and lead to a repression in both homopolymerization and homopolymer molecular weight. As a result, compared to the solid-state grafting, melt grafting is supposed to promote both graft ratio and graft efficiency especially for GMA and IPOZ. The above analysis is confirmed in Figure (2-9) The graft ratio for all three monomers grafted via melt grafting is much higher than those grafted via solid state grafting Among the three monomers, MA is still the one which can be grafted with the highest graft ratio although the conversion of MA is not the highest (Table (2-4)), GMA has the next highest graft ratio, while oxazoline has the lowest same sequence as solid state grafting

The effects of temperature and initiator on the graft ratio and graft efficiency are shown in Table (2-5) When the processing temperature is above 160°C, almost no homopolymerization for MA is observed This is because MA is not readily polymerized under the temperature employed here and is therefore grafted at a high efficiency without the accompanying formation of any homopolymerization. The ceiling temperature for GMA polymerization is not known, but since that for methyl methacrylate (MMA) at a concentration of 1M is estimated to be 155°C [54], it is expected to be under 180°C. It should be reasonable to infer that a high processing temperature of melt grafting (>160°C) can

eliminate the homopolymerization to a certain extent for GMA monomer. As shown in Table (2-5), when the temperature increases from 160°C to 180°C, the graft efficiency increases from 53% to 64%. Unfortunately, the high processing temperature makes monomer vaporize easier, this kind of consumption of monomer by processes other than grafting can also be a direct reason for the low graft efficiency and conversion of IPOZ (as shown in Table (2-4) and (2-5)) although graft ratio and conversion increased with high temperature.

Besides the temperature factor, from Figure (2-10), it can also be seen that graft ratio cannot be improved dramatically by just increasing the monomer concentration, which is similar to solid-state grafting. High monomer content leads to low graft efficiency, while low monomer content can usually keep graft efficiency effectively high. The reason for that is that the small amount of monomer has superior solubility in the melt compared to a large amount and the coalescence is rare which makes the monomer have more chances to contact not with the monomer itself but with the polymer chains.

The content of peroxide also has a direct effect on the graft ratio (GR) and graft efficiency (GE) (Table (2-5)), high initiator concentration resulted in high GE and GR. Unlike solid state grafting, the GR and GE of melt grafting is very sensitive to the change of peroxide concentration. Under high temperature, high content of peroxide can effectively abstract hydrogen atom on polyolefin backbone and produce PE macroradicals. The large amount of these PE macroradicals offer enough potential grafting sites for the monomer (Figure (2-5), step (2)) and increases the probability of polymer radicals to be attacked by monomer. Consequently, GR and GE increased dramatically along with the increasing of peroxide. Unfortunately, high contents of peroxide could induce a high crosslinking density which is shown by the decreasing MFI value of the grafted HDPE. As a result, determining

how to balance the graft ratio and crosslinking density is important for the melt grafting of HDPE. High crosslinking densities will result in poor processability while the high graft ratio is crucial for successful reactive compatibilization. The grafting rate could also be inferred from Figure (2-9). GR will not increase dramatically after the first 10 minutes of grafting which means the grafting can be mostly accomplished within the first 10 minutes, especially for MA and GMA. If the grafting is carried out in twin-screw extruder with high shear rate, the grafting rate could be increased even sufficiently. As a result, compared with other grafting techniques, melt grafting has the advantages of short processing time and continuous processing if the grafting is carried out in a twin screw extruder.

2.3.4 Solution Grafting

As illustrated before, IPOZ has a relatively low boiling point. Solid-state grafting usually results in a low graft efficiency (GE) because of the competition from homopolymerization, and melt grafting can not dramatically increase GE and conversion either because of its vaporization under the high processing temperature. These kinds of properties of IPOZ which is ready for homopolymerization and having a low boiling point make its grafting process turn back to the traditional solution grafting, in which monomer vaporization can be avoided by a condensation device. On the other hand, complete molecular contact between monomer and polymer chain would also be possible in a solution system, by which the coalescence of monomer can be minimized.

Figure (2-11) show the graft ratios of the three monomers along with the grafting time. In this case, both GMA and IPOZ can reach graft ratios as high as MA. The graft ratios of the monomers are highest compared with the other two grafting techniques. The high graft

ratio and efficiency can not only be attributed to a long grafting time but also to the ideal molecular dispersion of monomer in polymer solution and the high probability of molecular contact between monomer and polymer chain. The coalescence of monomer molecules is impossible because of the high solubility in polymer solution and low concentration of monomer.

The effect of the concentration of monomer is illustrated in Figure (2-12). At low monomer concentrations, the graft ratio (GR) increases along with the increasing monomer concentration until a large amount of monomer is added. The decreasing slope of the GR curve at high monomer concentrations means that homopolymerization begin to show up. However, unlike melt grafting and solid-state grafting, the GR is sensitive to the increasing monomer content. For all of the three monomers, the increment of monomer content from 2% to 6% could cause the GR to increase from around 1.8% to 4.2%. As a result, increasing the concentration of monomer is an effective method to increase the GR for solution grafting.

Similar to the melt grafting, increasing the temperature and the concentration of the initiator can also increase the GR and GE, but the resulted crosslinking is also observed (Table (2-6)). However, the increment of crosslinking is not as extreme as in melt grafting.

As illustrated before, the low GR of IPOZ in the other two methods is mainly because of the homopolymerization and vaporization of monomer. Due to the elimination of these problems in solution grafting, the GR and GE of IPOZ is the highest among the three grafting methods. It is interesting to notice that GMA and IPOZ have quite similar GR and GE values in solution grafting as well as in solid-state grafting. This kind of similarity between IPOZ and GMA might be due to the similar electron densities of their vinyl group as shown in Table (2-1) [57, 58].

2. 4 Conclusions

2.4.1 Solid State Grafting

1 Maleic anhydride can be successfully grafted onto PE particles by solid-state grafting while GMA and IPOZ are relatively difficult to graft with a high graft ratio The most likely reason is the predomination of homopolymerization for these two monomers in the solid state grafting condition. Homopolymerization is observed for all of the three monomers under the condition of solid state grafting

2 The graft ratio can not be effectively improved by increasing the concentration of monomer or peroxide, which only resulted in a low graft efficiency

3 Low crosslinking is observed for the solid state grafting which can be due to the incapability of peroxide to abstract hydrogen atoms from the PE backbone and form PE macroradicals under low temperature

4 The grafting rate is low because of the low concentration of PE macroradicals under the processing temperature.

2.4.2 Melt Grafting

1 All three monomers could be successfully grafted onto the polyolefin by melt grafting

2. There is competition between homopolymerization and grafting for GMA and IPOZ under low processing temperature However, the homopolymerization can be prohibited by the processing conditions like high temperatures, low concentrations of monomers and high concentration of peroxide. On the other hand these processing conditions can also bring in

some negative effects like high crosslinking densities

3 The required processing time for melt grafting is much shorter than that for solid state grafting and most of grafting can be finished within 10 mins of melt mixing at 70 rpm and 160°C

2.4.3 Solution Grafting

1 By solution grafting, all of the three monomers can be grafted onto PE with the highest graft ratios and efficiencies

2 Increasing the concentration of monomer to a certain extent is an effective route to increase both graft ratio (GR) and graft efficiency (GE) but high monomer concentrations can also result in a low GE.

3 Increasing the temperature and the concentration of peroxide will increase both the GE and GR, as well as increase the crosslinking density, but the crosslinking is not as sensitive to the peroxide as the melt grafting does.

4 GMA and IPOZ have quite similar grafting results which might be due to the similar electron densities for their vinyl groups

2.4.4 The Comparisons

Each of these three grafting methods has its own advantages and disadvantages The applications of them should be dependent on the specific monomer to be grafted Solid state grafting has the advantages of being free from toxic fumes and having low crosslinking densities Its main disadvantages are long processing time, poor monomer dispersion low graft ratios, and dominating homopolymerization which results in a low graft efficiency for

ready homopolymerizing monomers. Among the three monomers studied in this paper, MA is the best candidate for this technique by comparing Figure (2-2), (2-3), and (2-4).

Melt grafting has the advantages of short processing time, relatively high graft ratio and high efficiency if the polymer is processed under conditions like high processing temperature, low monomer concentration, and high peroxide concentration. The major disadvantage is the ease of forming toxic monomer fumes, especially for monomers with low boiling points like IPOZ. The presence of residue monomer and peroxide might have negative influences on the mechanical strength of final products. Also the crosslinking of PE caused by the high content of peroxide is another problem. MA and GMA are good candidates for this technique. In the reactive extruder used in the study of Chapter 4, the problem of monomer fume can be alleviated by a vacuum pump at the vent port, by which the unreacted residue monomer can be eliminated to certain extent. Grafting in a twin-screw extruder is also a continuous process in which high productivity and grafting efficiency can be both achieved simultaneously. It will be discussed in Chapter 4 in detail.

The traditional solution grafting technique is the most expensive process. The long reaction time, toxic solvent, and laborious procedure make it difficult to be used as a convenient and economical method to get functional polymer at a large scale, although the highest graft ratio can be achieved for all three monomers used in this study. The best candidates of the monomers for this technique are ones having low boiling points and chemical stability under high temperatures. In this study, it is found that only solution grafting can graft oxazoline monomer (IPOZ) onto PE backbone with high graft ratio and efficiency.

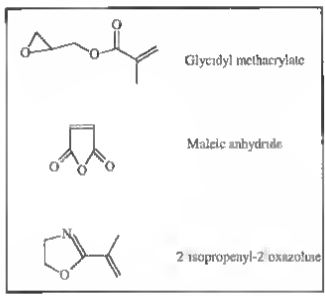

Figure (2-1) The molecular structures of the three monomers

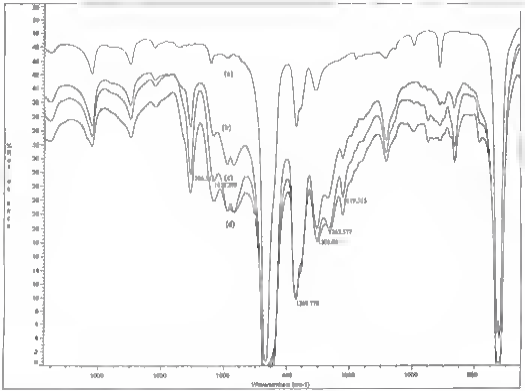

Figure (2-2) The FTIR spectra of maleic anhydride (MA) grafted HDPE by the three techniques The peak height ratios of the carbonyl groups of MA (1706.53 cm $^{-1}$) and the methyl group of PE (1369.37 cm $^{-1}$) are used to calculate the graft ratios. (a) Pure HDPE (b) Solid-state grafted HDPE, (c) Melt grafted HDPE, (d) Solution grafted HDPE.

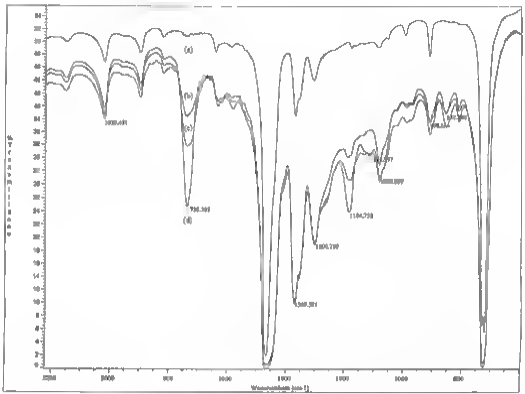

Figure (2-3) The FTIR spectra of glycidyl methacrylate (GMA) grafted HDPE by the three techniques The peak height ratios of the carbonyl groups of GMA (1738.38 cm^{-1}) and the methyl group of PE (1369.37 cm^{-1}) are used to calculate the graft ratios
(a) Pure HDPE, (b) Solid state grafted HDPE (c) Melt grafted HDPE, (d) Solution grafted HDPE

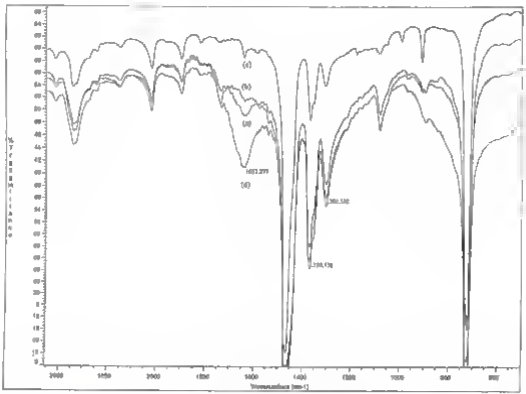

Figure (2-4) The FTIR spectra of 2 isopropenyl-2 oxazoline (IPOZ) grafted HDPE by the three techniques. The peak height ratios of the oxazoline ring of IPOZ (1637.28 cm-1) and the methyl group of PE (1370.13 cm-1) are used to calculate the graft ratios
(a) Pure HDPE, (b) Solid state grafted HDPE, (c) Melt grafted HDPE, (d) Solution grafted HDPE.

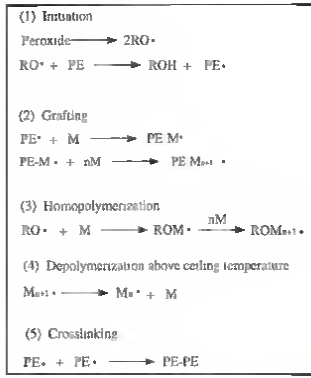

Figure (2-5). The possible reaction mechanisms during grafting

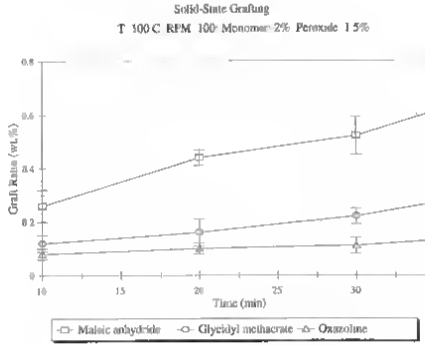

Figure (2-6) The graft ratios of the three monomers vs the reaction time for solid-state grafting

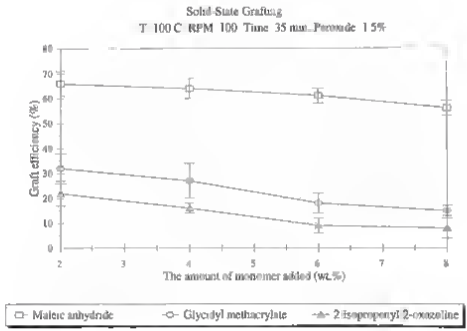

Figure (2-7) The graft efficiencies of the three monomers vs the amount of monomers added for solid-state grafting

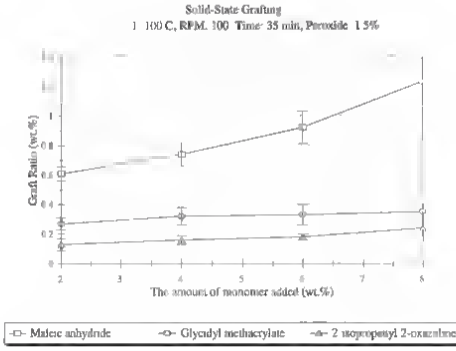

Figure (2-8) The graft ratios of the three monomers vs the amount of monomers added for solid state grafting

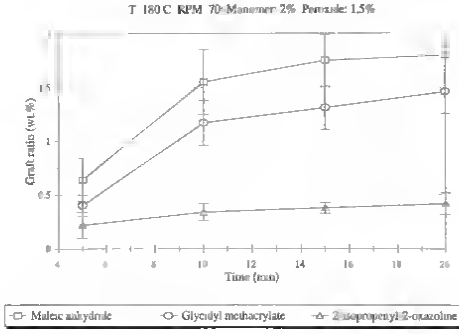

Figure (2.9) The graft ratios of the three monomers vs the reaction time for melt grafting

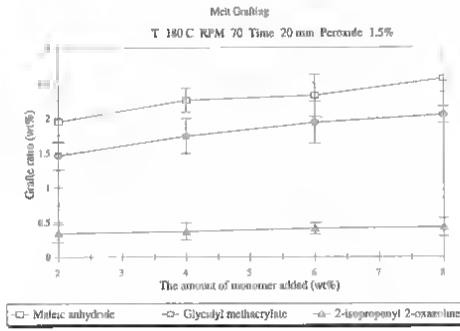

Figure (2 10) The graft ratios of the three monomers vs the amount of monomers added for melt grafting

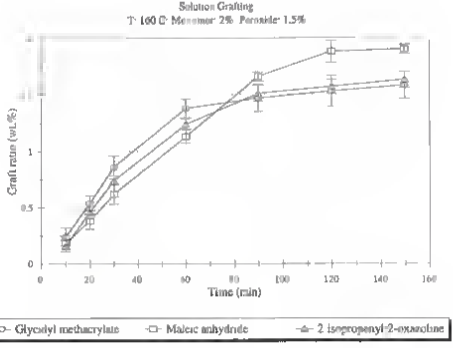

Figure (2.11) The graft ratios of the three monomers vs the reaction time for solution grafting.

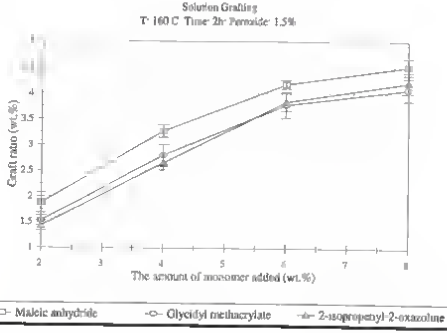

Figure (2-12) The graft ratios of the three monomers vs the amount of monomers added for solution grafting.

Table (2-1) Some physical properties of the three monomers.

Monomers	State	Mw	Fp (°C)	bp (°C)	Q Values*	e Values*
Maleic anhydride	Solid Crystal	98.06	103	200	0.86	3.69
Glycidyl methacrylate	Liquid	142.15	83	189	0.96	0.20
2 Isopropenyl 2-oxazoline	Liquid	111.00		50.5-51.5 (17 torr)	0.78	0.40

*Q and e are defined by Alfrey and Price Q and e equation [58]
Q and e are measures of the reactivity and polarity, respectively, of a vinyl monomer

Table (2-2) The comparison of conversions for the three monomers in solid state grafting

The amount of monomer added (wt %)	The conversion* of monomer (wt.%)		
	Maleic anhydride	Glycidyl methacrylate	2-isopropenyl-2-oxazoline
2	43	42	37
4	33	31	35
6	28	28	32
8	27	28	30

Temperature: 100°C Processing time: 35 min.
* Conversion was calculated as defined

Table (2-3) The influence of temperature and initiator concentration on the solid-state grafting reaction. Monomer ratio 2% Time 35 min RPM 100

Monomers	Temperature (°C)	Initiator (wt.%)	GR (wt.%)	GE (%)	Conversion (wt.%)	MFI * (g/10 min)
Maleic anhydride	80	1	0.39	47	41	4.8
	80	0.5	0.43	56	38	5.1
	100	0.5	0.52	62	42	4.8
	100	1.5	0.60	68	43	4.6
Glycidyl methacrylate	80	1	0.27	25	54	4.9
	80	0.5	0.26	25	51	4.7
	100	0.5	0.23	18	63	4.5
	100	1.5	0.28	19	72	4.4
2 Isopropenyl 2-oxazoline	80	1	0.12	14	43	4.6
	80	0.5	0.16	21	38	5.2
	100	0.5	0.13	17	36	5.1
	100	1.5	0.17	18	46	4.5

* The MFI of pure HDPE is 5.2 g/10 mm

Table (2.4) The comparison of conversions for the three monomers in melt grafting

The amount of monomer added (wt %)	The conversion of monomer (wt.%)		
	Maleic anhydride	Glycidyl methacrylate	2 isopropenyl-2 oxazoline
2	98	89	55
4	56	82	40
6	48	67	36
8	43	41	28

Temperature 180°C Processing time 20 min

Table (2 5) The influence of temperature and initiator concentration on the melt grafting reaction. Monomer ratio 2% Time 20 min RPM 70

Monomers	Temperature (°C)	Initiator (wt%)	GR (wt.%)	GE (%)	Conversion (wt.%)	MFI * (g/10 min)
Maleic anhydride	160	1	1 42	100	71	3 2
	160	0 5	0 92	100	46	3 4
	180	0 5	1 21	100	61	2 8
	180	1 5	1 95	100	98	1 9
Glycidyl methacrylate	160	1	1 17	71	82	3 3
	160	0 5	0 64	53	62	3 5
	180	0 5	0 81	64	63	2.7
	180	1 5	1 46	86	89	2.1
2 isopropenyl-2-oxazoline	150	1	0.32	37	44	3 5
	150	0.5	0 23	30	38	3 7
	170	0 5	0.31	34	45	3 3
	170	1 5	0 42	39	54	2.6

* The MFI of pure HDPE is 5.2 g/10 min.

Table (2.6) The influence of temperature and initiator concentration on the solution grafting reaction. Monomer ratio 2% Time 2 hr RPM 100

Monomers	Temperature (°C)	Initiator concentration (wt.%)	GR (wt.%)	GE (%)	MFI* (g/10 min)
Maleic anhydride	130	1	1.74	100	4.2
	130	0.5	1.65	-	4.4
	160	0.5	1.86	-	3.8
	160	1.5	1.88		3.1
Glycidyl methacrylate	130	1	1.54	77	4.4
	130	0.5	1.36	68	3.6
	160	0.5	1.48	74	3.5
	160	1.5	1.53	76	3.4
2 isopropenyl 2-oxazoline	130	1	1.51	75	4.6
	130	0.5	1.42	71	4.6
	160	0.5	1.48	74	4.1
	160	1.5	1.57	79	3.8

* The MFI of pure HDPE is 5.2 g/10 min

CHAPTER 3
THE REACTIVITIES STUDY OF GMA AND OXAZOLINE GRAFTED POLYOLEFIN IN THE MELT

3.1 Introduction

Chapter 2 illustrated the feasibility of grafting several monomers including maleic anhydride (MA), glycidyl methacrylate (GMA), and 2 isopropenyl 2-oxazoline (IPOZ), onto polyethylene by the solid-state, melt, solution grafting. As mentioned in Chapter 1, MA grafted polyolefin can only react with polymers with basic end groups like nylons, which have amine end groups. This restricts the applications of MA grafted polyolefin in polymers compatibilization. However, unlike MA grafted polymers, GMA and oxazoline grafted polymers can react very efficiently with both acidic and basic groups (carboxylic, hydroxyl groups, or amine groups) through nucleophilic ring-opening reactions, which makes them versatile precursors of compatibilizers.

As we know, the success of *in situ* reactive compatibilization can be determined by the optimization of interfacial reactions. Numerous publications have confirmed that the reaction speed of the interfacial reaction is very critical to the compatibilization. Normally, fast and efficient reactions can generate enough compatibilizer during the short melt processing, and achieve binary or multi phase compatibilization through strong interfacial adhesion. As a result, determining the most reactive functional polymers to maximize the compatibilization efficiency is very crucial to achieve successful compatibilization. In this

study, the reactivities of GMA and oxazoline grafted polyolefins with other nucleophilic groups including amine, carboxylic, secondary amine, and hydroxyl group, in the melt are investigated. The reasons for the reactivity study are:

1. Many polyesters (for example, PET, PBT, liquid crystalline polymers) have reactive carboxylic and hydroxyl end groups. If the grafted polyolefins are used in the compatibilization of polyester/polyolefin blends, the reactivity between grafted groups and the end groups of polyesters could have a direct influence on the compatibilization.

2. The nylon family can have amine reactive end groups. For the applications of the grafted polyolefin in the compatibilization of nylon/polyolefin blends, it is desirable to study the reactivities of these grafted groups with primary amine and secondary amine in order to know the extent of the reaction on the interface.

The mechanisms of these interfacial reactions are listed in Figure (3-1). For epoxy and oxazoline grafted polyolefin, the reaction mechanisms are quite similar. Both are ring-opening reactions which means their electrophilicities, hindrance factors, and the nucleophilicities of attacking groups should determine their reactivities. Based on the consideration of electrophilicity, both epoxy and oxazoline groups can react with secondary nucleophilic groups like secondary amine or hydroxyl generated in the first reaction (as shown in Figure (3-1)). As a result, one primary amine or carboxylic acid group might consume up to two epoxy or oxazoline groups. In this study, the reactivities of epoxy and oxazoline grafted polyolefin will be studied quantitatively without any discrimination of the first or secondary reaction.

Three small difunctional molecules (diacid, diol and diamine) are used as model compounds for polyester or nylon. There are two major reasons for using small difunctional

molecules First the concentration of these functional groups is easy to accurately control Secondly, since these difunctional small molecules can function as crosslinking agents for the epoxy or oxazoline grafted polyolefin the intensity of the reaction can be gauged by the torque value measurement or crosslinking density measurement by solvent extraction.

3.2 Experiment

3.2.1 Materials

1 10-Decanediol ($HOCH(CH_2)_{10}CHOH$) CORFREE ($HO_2C(CH_2)_{10}CO_2H$), 1,12 Diaminododecane ($H_2N(CH_2)_{12}NH_2$), glycidyl methacrylate(GMA) were bought from Aldrich Chemical Company GMA and IPOZ grafted HDPE were home made by solution grafting as illustrated in Chapter 2 with graft ratios at 1 4% and 1 2%, respectively

3.2.2 Procedures

The torque measurements were carried out by using a Brabender measuring head driven by Brabender plasti corder pl2000 The temperature of measuring head was kept at 180°C and 150°C for the crosslinking of GMA and IPOZ grafted HDPE, respectively The roller blades were rotated at 60 rpm. The torque data was acquired by computer interface. The difunctional small molecules were mixed with grafted HDPE in certain molar ratio before being put into the measuring head. FTIR detecting was conducted by Magna IR spectrometer 450 The sample film was prepared by taking melt after determined time of melt mixing and compression molding instantly into transparent film. The melt flow index (MFI) of the crosslinked polymers were measured according to ASTM D 1238, using Tinius Olsen

extrusion plastometer after the crosslinked HDPE was purified by washing the polymer in the form of a fine powder with boiling methanol. The gel amount was determined after the crosslinked polymers were Soxhlet solvent extracted by hot toluene for 2 days and vacuum dried the left gel. Thermal properties of crosslinked grafted HDPE were carried out in Solomat DSC 4000. The crystallization temperature (T_c) and melting temperature (T_m) were obtained with rising temperature at 10°C/min and cooling temperature rate at 40°C/min. The thermal history was deleted by heating the sample to 180°C then cooled down to 40°C, then reheated.

3.3 Results and Analysis

3.3.1 The Grafting of HDPE with GMA and IPOZ.

The detail of the solution grafting have been discussed in Chapter 2. Table (3-1) summarizes information about the GMA and IPOZ grafted HDPE used in this study. The graft ratios listed in Table (3-1) were obtained from FTIR analysis of solvent extracted grafted polyolefin. The calibration curves were obtained by comparing the ratio of the absorbance of the characteristic absorption peak of carbonyl of GMA (1753 cm^{-1}), or the oxazoline ring absorption of IPOZ (1637 cm^{-1}) to the methyl group of HDPE (1376 cm^{-1}) as illustrated in Chapter 2.

Both of the two grafted HDPE have higher T_m and T_c than unmodified HDPE due to the presence of a small amount of crosslinking initiated by the peroxide used during the grafting. The crosslink restricts the chain mobility of grafted HDPE, and makes them can only be molten at the higher temperature. In addition, a crosslinks can act as a local defects [10]

and lead to the reduction in crystallinity which is demonstrated by the decreasing of ΔH_c for both the grafted HDPE. The presence of crosslink is also confirmed by the lower MFI values of grafted HDPE than the unmodified HDPE.

3.3.2 The Reactivities of Carboxylic acid (-COOH), Amine ($-NH_2$), Secondary amine (-NRH), and Hydroxyl Groups (-OH) with GMA Grafted HDPE (HDPE-g-epoxy).

It is well known that the epoxy group is very reactive with amine or carboxylic acid group, this is why diamine or anhydride are usually used as crosslinking agents for the epoxy resin. The crosslinking can even be carried out at room temperature. The hydroxyl group can also react with the epoxy group, but the reactivity should not be as strong as the former's because of its relatively low nucleophilicity. However, under high temperature (above T_m of HDPE), the reactivity between epoxy and hydroxyl could be much higher.

Table (3-2) lists all of the reactive groups involved in the reactivity study. Products 1 to 4 are assigned to represent the crosslinked GMA grafted HDPE (HDPE-g-epoxy) by hydroxyl, secondary amine, primary amine, and carboxylic acid groups, respectively. Figure (3-2) is the FTIR spectra of products 1 through 4 after 5 mins' melt blending at 180°C in the Brabender measuring head. The absorption peaks at 911 cm^{-1} and 848 cm^{-1} are the characteristic peaks of epoxy group. After 5 min reaction with different kinds of same molar reactive small molecules, the intensity of epoxy characteristic peaks decreases noticeably for -OH and -NRH groups, while almost completely disappears for -COOH and $-NH_2$ group. It can be concluded that all of these four groups can react with epoxy groups under these conditions, and the disappearance of epoxy peaks indicates that the epoxy groups are completely consumed by -COOH or $-NH_2$ groups. Based on the decreased ratios of the peak

heights of epoxy to the internal reference (1467 cm^{-1}) (Table (3-3)) the approximate reactivity sequence of these four groups with the HDPE-g-epoxy is $-NH_2$ >-COOH >-NRH> -OH However, it is difficult to see the difference in reactivities between $-NH_2$ and -COOH by simply comparing the peak heights

Figure (3 3) is the FTIR spectra of mixtures with mixing ratio ((mole number of functional groups)/(mole number of epoxy)) at 0.5, and the mixing temperature of 150°C Both values are lower than in the former experiment Surprisingly for $-NH_2$ and -COOH group, the epoxy peaks still disappears although the molar ratio is less than 1 On the other hand, for the -OH and -NRH groups, the difference of the intensity of epoxy peaks for products 1 and 2 becomes obvious It appears that -NRH reacts with epoxy group more efficiently than -OH at the lower temperature The reactivities of $-NH_2$ and -COOH with epoxy group do not seem to be affected by the mixing temperature, also, one mole of $-NH_2$ or -COOH can effectively consume up to 2 mole of epoxy group The high efficiency of epoxy consumption by these two groups might be due to the secondary reaction as shown in Figure (3-1). After the first reactions the produced secondary amine or hydroxyl group still has certain reactivity with epoxy group, and the new generated groups keep on consuming the epoxy groups afterwards

Figure (3-4) shows the torque-time relationships for the reactions of HDPE-g-epoxy with diacid, diamine (primary and secondary), and diol. In the case of noncrosslinked HDPE-g epoxy the torque first increases quickly as the cold material is fed to the mixer As the material is heated by shear and conduction, it softens and the torque falls. The torque then levels off to a nearly constant value for the remainder of the mixing time In the cases of -NRH and -OH, after the mixer is molten, the torque values initially decrease then increase

at certain rate until a constant level is reached However, for these two groups the final torque values and the time needed to achieve there (t1) are different. This indicates that their reaction speed and reaction extent are different It seems that -NRH has a higher reaction speed and extent than -OH. In the cases of -NH_2 and -COOH, the torque continues to rise without dropping after the feeding is completed. This is caused by the extensive crosslinking reaction, which increases the molecular weights of the polymers dramatically in a very short time The torque value increase to a final constant value, which is much higher than values observed for the uncrosslinked HDPE g-epoxy or other two crosslinked HDPE g-epoxy sample. Also, the high reactivities of these two groups are demonstrated by shorter torque increasing time (t1) than those of the other two groups Based on the above torque measurement analysis, it can be concluded that the reactivity sequences of these four groups is NH_2, COOH > NRH > OH For -NH_2 and -COOH crosslinked HDPE they reach similar final torque values with different rates NH_2 crosslinked HDPE can reach the final torque value within 3 min, while -COOH crosslinked HDPE keeps a constantly increasing torque value until 7 min of mixing However, this does not mean the reactivity of amine with HDPE-g epoxy is higher than carboxylic acid because the secondary reaction between the new generated hydroxyl or secondary amine with epoxy must have participated in the crosslinking The delay of increasing of torque values for -COOH may be due to the lower reactivity of -OH group in the second reaction than that of -NRH (secondary amine) As a result, if we define the reactivity of primary amine or carboxylic acid based on the combination of first and secondary reactions, obviously, primary amine has higher reactivity than carboxylic acid with HDPE-g-epoxy However, if the reactivity is defined based on the first reaction, the relative reactivities of these two groups with epoxy group are still not clear

The increase of molecular weight of HDPE caused by the crosslinking can also be observed by a decrease in the melt flow index or by a increased amount of the crosslinked HDPE gel after solvent extraction. Table (3-4) shows that the products from the reactions of -COOH and $-NH_2$ with HDPE-g-epoxy (product 4 and 3) have MFI values much lower than those of -OH, and -NRH crosslinked HDPE (product 1 and 2). On the other hand, the gel amount of products 3 and 4 are much higher than those of product 1 and 2. This confirms that the increased molecular weight resulting from crosslinking of HDPE-g-epoxy by $-NH_2$ and -COOH are much higher than those by -OH and -NRH. From the point view of MFI and gel amount values, the extent of crosslinking of HDPE-g-epoxy increases in this order: -COOH, $-NH_2$ > -NRH, -OH. This is in agreement with the observation of the FTIR and torque-time profile as illustrated before.

Thermal properties such as crystallization temperature (T_c) and crystallinity of the HDPE-g-epoxy are expected to change after crosslinking with these four reactive groups. In this study, differential scanning calorimetry (DSC) is used for the thermal analysis of the crosslinked HDPE. The thermograms of pure grafted HDPE and crosslinked HDPE are shown in Figure (3-5) and the T_c and ΔH_c values are listed in Table (3-5). The crosslink caused by hydroxyl and secondary amine groups (product 1 and product 2) have certain effects on the crystallinity without any obvious shift of T_c to lower temperature. The constancy of T_c suggests no reduction in the crystallite size, while the decreasing of ΔH_c indicates the crystallinity of the samples is reduced after crosslinking since crosslinks act as local defects [61]. For primary amine and carboxylic acid (product 3 and 4), the effect of forming crosslinks on the crystallization behavior of grafted HDPE are more obvious; both T_c and ΔH_c are depressed dramatically in contrast to the pure HDPE-g-epoxy or other two

products. In this case, there is some differences of crystallization behavior for products 3 and 4. The T_c of product 3 (primary amine crosslinked HDPE) is lower than that of product 4 (carboxylic acid crosslinked HDPE), and the crystallinity of product 3 is higher than that of product 4. However, it is still difficult to judge the relative reactivity of primary amine and carboxylic acid group based on the overall consideration of T_c and ΔH_c.

Based on the T_c and ΔH_c comparison in Table (3-5), the reactivity sequence of these four groups is approximately NH_2, -COOH > -NRH > -OH, which is in agreement with the result from FTIR , MFI and torque measurement.

3.3.3 The Reactivity Carboxylic Acid (-COOH), Amine ($-NH_2$), Secondary Amine (-NRH) and Hydroxyl Groups (-OH) with Oxazoline Grafted HDPE (HDPE-g-oxazoline)

The reaction mechanisms of oxazoline with these four groups are shown in Figure (3-1). Similar to the reaction mechanism of epoxy, they are the ring opening reactions with the formation of an amide group. Based on this reaction mechanism, the consumption of an oxazoline ring and formation of an amide group after reaction could be detected by FTIR spectra by monitoring the characteristic peak of oxazoline ring (1658 cm^{-1}) and amide group (1668 cm^{-1}). Figure (3-6) shows the FTIR spectra of the reaction products of oxazoline grafted HDPE with these four reactive groups and the spectrum of the pure HDPE-g-oxazoline. In -NRH case, the generated amide group has very weak absorption (Figure (3-6)), but it becomes more and more obvious along with the sequence of -NRH< -OH <$-NH_2$ and -COOH. For -COOH case, the amide absorption peak is so strong that the absorption of the original oxazoline ring is overlapped. It seems that the reactivity of -COOH with HDPE-g-oxazoline is much stronger than with the other three groups. By observation, the final hot

reacting mixture of HDPE-g-oxazoline/diacid became a brown powder after 12 min of mixing indicating extremely high crosslinking density The high reactivity of -COOH with oxazoline group has been well known for a long time Its typical application of this is using bisoxazolines as chain extenders for polyesters such as PET and PBT by reaction with their carboxylic acid end groups [62] Unfortunately, the reactivity between NH_2 and oxazoline has not been well studied although it has been recently used in the compatibilization of oxazoline grafted poly(styrene-co acrylonitrile) (SAN)/nylon 6 blends [63] Based on the FTIR spectra in this study, the reactivity of amine with HDPE g oxazoline is relatively lower than carboxylic acid The further evidence for this difference in reactivities is shown in the torque measurements illustrated later Few publications have reported the different reactivities of amine and carboxylic acid groups with oxazoline group Fradet [64] in his recent publication, studied the reactivity of oxazolones, which have quite similar structure with oxazoline, with amine and carboxylic acid He concluded that both groups can react very efficiently with oxazolone group and the reaction can even be carried out at room temperature within 10 min of reaction time. No obvious difference in reactivity for these two groups with oxazolone were observed in Fradet s study In the case of oxazoline, the electrophilicity of oxazoline is much lower than oxazolone, the reaction between oxazoline and -COOH and NH_2 group could only be completed in the high temperature according to our observation As a result it is quite possible that the difference of reactivities for these two groups would show up No further investigation has been carried out aiming to the explaining of this reactivity difference, and till now still no clear explanation for that based on nucleophilicity of amine or carboxylic and electrophilicity of oxazoline. Solely according to the FTIR results the approximate reactivity sequences is -COOH >> NH_2 > -OH > -NRH

Figure (3-7) shows the torque-time relationships for the crosslinking of HDPE-g-oxazoline by these four reactive groups. Both -NRH and -OH group can form a certain amount of crosslink with oxazoline, but the final torque values are not much higher than that of pure HDPE-g-oxazoline, which indicates the low activities of these two groups with oxazoline. Compared with -NRH crosslinked HDPE (product 2'), -OH group seems to be more reactive based on the higher final torque of crosslinked HDPE (product 1'). This result is in agreement with the results of FTIR. The high reactivity of oxazoline with -COOH group is also confirmed by the extremely high final torque value of product 3'. The torque value keeps increasing until 9 min of mixing. As a comparison, the final torque values of -NH_2 are much lower than that of -COOH, but higher than those of -OH and -NRH. Interestingly, -COOH group can achieve complete crosslinking with higher final torques but in a longer period of time than -NH_2 group. This could be attributed to the secondary reaction as shown in Figure (3-1). Since -COOH has higher reactivity with oxazoline, the high reaction probability generates a large amount of amino structure, which still has certain reactivity with oxazoline. The high concentration of amino group keeps reacting with oxazoline within a certain long period of time because of its low reactivity. For the amine, although amino groups are generated, the relative low reactivity of it makes the concentration of formed amino group low, which results in shorter t1 and lower torque increasing rate.

Similar to the reactivity study of epoxy, the molecular weight increase of the crosslinked products is confirmed by a decrease in the MFI or by a increase of gel amount after solvent extraction (Table (3-6)). For diacid crosslinked HDPE (product 4'), the crosslinking density is so high that it could not be molten in MFI measurement. For product 3', although it shows much less gel amount and high MFI than product 4', its crosslinking

density is much higher than diol and secondary diamine crosslinked HDPE (product 2 and product 1')

Overall, the reactivity sequences from the study of MFI and torque measurements is -COOH > $-NH_2$ > -NRH OH which still fits well with the results from FTIR

Figure (3-8) is the DSC measurement of the four crosslinked HDPE along with the pure HDPE-g-oxazoline T_c and ΔH_c values are listed in Table (3-7) It is interesting that the crosslinking caused by secondary amine group has no direct effect on the crystallinity but shift T_c to higher temperature. In general, crosslinks act as local defects and reduce the total crystallinity However, it was reported that a few crosslinks often improve the packing of polymer chains into a crystalline structure since they properly restrict the flow of melt [65] The behavior described above could be attributed to that. Diol crosslinked HDPE has both low ΔH_c and T_c which means the reactivity of OH with HDPE-g-oxazoline is higher than -NRH The differences of thermal properties of the product 3' (amine crosslinked HDPE) and product 4 (carboxylic acid crosslinked HDPE) are very obvious in this case The higher reactivity of COOH with HDPE g oxazoline makes the crystallinity and T_c of product 4' much lower than those of product 3 As a conclusion, the reactivity consequence for the four groups based on DSC study is -COOH > $-NH_2$ > -OH > -NRH which fits well with the sequences got from other detectings.

3.3.4 The Reactivities of Epoxy Grafted HDPE (HDPE-g-epoxy) and Oxazoline Grafted HDPE (HDPE-g-oxazoline) with Carboxylic Acid (-COOH), Amine (NH_2), Secondary Amine (-NRH), or Hydroxyl (-OH) Groups

Since the two grafted HDPE used in this study have similar graft ratios (1.2% 1.4%) and other physical properties (ΔH_c, T_c and crosslinking density) the reactivity of HDPE-g

oxazoline and HDPE-g-epoxy with carboxylic amine, and hydroxyl groups could be studied transversely Based on the two sets of data, (Figure (3-4) and (3-7) Table (3-4) and (3-6)) HDPE-g oxazoline seems to be as reactive as HDPE-g-epoxy with -COOH group, while HDPE-g-epoxy is definitely more reactive than HDPE-g-oxazoline with -NH_2 group For NRH groups, HDPE-g-epoxy has higher reactivity with it than HDPE-g-oxazoline, while for OH groups their reactivities are quite similar

This information is very important in helping to choose proper functional polymers for the compatibilization of polymer blends. Currently, many of the reactive compatibilizations are based on the interfacial reaction between the polymer end groups and functional polymers with either oxazoline or epoxy reactive groups According to our previous study in Chapter 2, oxazoline functionalized polymer could only be synthesized by solution grafting or solution copolymerization process which are usually much more costly than epoxy functionalized polymer synthesized by melt grafting as will be illustrated in Chapter 4 Based on both economics and reactivity consideration epoxy grafted polyolefin should be the better choice for the compatibilization

3. 4 Conclusions

In this part of study the reactivities of epoxy and oxazoline grafted HDPE with amine, carboxylic acid, secondary amine and hydroxyl groups in the melt were studied The following conclusions are drawn

1 Epoxy and oxazoline grafted HDPE have certain reactivity with both acidic (carboxylic and hydroxyl groups) and basic groups (primary amine and secondary amine groups)

2. Based on the FTIR, MFI and DSC studies of small molecule model, the reactivity sequence of the functional groups with HDPE-g-epoxy is NH_2, -COOH > NRH > OH. There is still no enough evidence to show the reactivity difference between primary amine and carboxylic acid

3. By using the same characterization techniques, the reactivity sequence of the functional groups with HDPE g-oxazoline was found to be -COOH >> NH_2 > -OH > NRH. Oxazoline is far more reactive with carboxylic acid than with primary amine in this case

4. The reactivity sequence of HDPE-g-epoxy and HDPE g-oxazoline with carboxylic acid group is: HDPE-g-epoxy = HDPE-g-oxazoline. With primary amine group is, HDPE-g epoxy >> HDPE-g-oxazoline. With secondary amine group is: HDPE-g-epoxy > HDPE-g oxazoline. With hydroxyl group is: HDPE g-epoxy = HDPE-g-oxazoline

5. Due to the close overall reactivities of HDPE-g-epoxy and HDPE g-oxazoline and the difficulties of synthesizing HDPE g oxazoline, epoxy grafted polyolefin should be the better choice for the applications in polymers compatibilization

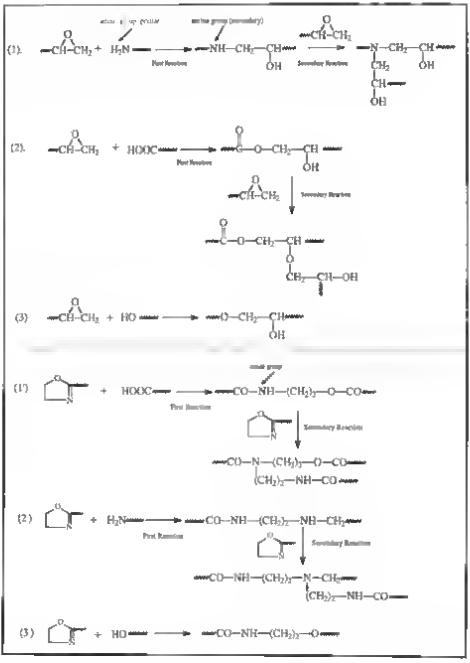

Figure (3-1) The reactions mechanisms of GMA or oxazoline grafted polyolefins with amine, hydroxyl, and carboxylic acid groups.

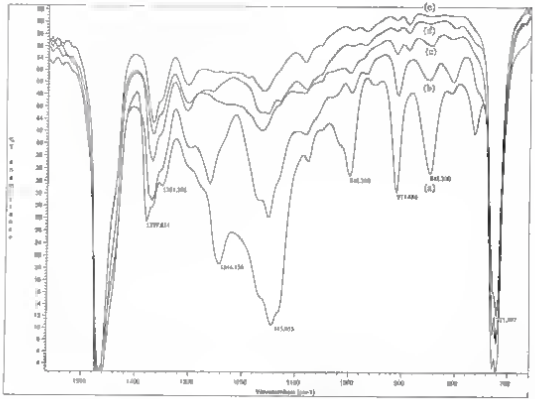

Figure (3.2) FTIR spectra of HDPE g-epoxy crosslinked by various difunctional molecules for 5 min at 180°C ((mole number of functional groups)/(mole number of epoxy group)) = 1
(a) Pure HDPE g-epoxy (graft ratio = 1.2%) (b) Diol crosslinked HDPE-g-epoxy; (c) Diamine (secondary) crosslinked HDPE g-epoxy (d) Diacid crosslinked HDPE g-epoxy (e) Diamine (primary) crosslinked HDPE-g epoxy

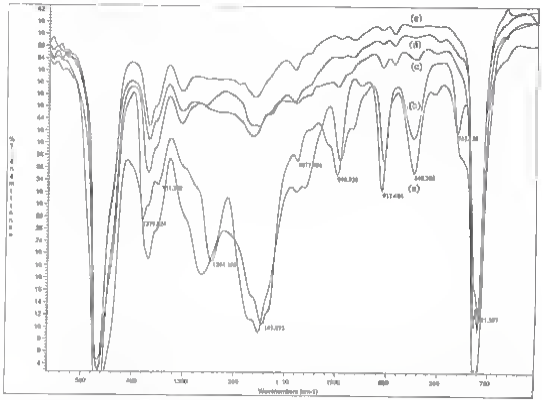

Figure (3-3) FTIR spectra of HDPE-g-epoxy crosslinked by various difunctional molecules for 5 min at 150°C; ((mole number of functional group)/(mole number of epoxy group)) = 0.5
(a) Pure HDPE-g-epoxy (graft ratio = 1.2%) (b) Diol crosslinked HDPE-g-epoxy; (c) Diamine (secondary) crosslinked HDPE-g-epoxy, (d) Diacid crosslinked HDPE-g-epoxy; (e) Diamine (primary) crosslinked HDPE-g-epoxy

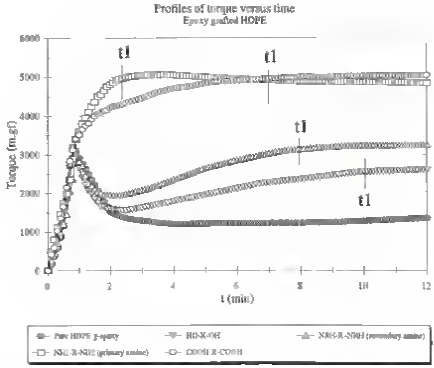

Figure (3-4) Profiles of torque vs. time during the crosslinkang of HDPE-g epoxy t1 represents the time when the constant torque values are reached

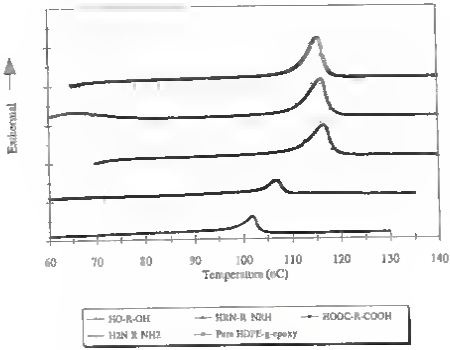

Figure (3 5) DSC spectra of the crosslinked HDPE g-epoxy

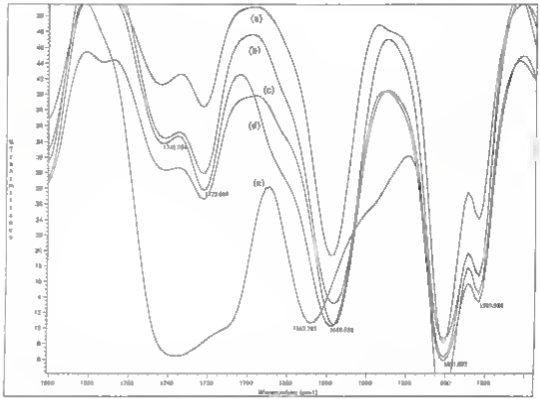

Figure (3 6) FTIR spectra of HDPE-g-oxazoline crosslinked by various difunctional molecules for 5 min at 180°C, ((mole number of functional groups)/(mole number of oxazoline)) = 1 (a) Pure HDPE-g-oxazoline, (b) Diamine (secondary) crosslinked HDPE g-oxazoline, (c) Diol crosslinked HDPE-g-oxazoline (d) Diamine (primary) crosslinked HDPE-g-oxazoline, (e) Diacid crosslinked HDPE-g oxazoline

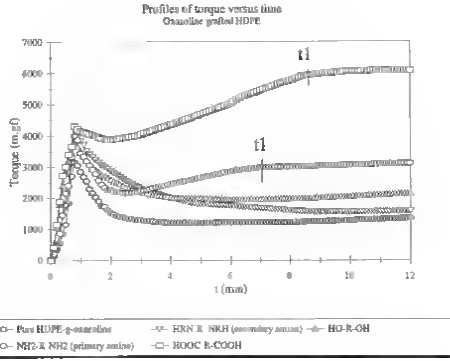

Figure (3-7) Profiles of torque versus time during the crosslinking of HDPE-g-oxazoline

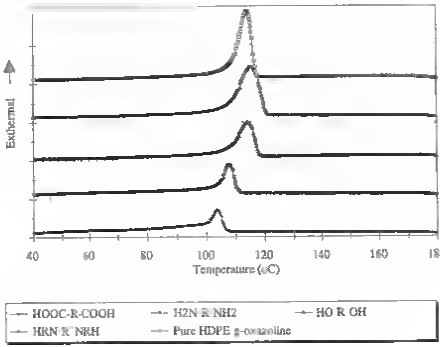

Figure (3 8) DSC spectra of the crosslinked HDPE g-oxazoline

Table (3-1) The comparisons of grafted HDPE with pure HDPE

Comparisons	Unmodified HDPE	HDPE-g-oxazoline	HDPE g-epoxy
Graft ratio (%)	0	1 2	1 4
T_c (°C)	111 4	114 3	116 2
T_m (°C)	136 8	137 2	138 6
ΔH_c (kJ/kg)	195 6	186,5	185 1
MFI (g/10 min)	5.2	4 6	3 6

Table (3-2) The reaction groups of the crosslinking of grafted HDPE

Functional HDPE			Difunctional small molecules	
Run No	Name	Reactive group 1	Name	Reactive group 2
Product 1	HDPE-g-epoxy	epoxy	diol	-OH
Product 2	"	"	diamine (secondary)	NRH
Product 3	"	"	diamine (primary)	$-NH_2$
Product 4	"	"	diacid	-COOH
Product 1	HDPE g-oxazoline	oxazoline	diol	-OH
Product 2	"	"	diamine (secondary)	NRH
Product 3	"	"	diamine (primary)	NH_2
Product 4	"	"	diacid	-COOH

Table (3-3) The peak height ratios of the absorption peaks undergoing changes due to the reaction of grafted HDPE with diols (product 1), diamine (secondary) (product 2), diacid (product 3) and diamine (primary) (product 4), relative to the internal reference absorption of PE backbone at 1467 cm^{-1}

Ratios of Absorption Peaks (911 cm^{-1}/1467 cm^{-1}) and (848 cm^{-1}/1467 cm^{-1})				
180°C 5min mole ratio 1			150°C, 5min mole ratio 0.5	
Pure HDPE g-epoxy	0.37	0.28	0.37	0.28
Product 1	0.14	0.07	0.25	0.20
Product 2	0.04	0.03	0.05	0.04
Product 3	0.01	0	0.01	0
Product 4	0.01	0	0.01	0

Table (3-4) Melt flow indices (MFI) and gel amount of the crosslinked HDPE-g-epoxy

Sample	MFI (g/10 mn)	Gel Amount (%)
Pure HDPE-g-epoxy	3 6	0 24
Product 1	1 8	12
Product 2	1 6	16
Product 3	0	38
Product 4	0	31

Table (3 5) DSC results for the crosslinked HDPE-g-epoxy

Sample	T_c (°C)	ΔH_c(kJ/kg)
Pure HDPE-g-epoxy	116 2	185 1
Product 1	116 6	181 2
Product 2	116 8	164 3
Product 3	107.3	46.7
Product 4	102.5	52.1

Table (3-6) Melt flow indices (MFI) and gel amount of the crosslinked HDPE-g-oxazoline

Sample	MFI (g/10 min)	Gel Amount (%)
Pure HDPE-g-oxazoline	4.6	0.18
Product 1	2.9	2.2
Product 2	3.2	1.6
Product 3	0.8	21.3
Product 4'	0	42.5

Table (3 7) DSC results for the crosslinked HDPE g-oxazoline

Sample	T_c (°C)	ΔH_c (kJ/kg)
Pure HDPE-g-epoxy	114 3	185 1
Product 1	116 8	143 2
Product 2	114 2	170 6
Product 3	108 3	84 7
Product 4	104 8	68 6

CHAPTER 4
THE MELT GRAFTING OF LLDPE, HDPE, AND PP BY GMA MONOMER IN REACTIVE TWIN SCREW EXTRUDER

4.1 Introduction

Chapter 2 reports that polyolefins can be grafted with maleic anhydride (MA), glycidyl methacrylate (GMA) and 2-isopropenyl-2-oxazoline (IPOZ) monomers by solid-state, melt, and solution grafting techniques. Based on the comparison of these three grafting methods, it was concluded that melt grafting has the advantages of short processing time, relatively high graft ratio (GR) and graft efficiency (GE). Chapter 3 compares the reactivities of GMA and IPOZ grafted HDPE and concluded that epoxy group has equal or higher reactivity than oxazoline group with most of acidic and basic groups. In this chapter, reactive twin-screw extrusion is employed to carry out the melt grafting of polypropylene (PP), low density linear polyethylene (LLDPE), and high density polyethylene (HDPE) with GMA monomer. There are several advantages for applying twin screw extrusion in melt grafting. First, it is a continuous process which could have high output; secondly, it has a higher shear rate than the batch mixer which could provide better dispersion of monomer and peroxide, a higher graft ratio, and improved graft efficiency. The melt grafting of PP by MA with twin-screw extrusion has been extensively reported [67-72], however few publication over grafting polyolefins with GMA in twin screw extruder. Although in the study of Chapter 2, some initial results were drawn about the melt grafting of HDPE by GMA and other two monomers

in a batch mixer. The melt grafting during twin-screw extrusion would be much more complicated and the study of this chapter will not be solely based on the results from Chapter 2. In this part of study, the effects of reaction temperature, screw speed, initiator concentration, and the amount of GMA on the percentage of grafting are studied in detail. The influence of the grafting procedures on gel content, the upgrading of graft ratio by comonomer technique are also investigated.

4.2 Experiment

4.2.1 Materials

The materials used in this part of study are listed in Table (4-1) below.

Table (4-1) The materials used in this study

Type of Materials	Materials	Properties	Manufacturers
Polymers	LLDPE (Escorene LL5103)	MFI 12g/10 min Mw 58,000	Exxon Chemical
	HDPE (PLS H6003)	MFI 5.2g/10 min	Eastman Chemical
	PP (Tenite)	MFI 2.6g/10 min	Eastman Chemical
Monomer	GMA	Boiling point 189°C	Dow Plastics
Initiators	dicumyl peroxide (DCP)	0.1 h t1/2 (half life) temperature 155°C	Witco Corporation
	2,5-dimethyl-2,5-di(t-butylperoxy)hexane (DDPH)	159°C	Akzo Chemie Co.
	di-t-butyl peroxide (DB)	162°C	Akzo Chemie Co.
	2,2'-azobis (isobutyronitrile) (AIBN)	148°C	Aldrich Chemical Co.

The selection of initiators is based on the requirement that the half-life of the initiator

needed for melt grafting should correspond to the residence time of the extrudates.

4.2.2 Grafting

The grafting of all three polymers was carried out in the same Brabender batch mixer used in Chapter 2 or in an APV reactive twin-screw extruder with L/D = 39 (as shown in Figure (4-1)). The polymers were fed at 80 to 120 g/min into the hopper. The monomer/peroxide solution was injected into the twin-screw extruder from the injection nozzle via a liquid pump.

The grafting reaction study of section 4.3.2 is completed in a Brabender batch mixer used in the study of Chapter 2. The RPM was kept at 80, temperature was 180°C, reaction time was 20 mins.

The grafting in the study of Section 4.3.3 is completed in the APV reactive twin-screw extruder. The operation parameters are listed below:

The polymer/monomer/peroxide weight ratio: 100/6/0.6.

RPM of screw rotation: 100, Temperature: 180°C.

Residence time (measured by dye detecting method): 1.5 min.

The grafting in the study of Section 4.3.4 is completed in the same reactive twin-screw extruder. The operation parameters are listed below:

The monomer/peroxide weight ratio: 7/1.5 to 6/0.6.

The monomer/peroxide pumping rate: 2.8 g/min to 6.0 g/min.

RPM of screw rotation: 100 to 200.

Temperature: 180°C to 220°C.

Residence time (measured by dye detecting method): 1.0 to 3.5 min.

4.2.3 Analysis

In order to evaluate the peroxide induced crosslinking density of polymer, the gel content was determined by placing the crude sample in Soxhlet extractor for 24 h with refluxing toluene. The dissolved grafted polymer was then precipitated in methanol and dried under reduced pressure at 50°C for 24 h. The content of carbon, hydrogen, and oxygen in the dried polymer were analyzed by an elemental analyzer. The content of oxygen could be related to the amount of GMA grafted. FTIR spectra was obtained to detect the graft ratios as illustrated in Chapter 2 and 3 and Appendix B.

4.3 Results and Analysis

4.3.1 FTIR Calibration Curves for the Detection of Graft Ratio

The FTIR spectra of the purified grafted LLDPE, HDPE, and PP are shown in Figure (4-3). The characteristic peaks are indicated. The absorption peaks at 1731.5 cm^{-1} (carbonyl characteristic peak) clearly demonstrates the presence of the grafted GMA structure on the backbones of these three polyolefins. The percentage of grafting is estimated by comparing the absorbance of the carbonyl group of the grafted GMA to the methyl group of PE or PP (1376 cm^{-1}). The absolute percentage of grafting can be determined by oxygen analysis. Combining the results of element analysis and FTIR absorbance ratio constructs the calibration curves shown in Figure (4-2).

4.3.2 The Comparison of Initiators

As illustrated before, the major function of initiator is abstracting hydrogen atoms from the backbone of polyolefin and form macroradicals which can let monomers graft on. A different initiator has a different hydrogen abstracting ability, as a result, it has a different effect on the final graft ratio (GR) of the grafted polyolefins. Table (4-2) lists the graft ratio (GR) and melt flow index (MFI) values for the three GMA grafted polyolefins by applying four different initiators: dicumyl peroxide (DCP), 2,5-dimethyl-2,5-di(t-butylperoxyl)hexane (DDPH), di-t-butyl peroxide (DB), and 2,2'-azobis (isobutyronitrile) (AIBN). With the exception of AIBN, which is a nitrile type of initiator, all of the other three are peroxided type initiators.

For LLDPE, all of the four listed initiators can graft monomer onto its backbone. The hydrogen abstraction by the initiators also generates some crosslinks which is indicated by the decreasing MFI values. In this case, DDPH and DCP can most effectively initiate the grafting with satisfactory graft ratio and medium crosslinking. Compared with DDPH and DCP, AIBN is relatively weak in hydrogen abstraction which is indicated by its low GR and high MFI. DB is not a strong initiator for grafting either, however, it generates the highest crosslinking density for some undetermined reasons.

Compared with the grafting of LLDPE, the grafting of HDPE seems more difficult to initiate. Both DCP and DB fail to initiate any grafting; only DDPH results in a graft ratio. However, all of the four initiators could generate crosslinks in HDPE although most could not bring any monomer onto the HDPE backbone.

The grafting of PP results in much higher MFI values compared with either LLDPE or HDPE. The high MFI values of the grafted PP indicates that all four initiators induce severe thermal degradation. Similar to HDPE, PP is very difficult to be grafted whose GR values are much lower than those of LLDPE. This similarity between HDPE and PP could be due to their high crystallinity, as we know most grafting is supposed to take place only in the amorphous phase.

In conclusion, both DCP and DDPH are useful in grafting GMA onto LLDPE, however, for HDPE and PP, DDPH is the only initiator to initiate grafting with satisfactory graft ratio. Among the four initiators, DDPH is the only effective initiator for the grafting of all three polyolefins. Unfortunately, the thermal degradation and crosslinking caused by DDPH is a potential problem for the GMA grafted polyolefins applied in the compatibilization of polymer blends. Further investigation is discussed later in this chapter and in Chapter 5.

4.3.3 The Different Types of Grafting Procedures

A usable grafting method requires initiators capable of abstracting hydrogen from the polyolefin to form reactive sites. Therefore, crosslinking and degradation - a decrease or increase of the melt index respectively -could also occur.

One way to reduce the crosslinking or degradation is to reduce the amount of initiator added. However, as illustrated in Chapter 2, less initiator generates less amount of macroradicals and consequently, results in lower graft ratio or graft efficiency. Obviously, decreasing the initiator content is not a ideal way to control crosslinking or degradation. An alternative way to suppress crosslinking and degradation while achieving a high graft ratio is to keep the overall feeding composition constant, but change the types of grafting procedure

in twin-screw extruder In this study, three kinds of processing procedures as shown in Figure (4-4) are tried.

The selection of proper processing procedures should be based on analyzing the grafting mechanisms. The mechanism for melt grafting is very complicated and still not quite clear Figure (4-5) lists all the possible reactions which could occur during the grafting reaction. Similar to the mechanisms analyzed in Chapter 2, first, the initiator decomposes and generates a primary $RO^{\bullet}$ radical which abstracts a hydrogen atom from the polymer chains (reaction (2)) The generated $P^{\bullet}$ macroradicals will either undergo crosslinking (for PE) or degradation (for PP) At the same time, the monomer can also be grafted onto the macroradicals and form the grafting structure. Besides these reactions another major reaction is homopolymerization of the GMA monomer The radical of the GMA homopolymer can also recouple with the grafted macroradical and extend the grafted chain As a result there are three major reactions taking place crosslinking (or degradation for PP), homopolymerization of monomer, and grafting

Whether these reactions take place in sequence or simultaneously is dependent on the grafting procedure For process 2 in Figure (4-4) the crosslinking density and degradation rate are considerably high for PE and PP respectively based on the MFI values shown in Table (4-3) This phenomena could be due to the premixing of polymer with peroxide which makes reaction (1) to (4) (Figure (4-5)) dominant before any monomer contacts with the radicals The favored crosslinking and degradation also consume most of the reactive sites on polymer backbone making it hard for the monomer to be grafted onto This could be the reason for the low graft rates of the three polymers processed by this procedure. For process 1 in Figure (4-4) the polymer is molten before contacting any peroxide therefore avoiding any

crosslinking or degradation during the melting. Once the molten polymer is mixed with peroxide and monomer, the $P^{\bullet}$ macroradical will be consumed by both monomer and radicals of monomer (reaction (5), (6) and (8)) which decrease the chances of crosslinking or degradation (reaction (3) and (4)). This may explain the high graft ratio of polymers processed by process 1. For process 3 in Figure (4-4), all of the possible reactions take place simultaneously (reaction (1) to (8)) and the crosslinking (or degradation) compete with grafting during the melting of the polyolefins. Thus, the degree of crosslinking, degradation and the graft ratio are between the process 1 and process 2. Based on above analysis, the process 1 should be the optimal procedure for the highest graft ratio and lowest degree of crosslinking or degradation.

4.3.5 The Influence of Extrusion Parameters and Compositions on the Graft Ratio (GR).

The data in Table (4-4) shows that a higher reaction temperature results in a higher graft ratio. This is attributed to the fact that the higher temperature can shorten the reaction time and the half life of initiator. A high initiator concentration during high temperature processing generates more reactive sites on polymer backbone, which also increases the graft ratio. However, similar to the batch mixer results illustrated in Chapter 2, the high processing temperature and peroxide concentration could result in a high degree of crosslinking and degradation as shown by the MFI values.

The influence of screw speed on the graft ratio is opposite to the influence of temperature. Although high shear rate could bring in better dispersity of monomer and initiator into the molten polymer, the residence time of reactants in the twin screw extruder shortens when the screw speed increases. This indicates that relatively lower screw speed will

provide longer grafting time resulting in higher graft ratio

4.3.6 The Effects of Comonomer

Although the graft ratio could be improved by employing proper grafting procedures and extrusion parameters, the grafted polymers still suffer from crosslinking or degradation, as shown in Table (4-3) and Table (4-4). Additional difficulty also arises from the competition between monomer grafting and homopolymerization (Figure (4-5) reaction 5 and 7), and the limited solubility of monomers in the polyolefin melts [73]. These detrimental factors could be attributed to the low graft ratios of the grafted polyolefins, especially polypropylene. However, if somehow the graft initiation step (reaction 5 in Figure (4-5)) could be accelerated and consume most of the P• crosslinking, degradation, and homopolymerization (reaction 3, 4, and 7 in Figure (4-5)) would be suppressed.

The comonomer technique was first proposed by *Hu et al.* [74] in the melt grafting of PP with maleic anhydride (MA). It was reported that the free radical reactivity of MA can be substantially enhanced and the degradation can be reduced by the addition of an electron-donating monomer such as styrene. Sun and Lambla [75] also used styrene as a comonomer for the grafting of MA onto PP and found that the graft ratio of MA could also be enhanced. They also reported that the extent of chain scission of PP is less severe as indicated by the increased molecular weight of the grafted materials upon the addition of styrene. The exact mechanism of this synergistic effect is, however, still unclear. It is the intent of the study of this section to examine how the graft ratios of GMA grafted LLDPE, HDPE, and PP are affected by the addition of styrene as a comonomer.

The effect of adding styrene as a comonomer for the grafting of GMA onto the three polymers is shown in Figure (4-6 a). The graft ratios for all three polymers are much higher in the presence of styrene. Based on overall considerations, the explanation for this phenomena might lie in three factors. First, it is believed that the polymer macroradical reacts preferentially with styrene monomer to form a more stable styryl macroradical, which then reacts with GMA in a chain propagation step. The higher reactivity of styrene towards the macroradical is primarily due to the conjugated double bond of styrene. Secondly, styrene and GMA may form a so called charge transfer complex (CTC) [74], which is believed to be more reactive than MA alone towards the PP macroradical. The CTC structure is shown below in Figure (4-7)

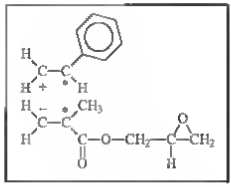

Figure (4-7) Charge transfer complex (CTC)

The third factor which might contribute to the improvement of the graft ratio is the higher solubility of polyolefins in styrene than in GMA. Solubility tests reveal that LLDPE, HDPE, and PP pellets dissolve readily in refluxing styrene while remaining insoluble in GMA at 140°C after 20 minutes. This enhanced solubility of polyolefins allows for more intimate mixing of the styrene monomer with the polyolefins thus creating an environment more

suitable for grafting. According to Dhal *et al* [76], the reactivity ratios of GMA and styrene are 0.78 and 0.29 respectively at 60°C. If graft initiation occurs with the addition of styrene, the propagation of grafting should occur preferentially with the addition of GMA, based on the reactivity ratios. As a result, the major grafted monomer is still GMA, although styrene is grafted first.

The addition of styrene monomer is supposed to serve another purpose: reducing the amount of crosslinking or degradation during grafting. Hu and Lambla [73] reported high molecular weights for MA grafted PP with the addition of styrene. It was explained that the PP macroradicals are consumed more rapidly by styrene in the comonomer system than by MA alone, so that the amount of chain scission is reduced. However, in this case, GMA is being used as the monomer instead of maleic anhydride, the depression of crosslinking or degradation is not so obvious as shown in Figure (4-6 b), where the MFI values of grafted polyolefins with or without styrene are about the same. This means the increasing rate of the grafting is not high enough to consume most of the macroradicals. There are still large amounts of macroradicals undergoing crosslinking or degradation. Conflicting with the published results of MA grafting study [74], this phenomena reveals that the thermal degradation and crosslinking of polyolefins during the melt grafting of GMA could not be effectively suppressed by comonomer technique.

4.4 Conclusions

In this part of the study, the melt grafting of LLDPE, HDPE, and PP with GMA monomer is carried out in a reactive twin screw extruder. Following conclusions are drawn.

1. Various kinds of initiators with proper half lifes are tried and compared. It is found

that 2,5-dimethyl-2,5-di(t-butylperoxy)hexane is the most effective initiator for the grafting of all three polyolefins although it also results in a certain amount of crosslinking for PE and degradation for PP respectively

2 Different types of grafting procedures are also studied Injecting monomer/peroxide into the molten polyolefins will result in high graft ratio and less crosslinking or degradation, while mixing peroxide with polyolefins first then monomer or mixing polyolefins with peroxide and monomer together before extrusion would result in lower graft ratio and severe crosslinking or degradation.

3 The processing parameters are studied in detail and it is found that increasing the grafting reaction temperature, the initiator concentration, the amount of GMA, or decreasing the screw speed would result in a higher graft ratio

4 The comonomer technique is studied in order to upgrade the graft ratio and suppress crosslinking or degradation Styrene, as a comonomer, dramatically upgrades the graft ratios for all three polyolefins The most likely reason for that is the high solubility of styrene in polyolefins and the high stability of the macroradical formed between polyolefins radicals and styrene monomer The details of this mechanism are still not clear Unfortunately the addition of styrene does not effectively suppress crosslinking or degradation

Table (4-2) The Influence of different initiators on the graft ratio and crosslinking

Initiator	LLDPE			HDPE			PP		
	vCO/ δCH_2	GR (%)	MFI (g/10min)	vCO/ δCH_2	GR (%)	MFI (g/10min)	vCO/ δCH_2	GR (%)	MFI (g/10min)
None	/	/	12	/	/	5.2	/	/	2.6
DCP	0.80	1.48	4.7	0	0	2.2	0	0	54.2
DDPH	1.54	2.71	5.6	1.21	1.82	2.7	0.47	0.78	67.8
DB	0.21	0.34	4.3	0	0	1.1	0.04	0.21	72.1
AIBN	0.15	0.27	6.8	0.08	0.03	4.3	0	0	24.3

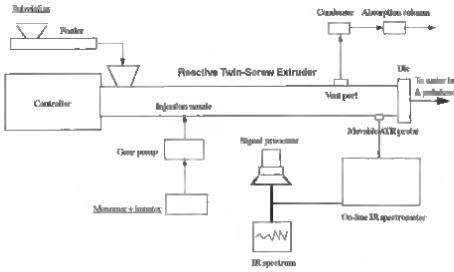

Figure (4-1) The set up of reactive twin-screw extrusion.

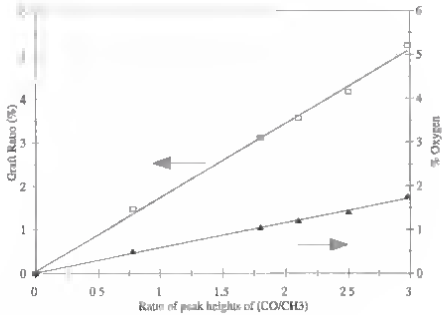

Figure (4.2.a) The calibration curve for the calculation of the graft ratio of GMA grafted LLDPE

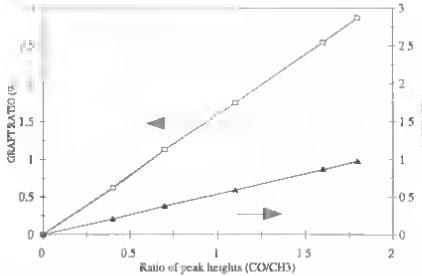

Figure (4-2 b) The calibration curve for the calculation of the graft ratio of GMA grafted HDPE

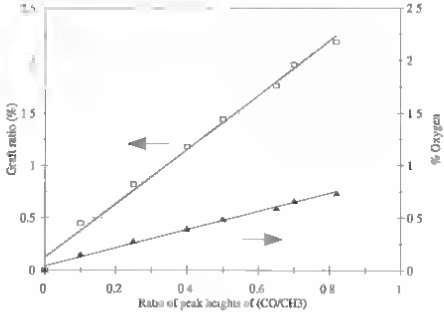

Figure (4-2 c) The calibration curve for the calculation of the graft ratio of GMA grafted PP

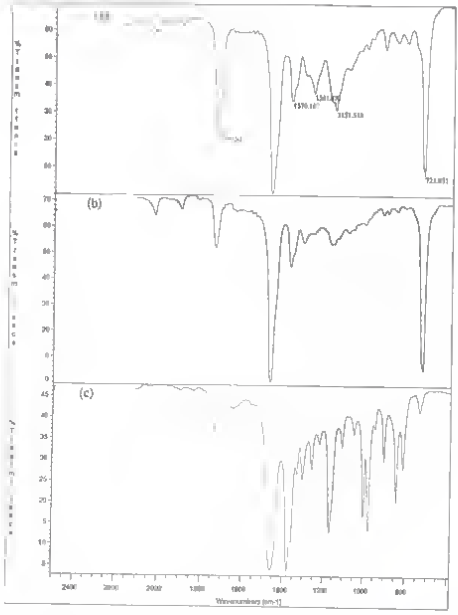

Figure (4.3) FTIR spectra of the grafted polyolefins
(a) LLDPE g-epoxy , (b) HDPE-g epoxy , (c) PP-g-epoxy

Table (4-4) The influence of reaction parameters on the GR and MFI values

Polymer/GMA /Peroxide (wt)	Screw Speed (rpm)	Temperature (°C)	Graft Ratio (GR) (%)	MFI (g/ 10 min)
LLDPE 100/6/0 6	100	180	1 65	7.4
100/6/0 7	100	180	1 77	5.5
100/6/0 7	200	180	1.43	9 6
100/7/0 7	150	215	2 89	2.3
HDPE 100/6/0 6	100	180	1.12	2.1
100/6/1.0	150	180	1 23	1.8
100/6/1.0	150	200	1.94	0.9
100/7/1 3	200	220	1 96	1 1
PP 100/6/0 6	100	180	0 78	67 8
100/6/0 8	100	180	0 84	93.4
100/6/1.0	150	200	1 45	/
100/7/1 5	200	200	1.52	/

Table (4-3) The effects of different processing procedures on GR and MFI values

Procedure Used	LLDPE		HDPE		PP	
	GR (%)	MFI (g/10min)	GR (%)	MFI (g/10min)	GR (%)	MFI (g/10min)
Process 1	1 65	5 6	1 12	1 7	0 78	67 8
Process 2	0 73	1.2	0 58	0 8	0 46	~94 5
Process 3	0 85	1 8	1 05	0 9	0 52	~89 6

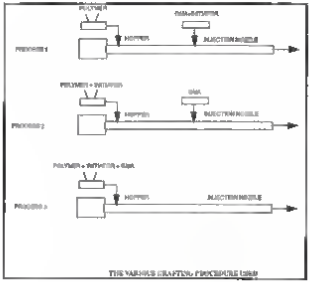

Figure (4-4) The three grafting procedures used in this investigation

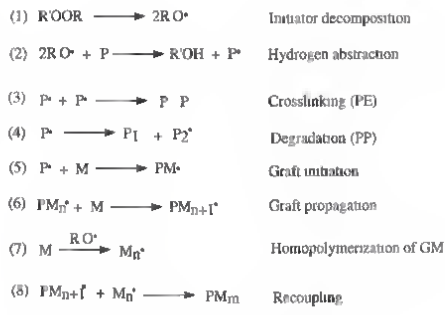

Figure (4-5) The mechanisms of main reactions in the grafting process

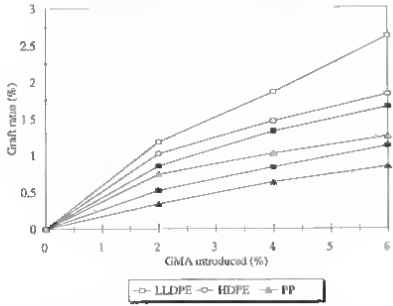

Figure (4-6 a) The effects of adding styrene as comonomer on the graft ratios of these three grafted polymers.

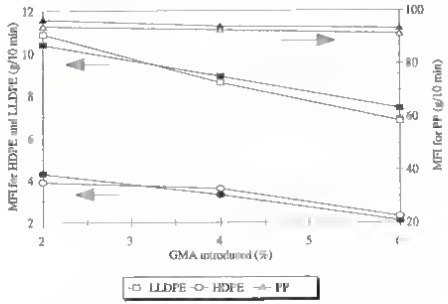

Figure (4-6 b) The effects of adding styrene as comonomer on the MFI of these three grafted polymers

CHAPTER 5
CROSSLINKING THE GMA GRAFTED POLYPROPYLENE (PP-G EPOXY) BY MUTIFUNCTIONAL MONOMER

5.1 Introduction

The accelerated thermal degradation of PP in the presence of peroxide during its melt grafting by GMA (glycidyl methacrylate) was briefly discussed in Chapter 4. Normally the thermal degradation of PP during its processing can be avoided by adding thermal stabilizers (antioxidants). However this kind of stabilizing mechanism cannot be applied to the grafting process because the stabilizer eliminates the free radicals which initiate the grafting. Effort was made in Chapter 4 to accelerate the grafting in order to inhibit the disproportionation of the radicals by using styrene as a comonomer of GMA. It turned out that styrene did facilitate the grafting but its inhibiting effect was very trivial.

The failure to suppress the degradation of during the grafting of PP could directly affect the final properties of PP blends if the degraded PP is used as a precursor of the compatibilizer. First, the poor mechanical properties of GMA grafted PP (PP g-epoxy) attributed to their short molecular chains and little amount of entanglement could be the cause of the poor bulk properties of PP based blends. Secondly the low melt viscosity of PP-g-epoxy brought by low molecular weight would make it difficult for PP g-epoxy to disperse into other phases with the higher melt viscosities. It has already been established that the viscosity ratio of blending components has direct effect on the morphology and physical

properties of the blends. Wu [77] indicated that smallest dispersing domains size can only be achieved when the viscosity ratio is close to one. Due to its low melt viscosity, degraded PP-g-epoxy, when it was used as reactive compatibilizer in blending systems, would tend to agglomerate without dispersion to the interface of PP and other polymers.

As a potential application, PP-g-epoxy can also be used as a coupling agent for PP/(wood or glass fiber) composite. The epoxy group of PP g-epoxy and hydroxyl group of wood or glass fiber make it possible to develop interfacial bonding between the PP matrix and the fibers. It has been proven that when a large amount of the PP g-epoxy is applied, its low molecular weight and poor mechanical properties have an inferior effect on the bulk properties of the composite, especially for the tensile strength and elongation properties [78].

In this chapter, a chemical crosslinking method is used to improve the bulk properties of grafted PP. By using a multifunctional monomer along with GMA monomer, the degraded chain segments are supposed to be recoupled. Crosslinking of PP by the class of methacrylates or allyl multifunctional monomers has been widely published [79, 80]. Recently, Yoshi *et al.* [81] used multifuctional monomer (trimethylolpropanetriacrylate) (TMPTA) in the presence of electron beam irradiation to upgrade the melt strength of PP by increasing its amorphous phase content. It was found that the crosslinked PP has extremely high elongation properties and melt strength. In the study of this chapter, similar multifunctional monomer is used to generate a certain level of crosslinking density during the melt grafting. As mentioned before, the major purpose of crosslinking is not only to increase the mechanical properties of grafted PP, but also to increase its melt viscosity which may facilitate its dispersion into other phases during melt blending. The effect of the crosslinking on the rheological, thermal, and mechanical properties of the grafted PP are studied in this

chapter

5.2 Experiment

5.2.1 Materials

The PP (Tenite with MFI 2.6 g/10 min) used in this study was donated by Eastman Chemical Co. Another high molecular weight PP (MFI 1.1 g/10 min, η_a 89,300 Pa.s) is donated by Himont Chemical Co. The initiator (2,5-dimethyl-2,5-di(t-butylperoxyl)hexane (DDPH)) was purchased from Akzo Chemie Co. Both multifunctional monomer (trimethylolpropanetriacrylate (TMPTA)) and monomer (Glycidyl methacrylate (GMA)) were purchased from Aldrich and purified by column chromatography before application.

5.2.2 Grafting

The grafting was carried out in the same APV reactive twin-screw extruder as illustrated in Chapter 4. The extrusion parameters were kept at PP/GMA/peroxide 100/6/0.6 or 100/6/0.2, 100 rpm, 180°C. The multifunctional monomer was premixed with GMA/peroxide with predetermined ratios.

5.2.3 Analysis

The pellets of crosslinked PP-g-epoxy were injection molded to standard tensile test specimens with 3000 psi under 180°C. The tensile test was carried out according to ASTM D638, type V in a MTS 880-14 servo-hydraulic testing machine with strain rate at 5 in/min. Hardness (Rockwell) was tested according to ASTM D785.

The melt flow index (MFI) of the blends were measured according to ASTM D1238 using Tinius Olsen extrusion plastometer

The Thermal testing was carried out by using the same DSC as previously illustrated. The 10°C/min heating and 40 C/min cooling down program was employed to cancel the thermal history

A SR-200 double plate rheometer was used to perform the rheological study The diameter and gap of the parallel plates are 25 0 mm and 1 0 mm Stress and temperature were kept at 250 Pa and 180°C, respectively The frequency changed from 0 03 Hz to 79.5 Hz.

^{1}H-NMR testing was carried out in GEMINI 300 NMR spectrometer by using toluene-d_8 as the solvent. The sample was dissolved in the solvent in high temperature before detecting All of the samples used in ^{1}H NMR or FTIR were purified by solvent extraction

5.3 Results and Analysis

5.3.1 The mechanisms.

As shown in Figure (5 1) the whole proposed mechanism is composed of three parts Peroxide will cause chain scission while the multifunctional monomers recouple all of these scissized chains together Meanwhile GMA monomers are grafted onto the macroradicals. All of these three processes take place simultaneously The scission and recoupling are two opposite but irreversible processes. Chain scission keeps the linearity of molecular chain structure while recoupling makes PP chain geography shift from linear to branching Recoupling cannot only reconnect the segments of scissized chains it can also stabilize the macroradicals by the "resonance effect" as shown in Figure (5 1) [80] On the other hand the

recoupling and grafting could form a competitive pair for the free radicals because both consume the macroradicals As multifunctional monomer has high functionality, in worst case large amounts of it can consume the majority of macroradicals and leave GMA without a reactive site to graft onto As a result, the optimal ratio of multifunctional monomer/GMA monomer should be determined to keep the maximum graft ratio of GMA and simultaneously, the chain scission caused by peroxide can be compensated to certain extent by chain recoupling

5.3.2 The Detection of GMA Graft Ratios

Normally the graft ratio is measured by the FTIR absorption of carbonyl group of the grafted GMA monomer after the grafted PP is solvent extracted as illustrated in Chapter 2 3 4, and Appendix B In this study, as TMPTA is used as coagent the carbonyl groups of TMPTA may interfere with the analysis. As a result, the carbonyl peak cannot be used for quantitative analysis in this case Another characteristic peak that can be used to detect the GMA graft ratio is the epoxy group at 998 92 cm^{-1}, 911 49 cm^{-1} and 848 20 cm^{-1}, which has no interference from TMPTA. However, these peaks are not intense and sensitive enough to the changing of graft ratio In order to perform quantitive grafted GMA measurements, ^{1}H-NMR was used in this study (Fig (5-2)) Toluene-d^{8} was used as solvent for the grafted PP A heating stage was used during NMR experiments to insure that grafted PP was soluble in solution. The degree of grafting was calculated from the ratio of the integral of peaks located at approximately 4 05 ppm (assigned for the two hydrogen atoms that are adjacent to the ester oxygen atom) to the integral of the peaks that occur between 0 5 and 1 8 ppm (assigned for the six hydrogen atoms of PP)

5.3.3 The Effects of Peroxide During Melt Grafting

The effect of peroxide accelerated thermal degradation on the mechanical and thermal properties of PP has been well studied [81-83]. As shown in the Table (5.1) below, with the increasing amount of peroxide, the graft ratio does obviously increase, but the MFI increases even more dramatically. It is clear that peroxide accelerates the thermal degradation of PP much more than it upgrades the grafting. The severe degradation resulted in low yield strength, hardness, melting point, and, most obviously, the elongation properties. In other word, if we want to increase the graft ratio by increasing the peroxide concentration, the molecular weight and mechanical properties would be inevitably sacrificed. From the MFI value shown above, we can see that PP is extremely sensitive to the presence of peroxide, up to 0.5% of peroxide may cause the avalanche of PP molecular structure and consequently deteriorate its mechanical properties. The poor mechanical properties could be due to the slippage failure of short molecular chains lack of entanglements. Figure (5.3) shows G', G", and η^* of unmodified and degraded PP g-epoxy as a function of frequency. It is observed that G', η^* curves of degraded PP-g-epoxy lie much lower (especially at the low frequency range) than that of the unmodified PP indicating the low entanglement density at low frequencies and, therefore, shorter chains for the degraded PP g-epoxy. Since the molecular weight distribution of PP has a linear relationship with "polydispersity index" (PI value) [84] which can be calculated from the cross-over of the G' and G" curves by

$$PI = 10^5 / G_c \quad (G_c \text{ the cross-over modulus value})$$

The calculated low PI value of degraded PP (4 8) indicates that the degraded PP has a narrower molecular weight distribution than that of unmodified PP (5 7), although its molecular weight is much lower than unmodified PP. This result conforms to the well observed phenomena, chain scission can narrow down the molecular weight distribution of PP.

The short molecular chain of degraded PP g-epoxy can also be demonstrated from its G'–G" plot (Figure (5-4)). G" is larger than G throughout the frequency region (10^{-2} to 10^{2} Hz). That means the deformation is mainly viscous at even higher frequencies. Normally, G" is only larger than G at low frequency for the typical thermoplastics [61]. As a comparison, the G'–G" curve of unmodified PP demonstrates the typical thermoplastic rheological properties.

5.3.4 The Degradation Rates of Two Types of PP with Different Molecular Weights

Since the rate of thermal degradation of PP has a direct relationship with its molecular weight, in this section of study, high molecular weight PP (from Himont Chemical η_0 89,300 Pa s ± MFI 1 g/10mins) is used as parent materials in order to get PP g-epoxy with relatively high molecular weight. The decrease of η_o (zero shear viscosity) with the increasing of peroxide added was shown in Figure (5-5). The η_0 of the normal molecular weight PP decreases dramatically within the first addition of 0.2% peroxide, after which η_0 does not change much. It may be inferred that this point corresponds to the critical molecular chain length for the formation of entanglements. For high molecular weight PP, η_0 is not so sensitive to peroxide within first 0.05% and there is a plateau region for η_o value. However, η_0 dropped obviously between 0.05% and 0.2% and after the critical point of 0.4%, the η_0

curve tended to be flatter When the amount of peroxide added exceeds 0.4%, both normal and high molecular weight PP reach quite similar final η_0 values.

In Figure (5-5), both PP have a "peroxide sensitive region", where the η_0 values drops dramatically PP with high molecular weight seems to have a higher and a broader region (around 0.05% to 0.4%) while normal molecular weight PP has a lower and a narrower region (around 0– 0.2%) However, after this region PP with different molecular weights results in quite close final η_0 value. As the peroxide concentration for melt grafting of PP is usually above 0.3%, it is clear that selecting unmodified PP with high molecular weight does not necessarily increase the molecular weight of the grafted PP

5.3.5 The Effect of Crosslinking by Multifunctional Monomer (TMPTA).

5.3.5.1 High peroxide concentration (0.6%).

The peroxide concentration was set at 0.6% in our previous reactive extrusion Based on the work done in Chapter 4, it has been concluded that using high peroxide concentrations and low monomer concentrations is an effective method to increase the grafting efficiency and inhibit the homopolymerization of GMA monomer during the melt grafting However as illustrated before, high concentration of peroxide causes severe degradation. In this study, the concentration of multifunctional monomer (TMPTA) is increased from 0 to 1.0% in order to see if the effect of chain recoupling and crosslinking can compensate for the chain scission to certain extent

The comparisons of thermal, melt and mechanical properties of degraded and crosslinked PP-g-epoxy are shown in Table (5-2) Based on the comparison of MFI values, PP is more sensitive to peroxide than multifunctional monomer The degradation caused by

0.6% peroxide overwhelms the chain recoupling by up to 1.0% multifunctional monomer However, 1.0% of TMPTA does reduce the MFI value of PP from 52.4 to 21.4 along with the increasing of gel amount from 0 to 0.35% Since the gel amount (crosslinking density) is low while the decreased MFI is large, it may indicate that the main effects from multifunctional monomer is not just crosslinking or chain recoupling but also minimizing the β-scission by stabilizing the macroradicals via "resonance effect", as shown in Figure (5-4) On the other hand, the graft ratio is not affected by the increase of TMPTA and almost remains constant. This means that the number of macroradicals initiated by peroxide is large enough to have both grafting and chain recoupling happen simultaneously without any competition.

Due to the low molecular weight caused by chain scission, the degraded PP g-epoxy has a much lower T_m and crystallinity (shown as ΔH_m) than unmodified PP Once TMPTA was added there is certain increase of T_m due to the restriction of the flow of melt by crosslinks As we know, in general, crosslinks act as local defects and together with the reduced supercooling, reduction in total crystallinity is expected However, according to Baird *et al* [85] few crosslinks often improve packing of polymer chains into a crystalline structure. Our results with a certain amount of increasing ΔH_m value along with the increasing amount of TMPTA added may correspond to this. The similar phenomena was also observed in the reactivity study of grafted HDPE in Chapter 3

There is no obvious change of hardness with the addition of TMPTA. For semicrystalline polymer like PP the hardness mainly depends on the level of crystallinity When the crystalline is disturbed by the chain scission, the hardness would decrease But if the crosslinking and chain recoupling are introduced in, the increase of hardness by

crosslinking can compensate for the decrease caused by chain scission. So the overall hardness can remain constant. The chain recoupling and crosslinking also bring in certain improvements on the elongation property of degraded PP. In this case, both chain scission and chain recoupling happened simultaneously, but the chain scission is still predominate. As a result, the elongation at break value of highest crosslinked PP is still lower than pure PP.

The increase of yield strength is mainly due to the presence of crosslinks, it may also be due to the interactions between the grafted GMA chains. The graft structure makes the specific interaction between grafted chains as a kind of physical crosslink which might improve the mechanical properties.

5.3.5.2 Low peroxide concentration (0.2%).

In order to have grafted PP with similar rheological, mechanical and thermal properties as unmodified PP, the chain scission and recoupling rates should be kept balanced. As shown above, PP is more sensitive to the peroxide concentration, so low peroxide concentration (0.2%) was chosen in the study of this section. Low peroxide concentration can avoid the excessive degradation but this comes with a sacrifice in graft ratio. In this case, the graft ratio was around 0.63%, which is lower than the case of high peroxide concentration.

Since the amount of TMPTA is much higher than peroxide in this case, chain recoupling begins to dominate over chain scission and consequently the MFI values decrease along with the increasing amount of TMPTA as shown in Table (5-3). Compared with the case of high peroxide content, gel amount has a dramatic increases which means the crosslinking density increases. However, this number of crosslinks still has no influence on the smoothness of extrusion and the surface finish of the samples from injection molding according to our observation.

The yield strength increases in the presence of crosslinks initiated by high content of TMPTA. Unlike the case of high peroxide concentration, the elongation increases dramatically along with the increasing of TMPTA in this case. The same phenomena was observed by Kim *et al* [83] in his PP crosslinking study. The most reasonable explanation for this observation is the presence of increased content of amorphous phase, which is indicated by the decreasing ΔH_m values. The resulting PP has an extremely improved ductility and makes specimens difficult to be broken (elongation at break is above 664%) even under high strain rate (5 inch/min). For the thermal properties, T_m increases first, then decreases, and ΔH_m keeps decreasing. It confirms that the crystalline is disturbed and the crystallinity is reduced by the chains recoupling which causes branching or a crosslinked structure. As chain crosslinking and recoupling dominate in this case, the increased molecular weight and crosslinking density increased the hardness.

The effect of both TMPTA and peroxide on rheological properties of the grafted PP is illustrated in Figure (5-6). As compared to the corresponding binary PP/peroxide and PP/TMPTA systems, the persistence of G' into the low frequency region in the case of PP/TMPTA/peroxide systems clearly indicates the existense of highly branched PP chains. On the other hand, the lower G" value in the high frequency range compared with the TMPTA crosslinked PP, suggests lower entanglement density caused by degraded PP chains. Both observations agree with the proposed competition between chain scission and recoupling reactions.

5.3.5.3 The contribution of TMPTA and GMA to the crosslinking.

Based on the study of PP grafting by maleic anhydride (MA), a number of papers have reported that the presence of monomer, like MA, enhanced the crosslinking [86]. The

mechanism for that is still not well understood. In the current study, it is still not clear how much contribution GMA has made to the amount of observed crosslinking. In order to clarify the proportion of crosslinking from GMA and TMPTA, the variation of G' with different GMA levels without TMPTA and different TMPTA without GMA were measured and results are showo in Figure (5 7 a) and Figure (5-7 b) respectively. With no GMA, significant contributions of TMPTA to chain recoupling in the crosslinked PP can be clearly identified, indicating dramatically enhanced crosslinking in the presence of TMPTA. In contrast, the effect of GMA on chain connectivity is much less apparent, as is shown in Figure (5-7 b). As a result, TMPTA is the major contributor to the formed crosslinking rather than GMA. However, GMA does enhance the crosslinking to certain extent level based on the limited increase of G in Figure (5-7 b)

5.3.5.4 The rheological properties recovery of PP recoupled by TMPTA

Figure (5-8) shows the recovery of complex viscosity along with the addison of TMPTA. It is observed that with 0.8% of TMPTA and 0.2% of peroxide, the crosslinking and chain scission can reach a balanced point, where the grafted PP has almost exactly overlapped viscosity curve with unmodified PP. That means by adjusting the TMPTA/peroxide ratio, the introduced chain recoupling can compensate for the opposite rheological effect from peroxide. Figure (5 9) shows the opposite effect of peroxide and TMPTA on the complex viscosity of grafted PP. 0.2% of peroxide can drop the η_0 from above 10,000 Pa.s to low 1000 Pa.s, while the amount of TMPTA needed to restore the orgnal viscosity is as high as 0.8%. This result confirms the conclusion drawn early, PP is more sensitive to peroxide than to multufunctional monomer. The comparison of G~G" plot of unmodified PP and degraded PP has been made in Figure (5 10). It is found that the deformation of degraded PP

is mainly viscous throughout the frequency range. However, along with the increasing amount of TMPTA introduced, the storage modulus (G') began to be slightly larger than dissipation modulus (G") at high frequency. As we know, for typical thermoplastic materials, the deformation should be mainly viscous at low frequency and elastic at high frequency, while the opposite is typical for elastomer materials. In this case, the G'-G" curve indicate that crosslinked PP still demonstrates a typical thermoplastic rheological properties. This means that although crosslinking occurs in this type of recoupling caused by TMPTA, an extensive three dimensional network of crosslinking does not form. The absence of extensive crosslinking allows the PP to retain its processability.

5.4 Conclusions

In the study of this chapter, a multifunctional monomer, trimetylolpropanetriacrylate (TMPTA), is used to form certain crosslinking during melt process in order to compensate the degradation initiated by the peroxide used for grafting. The following conclusions are drawn:

1. Peroxide used for the melt grafting of PP can cause severe thermal degradation of PP. TMPTA, as a multifunctional monomer, can be used to control the rheological properties of degraded PP by forming a certain amount of crosslinking or chain recoupling. With the proper ratio of TMPTA/peroxide, the grafted PP can keep similar melting and mechanical properties as pure PP.

2. PP is more sensitive to peroxide than to multifunctional monomer (TMPTA). In the case of high peroxide concentration, TMPTA cannot effectively restore the rheological properties of degraded PP. Only under low concentration of peroxide, the crosslinking or

chain recoupling caused by TMPTA could compensate the negative effect of chain scission, and improve the bulk properties of grafted PP

3 High molecular weight PP (MFI 1 1 g/10 mins) can restrain the rate of degradation when the peroxide concentration is below 0 1% There is a plateau region (0–0.05% peroxide) where the shear viscosity of PP is not sensitive to the presence of peroxide However, when the peroxide concentration exceeds 0 3%, high molecular weight PP results in a quite close viscosity to the low molecular weight PP (MFI 2.6 g/10 mins) That means that using PP with high molecular weight could not generate high molecular weight grafted PP if the peroxide concentration is above 0 3%

4 There is no obvious competition for macroradicals between grafting and chain recoupling in the both cases of high and low concentrations of peroxide The amount of TMPTA added seems to have no effect on the graft ratio of grafted PP

5 Based on the rheological study it was concluded that the crosslinks of PP are mainly contributed by TMPTA while the effect from GMA is very trivial

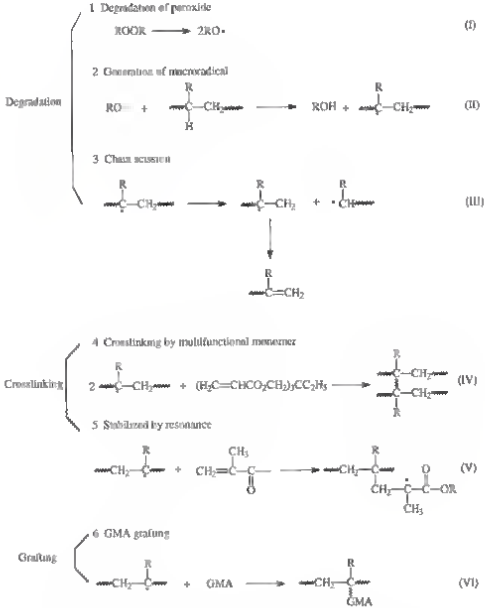

Figure (5-1) Proposed mechanisms of chain scission, chain recoupling, and grafting of PP

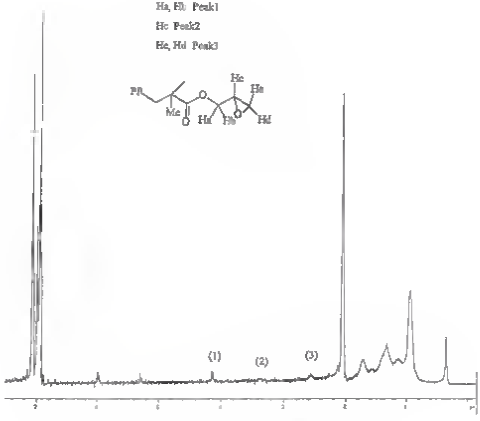

Figure (5-2) ^{1}H NMR spectrum of the crosslinked PF-g-epoxy

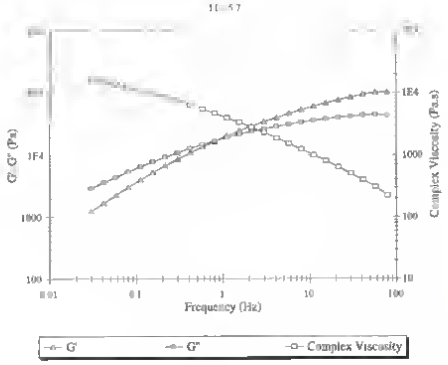

Figure (5.3.a) Shear storage modulus (G') shear dissipation modulus (G") and complex shear viscosity (η*) of pure PP PI polydispersity index.

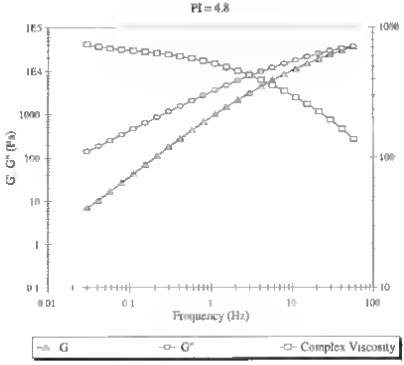

Figure (5.3.b) Shear storage modulus (G') shear dissipation modulus (G"), and complex shear viscosity (η*) of degraded PP g epoxy PI polydispersity index.

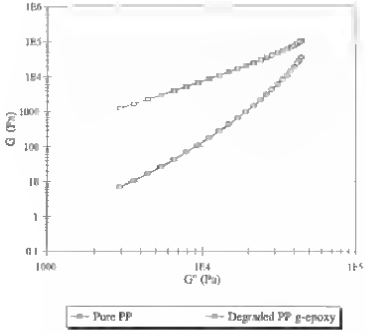

Figure (5-4) G –G'' curves for pure PP and PP g-epoxy

Figure (5.5) The decreasing of zero shear viscosity (η_0) along with the increasing of peroxide amount for high molecular weight PP (MFI 1.1 g/10 min) and currently used PP (MFI 2.6 g/10 min)

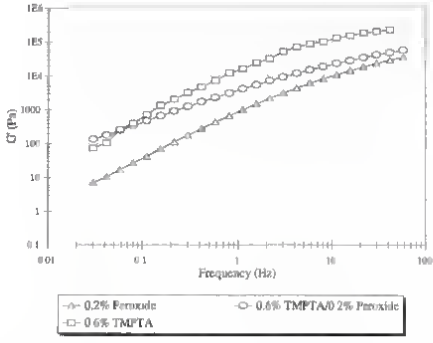

Figure (5-6) The simultaneous effects of peroxide and TMPTA on the rheological properties of PP

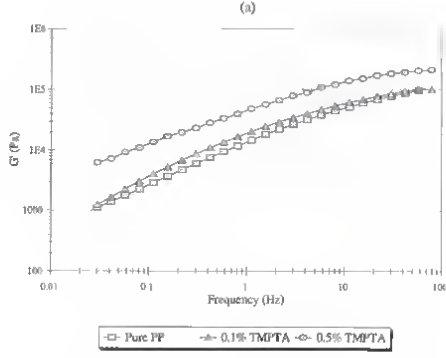

Figure (5-7 a) The variation of G of PP with different amount of TMPTA.

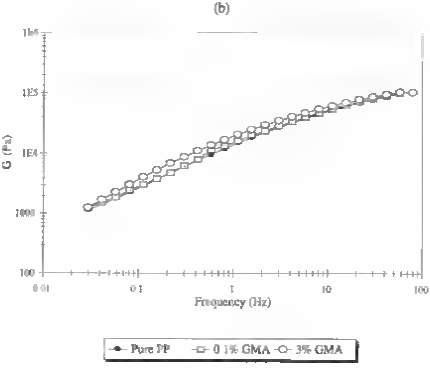

Figure (5.7 b) The variation of G' of PP with different amount of GMA.

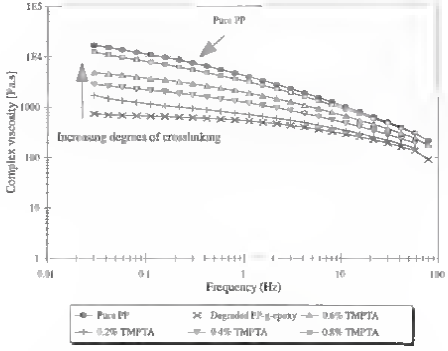

Figure (5.8) The rehabilitation of G' with the increasing amount of addition of TMPTA.

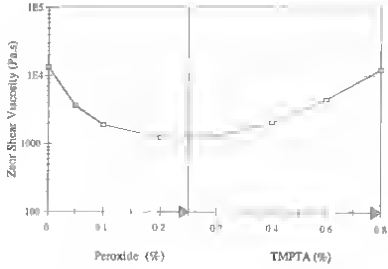

Figure (5-9) The opposite effects of peroxide and TMPTA on the zero shear viscosity of PF grepoxy

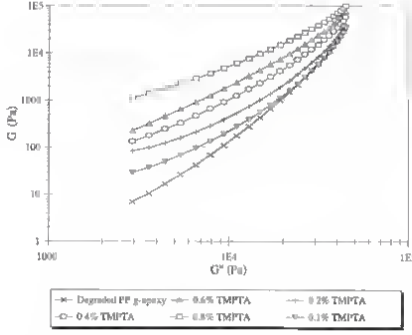

Figure (5 10) The G ~G ' curves of degraded and crosslinked PP-g epoxy

Table (5 1) The effect of peroxide on the properties of PP

Peroxide (%)	MFI (g/10min)	T_m (°C)	ΔH_m (J/g)	Gel (%)	Yield Streng (Mpa)	Elong (%)	Hardness (Rockwell)	Graft ratio (%)
0	2 6	165 5	106 7	0	32 83	430	95 8	0
0 1	34.5	162.1	104 5	0	31.46	446	94 1	0.65
0 2	38.7	159 5	103 2	0	31.09	428	93.6	0 63
0 3	52 4	155 6	103 6	0	30 66	411	93 7	0 71
0 4	67.8	153 2	103.5	0	30 14	386	93.5	0.78
0 6	93.4	152 8	102.7	0	29.36	361	93 1	0 84

Table (5.2) The effect of multifunctional monomers (TMPTA) on the graft ratio and properties of PP (The peroxide concentration was kept at 0.6%)

TMPTA (%)	MFI (g/10mins)	Tm (°C)	ΔH_m (J/g)	Gel (%)	Yield Streng (Mpa)	Elong (%)	Hardness (Rockwell)	Graft Ratio (%)
0	93.4	152.8	102.7	0	29.36	361	93.1	0.84
0.4	40.4	157.7	103.2	0.17	30.67	417	95.6	0.79
0.6	32.6	158.8	104.1	0.26	31.08	416	94.7	0.85
0.8	28.8	160.2	103.8	0.31	31.14	419	93.3	0.81
1.0	21.4	161.8	104.9	0.35	31.62	414	95.5	0.76
PP	2.5	165.5	108.6	0	32.83	430	95.8	0

Table (5-3) The effect of multufunctional monomers (TMPTA) on the graft ratio and properties of PP (The peroxide concentration was kept at 0.2%)

TMPTA (%)	MFI (g/10min)	Tm (℃)	ΔH_m (J/g)	Gel (%)	Yield Streng (Mpa)	Elong (%)	Hardness (Rockwell)	Graft Ratio(%)
0	38.70	159.5	103.2	0	31.09	428	93.6	0.63
0.4	26.34	162.4	104.1	0.47	31.68	527	94.2	0.67
0.6	10.59	161.9	102.7	0.56	33.68	575	95.8	0.61
0.8	2.78	161.4	101.6	0.63	36.59	>664	97.7	0.63
1.0	1.79	161.2	101.9	1.34	38.64	>664	98.8	0.57

PART II THE APPLICATIONS OF GLYCIDYL METHACRYLATE (GMA) MONOMER GRAFTED POLYOLEFINS IN THE REACTIVE COMPATIBILIZATIONS OF POLYMER BLENDS

CHAPTER 6
THE REACTIVE COMPATIBILIZATION OF HDPE/PET BLENDS

6.1 Introduction

The polymer mixture of poly(ethylene terephthate) (PET) and high density polyethylene (HDPE) constitute a significant portion of post-consumer waste. The two polymers, however, are immiscible and need to be compatibilized in order to be used in commercial applications. The immiscibility of PET and HDPE is because of their quite different molecular structures, polarities, and crystallization behaviors. Theoretically, immiscible blends are generally preferred over miscible blends as one can take advantage of the useful properties of each blend component. However, immiscible blends quite often have poor phase dispersion. The unfavorable interactions between the molecular chains would lead to large interfacial tension in the melt and make it difficult to disperse the components well during mixing. Such unfavorable interactions also lead to unstable morphology and poor interfacial adhesion, resulting in inferior mechanical properties. If the morphology can be better stabilized and the mechanical properties cost effectively improved, then we have an additional value-added use for post-consumer household waste. This objective could be achieved by compatibilization.

Currently there are two main compatibilization routes for PET/HDPE blends. One route is PET/HDPE g-maleic anhydride/HDPE blends [87]. Here, HDPE g-maleic anhydride (HDPE-g-MA) is synthesized by melt grafting of HDPE with maleic anhydride. Adding

HDPE-g-MA in the blends can increase the polarity of non-polar HDPE phase so that certain hydrogen bonding can be formed between the functional maleic anhydride group of HDPE-g-MA and polar structure of PET. The possibility of forming chemical bonding between MA and some hydroxyl end groups of PET is very rare because of the poor reactivity between maleic anhydride and hydroxyl or carboxylic groups. As a result, the biggest problem of this system is the lack of strong chemical bonds between the incompatible PET and HDPE phases although several authors [87-89] have claimed that they had decreased the domain size of HDPE and improved the mechanical properties of the blends by using this technique.

Another technique is PET/EGMA/HDPE blends using EGMA (ethylene glycidyl methacrylate copolymer) [90-92] as the precursor of compatibilizer. EGMA is a recently developed functional copolymer which has reactive GMA units on its polyethylene backbone. This system could achieve much better mechanical properties than the former one because of the chemical bonding formed between the epoxy group of GMA and the carboxylic or hydroxyl end groups of PET. Unfortunately, there are also disadvantages to this technique. The commercially available EGMA, which is synthesized by solution copolymerization, is relatively expensive (~$3.50/lb) [93]. It is economically impractical to use this kind of compatibilizer in large quantity. Also, the inserted GMA unit in PE backbone could influence the cocrystallization between EGMA and HDPE and reduce the compatibilizing efficiency.

In the study of this chapter, GMA grafted HDPE (HDPE-g-epoxy) by melt grafting is used as reactive precursor of compatibilizer for the blends. Melt grafting technique has been discussed extensively in the previous chapters. Compared with EGMA, HDPE-g-epoxy has the same compatibilization mechanism but it offers two advantages. First, low synthesizing costs and Second, HDPE-g-epoxy has similar backbone structure as pure HDPE. HDPE-g-

epoxy could be synthesized based on the HDPE to be compatibilized. The grafting will not change the original structure of PE backbone therefore, it has quite similar molecular structure molecular weight, crystallinity and melt viscosity as its original HDPE, although some crosslinking exist during melt grafting These factors facilitate the cocrystallization and dispersion of the grafted HDPE into HDPE component

6.2 Experiment

6.2.1 Materials

Pelletized PET (Eastman Chemical Co Intrinsic viscosity 0 8) and HDPE (Eastman Chemical Co , Tenite PLS H6001-A) are two mixing components for this study HDPE g-epoxy was synthesized by melt grafting during twin-screw extrusion, which was illustrated in Chapter 4 The graft ratios are from 0 8% to 1 9% for different items.

6.2.2 Compatibilization

The compatibilization of HDPE/PET blends was carried out in the same APV extruder illustrated in Chapter 4 The barrel temperature ranged from 230°C to 270°C from beginning to end heating zone PET was dried overnight in vacuum oven before compounding HDPE PET and HDPE g-epoxy was dry premixed in predetermined ratios and then compounded by the extruder at the feeding rate of 10 kg/hr and 300 rpm The residence time for the blends in the extruder was around 55 sec The extrudates were pelletized and dried in oven.

6.2.3 Characterizations

Tensile properties detection was carried out according to ASTM D638. The specimens were molded from predried blend pellets in a injection molding machine, the injection pressure was kept at 3000 psi. Standard notched Izod impact test (ASTM D256) were carried out in ambient conditions. For the morphological evaluation, the blends samples were cryogenically broken in liquid nitrogen, then samples were examined by scanning electron microscopy (SEM) after they were coated with a thin gold film. The detecting of melting points and crystallinity of blending components were completed in Solomat DSC 4000. The heating and cooling scans were carried out at a rate of 10°C/min in the temperature range of 30-300°C. The melt flow index (MFI) of the blends were measured according to ASTM D 1238 using Tinius Olsen extrusion plastometer. The gel content of grafted HDPE was determined by placing the crude extradates in Soxhlet extractor and extract for 24 h with refluxing toluene. All blends were predried overnight before detecting. The torque values used to judge the compatibilization reaction were detected by using a Brabender measuring head driven by Brabender plasti-cord pl2000. The temperature of the measuring heading was kept at 280°C and roller blades were employed at 60 rpm. The torque data were acquired by a computer interface.

6.3 Results and Discussion

6.3.1 The Comparisons of HDPE-g-epoxy and Pure HDPE

The major difference of chemical structures between grafted and pure HDPE is the grafted GMA unit on the HDPE backbone. In addition, as illustrated in previous chapters,

grafted HDPE could have certain crosslinks which is initiated by the peroxide used in the grafting. The crosslinking density is detected by measuring gel amount after solvent extraction of the extrudate. Table (6-1) shows the increasing tendency of crosslinking density along with the increasing graft ratios which is caused by increasing amount of peroxide added during grafting.

6.3.2 The Compatibilization Reaction between Epoxy Group and End Groups of PET.

The reactive end groups of PET(carboxylic or hydroxyl groups) make it possible for PET to be compatibilized with various functionalized polymers [94-97] by generating *in situ* formed compatibilizer. Most of the reactivity study of these reactions are carried out by measuring the changing of torque values along with reaction time in Brabender mixer. This kind of measurement is based on the mechanism that the chemical reaction between the phases increases the molecular weight and thus increases the viscosity of the system which results in an increase in mixing torque required to drive the rotors. It has been heavily used in the reactivity study of epoxy and oxazoline groups in Chapter 3. The same technique is used in this study. The torque vs. time curves for the control HDPE/PET and reactive HDPE/HDPE-g-epoxy/PET with different ratios are given in Figure (6-1) and (6-2). In order to exclude the effect from side reaction between PET and GMA oligomer remaining in the grafted HDPE, the grafted HDPE had been purified by precipitating from hot toluene in methanol before application. The reactive blends show a much higher torque than the nonreactive blends of similar composition. Both the large amount and high graft ratios of HDPE-g-epoxy lead to high torque values. Obviously, this is due to the chemical reaction between the phases. For most of the compatibilized blends, the highest torque values are

reached within 3 mins of mixing, after that a constant value is approached It can be inferred that most of the reaction are finished within the very beginning 3 mins of mixing As the twin screw extruder has a much higher shear rate and better dispersing effect than the Brabender mixer, it is quite safe to conclude that the reaction could be completed within a much shorter time in the twin screw extruder Figure (6 3) and (6-4) shows the torque values of reactive and control blends at 6 mins of mixing The beginning addition of grafted HDPE could increase the torque values dramatically, then, with more grafted HDPE added, the torque values are not as sensitive as in the beginning This kind of phenomenon is also observed in the morphology study below It could be due to the exhausting of all PET end groups by excessive grafted epoxy group. For the practical application, keeping proper but not excessive amount of grafted HDPE is the desirable way for the compatibilization, not only because of the economical consideration, but also for the avoiding of crosslinking formed among the excessive reactive groups [92, 95] The effect of crosslinking on the mechanical properties of the blends will be studied in the following mechanical property study

Parallel to the torque value measurement melt flow index (MFI) values of the blends are also detected to confirm the presence of the interfacial reaction. Figure (6-5) shows the change of MFI values along with the change of blending ratio while the concentration of grafted HDPE is held constant It is demonstrated that the presence of 10% grafted HDPE can greatly decrease the MFI value of the blends The drop of MFI has the same reasons as the increment of torque value illustrated above. From the same plot, we can see that the MFI values decrease along with the increasing amount of PET and the lowest MFI value shows up when PET component was around 50% This behavior may due to the increasing amount of reactive end groups of PET which have high probability to react with epoxy groups

Similarly Figure (6-6) shows that the MFI decreases along with the increasing amount of grafted HDPE added on the other hand the additions of grafted HDPE with higher graft ratio also results in lower MFI values of the blends

From the above torque and MFI measurements it appears that the reaction intensity can be increased by either increasing the amount of added grafted HDPE or adding the grafted HDPE with higher graft ratio Usually higher reaction intensity results in a high degree of compatibilization. However, according to the extremely low MFI value shown above for the blends with high reaction intensity, excessive concentrations of reactive groups might result in poor processability and certain crosslinking Again, the intensity of the interfacial reaction should be well controlled in order to satisfy both requirements of compatibilization and processability

6.3.3 The Processability

The extrusion of the incompatible blends of PET and HDPE without the presence of the compatibilizer results in grossly phase separated materials that are unusable for profile or any other application. Die swelling and melt fracture occur at all composition ratios However, by adding up to 5% of HDPE-g epoxy into the HDPE/PET (50/50) blends smooth extrusion is achieved and the RPM and feeding rate can be increased without disturbing the smoothness of the extrusion That means the poor processability of the blends caused by the phases separation can be dramatically improved by the compatibilization By adding up to 30% of HDPE-g-epoxy, rough surface of the extrudate begun to show up, which indicates the extensive crosslinking formed by the excessive interfacial reaction. As a result the proper content of HDPE g-epoxy for HDPE/PET (50/50) blends in order to maintain

certain processability should be between 5% to 30%

6.3.4 The Morphologies

Figure (6-7) and (6-8) show the SEM pictures of the cryogenic fracture surfaces without solvent etching of the HDPE/grafted HDPE/PET blends and their control samples (HDPE/PET 35/65 and 50/50) The dispersed and spherical particles with different dimensions have been identified to be HDPE domains by solvent etching For the control samples in both ratios HDPE has coarse morphology with larger domain sizes (6-10 μm) than any compatibilized sample. The large particle size, with no evidence of adhesion between the matrix and dispersed phase confirmed the incompatibility of the two components. In comparison, the compatibilized blends show the dispersed HDPE particles as being well separated and with a much smaller and uniform size when only 5% of HDPE-g-epoxy is added, Adding additional amount of HDPE-g-epoxy resulted in smaller HDPE particles The decreasing domain sizes along with the increasing amount of grafted HDPE added are plotted in Figure (6-9) Here, the calculation of domain size is based on the average value of at least 60 dispersed particles from 6 SEM pictures of different areas. Obviously, initial addition of small amount of grafted HDPE can affect the domain size efficiently and make domain particle in the blend deeply embedded in the matrix as shown in Figure (6-7) and (6-8) It is interesting to notice that after the initial dramatic decrease of the domain size with increasing amount of grafted HDPE, the domain size reaches a constant value of about 0.5 μm, increasing HDPE g-epoxy further has no effect on particle size It is quite possible that at certain critical point for example, 15% of HDPE-g epoxy most of the PET end groups have been consumed After that, the extra addition of HDPE g-epoxy does not have any effect on

the compatibilization. The reduction of domain sizes by the compatibilization has been widely studied and used a judgement of the degree of compatibilization. There are many factors contribute to this behavior: the copolymer formed by the interfacial reaction reduces the effective interfacial tension in the system, the chemical reaction increases the viscosity of the blends which increases the applied shear stress during the blending, also the presence of the copolymer at the dispersed phase interface retards coalescence which stabilize the morphology [43]. It is difficult to say which factor is most effective in the decreasing of domain size in this case, most possibly, the decrease of domain size could be due to the combination of all these factors.

The morphologies of the interface between HDPE particles and PET matrix can also offer us some information about the interfacial reaction. Figure (6-10) show the comparison of interfacial morphologies of control and compatibilized blends. For the uncompatibilized blend, the domains are, not only large and smooth, but also have a clear crevice with the matrix. In addition, there are some smooth and spherical "pull out" holes on the fracture surface. Both of these phenomena are the typical signs of poor interfacial interaction. In contrast, the compatibilized blend has a rough and blurred interface which indicates the strong interaction. The chemical bonding between the two phases formed during melt blending contributed to this rough interfacial morphology. Figure (6-11) shows a very interesting phenomena, the interfacial interaction is so strong that when the sample is cryogenically broken, the fracture surfaces are not the interfaces of the two phases but the right through HDPE phase itself. As an analogy, the graft copolymer formed between graft HDPE and PET is just like a binder for the two phases. It could hold the two phases tightly enough to resist the crack

The stability of the morphology is one of the greatest advantages of the compatibilized blends. In this study it is investigated by using annealing experiments. Figure (6-12 (a) and (c)) are the morphologies of uncompatibilized and compatibilized blends without any annealing processing. Figure (6-12 (b) and (d)) are the morphologies of blends after annealing at 260°C for 10 min. The coalescence can be observed easily in the uncompatibilized blends which is caused by the high interfacial tension between the phases. However, for compatibilized blends, there is almost no morphological change before and after annealing. Many authors have discussed the mechanism of phase stabilization by compatibilization [43-98-100]. Basically, the interfacial interaction reduces the interfacial tension, consequently decreases the thermodynamic driving force for coalescence. Another possible mechanism is the formation of certain crosslinks during the interfacial reaction which trap individual domain and hinder any possible coalescence.

6.3.5 The DSC Spectra

The crystallization transition temperatures of the uncompatibilized and compatibilized blends are analyzed by DSC (Figure (6-13)) spectra. There seem to be no significant shift for the T_c of HDPE component. However, the crystallization temperatures of PET component shift to lower values and the $\Delta H_{crystallization}$ value decreases in proportion to the amount of graft HDPE added (Table (6-2)). With 20% of grafted HDPE added, the shift was about 6.2°C. This kind of T_c shifting and decreasing of crystallinity means the interfacial chemical reaction interfered with the crystallization of PET and altered the nature of the phase. This could be due to the large amount of copolymer of PET and HDPE formed by the binding reaction between epoxy of HDPE-g-epoxy and PET end groups. Thus, indirectly, it has been proven

again that the compatibilizer formed during the compounding is an effective interfacial agent between the two compatibilized components

6.3.6 The Side Reactions

Strictly speaking the shifting of PET crystallization peak in DSC spectra discussed above could also be attributed to the side reaction between PET and residue GMA monomer or GMA oligomer remaining in the grafted HDPE. Since the grafted HDPE used in the compatibilization was not purified, there could be certain amount of unpolymerized GMA monomer and GMA oligomer in the grafted HDPE. Some amount of them might have been vaporized at the vent port of the extrusion system (as shown in Figure (4-1)), but it is still quite possible that residual amounts of GMA or GMA oligomer will remain in the extrudate. The residue GMA monomer could consume some PET end groups during the compounding while GMA oligomer, as it has above two epoxy units, might connect PET and extend PET molecular chains. This kind of chain extending of PET might have shifted the crystallization peaks of PET as illustrated above. From bulk properties point of view the extending of PET molecular chains might help PET trap and stabilize HDPE domains, and increase the tensile strength of PET component However, excessive chain extending and branching may decrease the ductility of PET component, extremely consume the PET end groups, and form a competitive pair with the main reaction of epoxy grafted HDPE and PET

In order to clarify the influence of residual GMA oligomer on the compatibilizing reaction, a certain amount of GMA oligomer was extruded with the HDPE/PET (50/50) blends. The GMA oligomer had M_n of 3 000 by GPC measurement and was synthesized by bulk radical polymerization, quenched in methanol and dried in vacuum oven. Figure (6-14)

shows that the T_c of PET increases with the increasing amount of oligomer. Obviously this is because of chain extending of PET caused by chain knitting of GMA oligomer which dramatically increased the molecular weight of PET. As a result, GMA oligomer, if remains in the grafted HDPE, could only increase the T_c of PET component in the blend instead of decreasing the T_c. If PET chains extending caused by residue GMA oligomer predominates over the interfacial reaction between PET and grafted HDPE, the T_c of PET component should increase after blending with grafted HDPE. However, from DSC spectra shown in Figure (6-13), the T_c of PET unidirectionally shift to low temperature. Based on this phenomenon, it can be concluded that the reaction between PET and grafted HDPE dominate over PET and GMA oligomer. In other words, under the current grafting condition, the residual amount of GMA oligomer is so trivial that the main reaction is still the interfacial reaction between PET and grafted HDPE.

6.3.7 The Mechanical Properties

In order to clearly indicate the effect of compatibilization on the mechanical properties, compatibilized HDPE/PET (50/50) ratio which originally had the worst mechanical properties among all of the ratios, is chosen to detect the tensile and flexural properties. As shown in Table (6-3), the overall improvement of the mechanical properties after compatibilization is very obvious. For tensile properties, both tensile strength and elongation at break have been increased dramatically. This is attributed to improved adhesion in the compatibilized blends that facilitated stress transfer and increased the load-bearing capacity. However, extra high concentrations of grafted HDPE (35%) dose not result in higher elongation. This is due to the high degree of crosslinking caused by the excessive

reaction. The high crosslinking density can also be seen from its high modulus and yield strength values of the blends.

HDPE has better impact properties than PET. In this case, HDPE could function as an impact modifier for PET. However, without any compatibilization, the impact strength is very poor because of the poor adhesion between the two phases. After only 10% of grafted HDPE is added, the impact strength jumps to double the original value. With more compatibilization introduced, the impact strength increased even more.

In conclusion, the compatibilization can bring in dramatic improvements on both impact and tensile properties. The mechanical properties improvement could be attributed to many factors, especially to the morphologies as previously illustrated. It seems that the fine and uniform distribution of the dispersed domains in addition to the intimate and rough interfacial morphology would usually result in high mechanical properties. However, in polymer compatibilization, the relationship between morphologies and mechanical properties is not so regular. As will be discussed in Chapter 8, in some cases, a finer morphology does not guarantee better mechanical properties.

6.4 Conclusions

In this study, HDPE-g-epoxy are used to compatibilize the HDPE/PET blend. The effect of compatibilization can be manifested by the great improvement of the overall properties including processability, morphology and mechanical properties. The compatibilization mechanism is studied by torque measurement, DSC detecting and morphology study. Following conclusions can be drawn.

1. Compared to the uncompatibilized control blends, the reactive compatibilized

blends of HDPE/PET show greatly reduced HDPE domain size, uniform domain distribution, and blurred interfaces according to the morphological study. This can be attributed to the copolymer of HDPE and PET formed by the chemical reaction between the grafted epoxy group on HDPE backbone and the end groups of PET. The copolymer functioned as a compatibilizer for the two phases and effectively increased the interfacial adhesion, reduced dispersed phase size, and stabilized the morphology.

2. Based on the torque measurement, it can be concluded that most of the reaction could be achieved within the first 3 mins, which could be shortened further in the twin-screw extruder via high shear rate. The reaction intensity increased with the increasing amount or the increasing graft ratio of the grafted HDPE, but the excessive reaction might result in the poor processability of the extrudate.

3. The compatibilization has a clear reflection on the crystallization transition of PET component of the blends, the peak position shifts to the lower temperature and the crystallinity decreases as the degree of compatibilization increases. The similar DSC study was used in the investigation of the PET chain extending, which was caused by the residue GMA oligomer formed during the grafting. It is concluded that the chain extending of PET by the GMA oligomer is trivial.

4. There is an obvious improvement in mechanical properties for the compatibilized blends compared with the uncompatibilized blends. Both tensile and impact strength are dramatically improved. The tensile testing indicated that there was an optimum concentration of grafted HDPE for the compatibilization. Above the optimum concentration, the excessive reaction may result in high modulus and poor ductility.

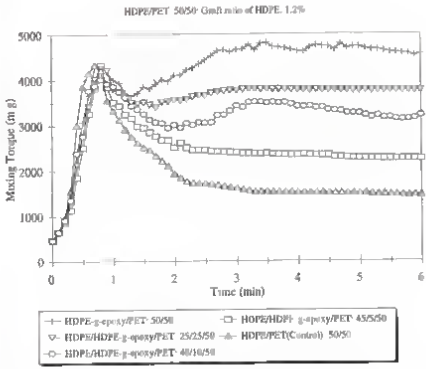

Figure (6.1) The torque vs time curves for the control and compatibilized HDPE/PET (50/50) blends with varied amount of grafted HDPE added. The graft ratio of grafted HDPE, 1.2%. Temperature of the measuring head was 280°C, RPM 60.

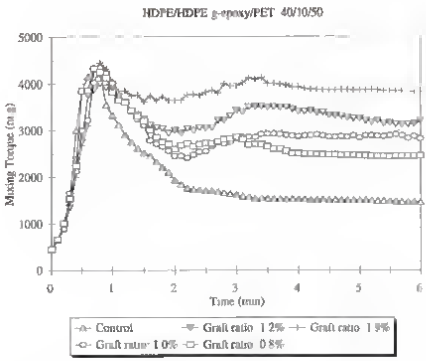

Figure (6-2) The torque vs. time curves for the compatibilized HDPE/grafted HDPE/PET (40/10/50) blends with varied graft ratio of the grafted HDPE. Temperature of the measuring head was 280°C. RPM 60

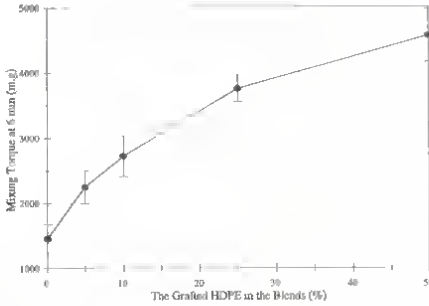

Figure (6-3) Effect of grafted HDPE concentration on the mixing torque at 6 min of mixing for HDPE/PET (50/50) blends

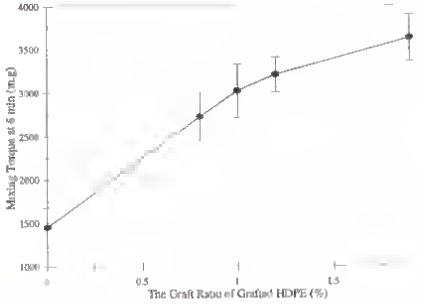

Figure (6-4) Effect of the graft ratio on the mixing torque at 6 min of mixing for HDPE/grafted HDPE/PET (40/10/50) blends

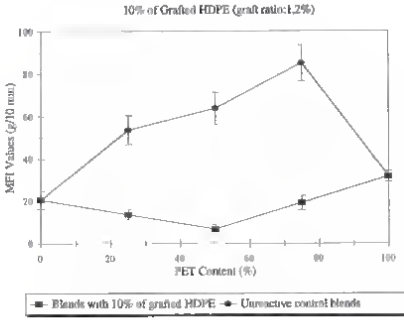

Figure (6-5) Effect of 10% of grafted HDPE on MFI of HDPE/PET blends with various ratios

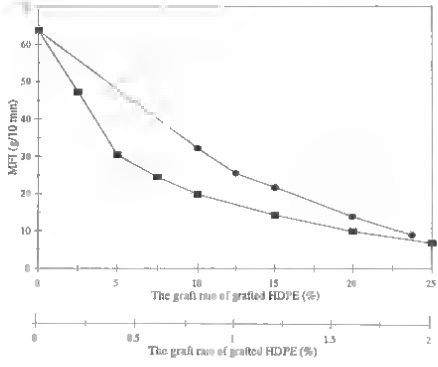

Figure (6-6) (■) Effect of different amount of grafted HDPE (graft ratio 1.2%) on the MFI values of the HDPE/PET (50/50) blends (●) Effect of different graft ratios of grafted HDPE on the MFI values of HDPE/grafted HDPE/PET (40/10/50) blends

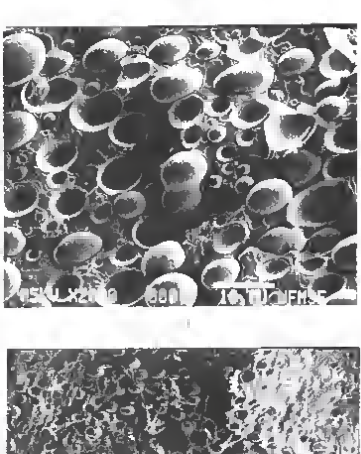

Figure 16.71 SEM fracture surfaces (X2000)
(a) Blend with composition HDPE/PET = 35/65 (Control sample)
(b) Blend with composition HDPE/grafted HDPE/PET = 32.5/2.5/65

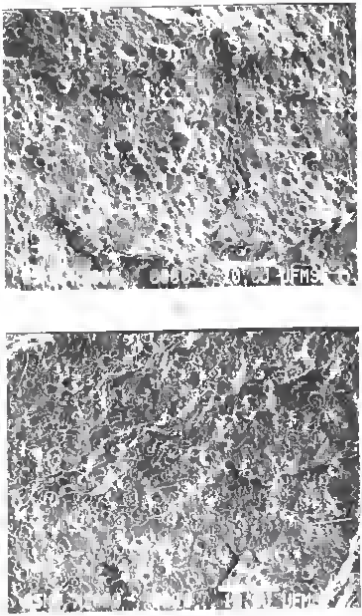

(d)

Figure (6.7 continued) SEM fracture surface. (X2000)
(c) Blend with composition HDPE/grafted HDPE/PET = 30/5/65
(d) Blend with composition HDPE/grafted HDPE/PET = 30/15/65

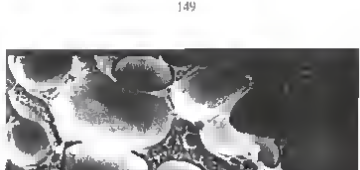

(a)

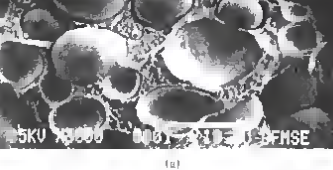

(b)

Figure (6.8) SEM fracture surface (X3000)
(a) Blend with composition HDPE/PET = 50/50 (Control sample)
(b) Blend with composition HDPE/grafted HDPE/PET = 45/5/50

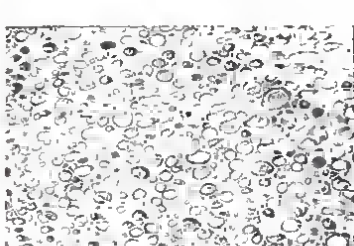

(c)

(d)

Figure (6-8 c continued) SEM fracture surfaces (X3000)
(c) Blend with compatibilizer HDPE/grafted HDPE/PET = 40/10/50
(d) Blend with compatibilizer HDPE/grafted HDPE/PET = 35/15/50

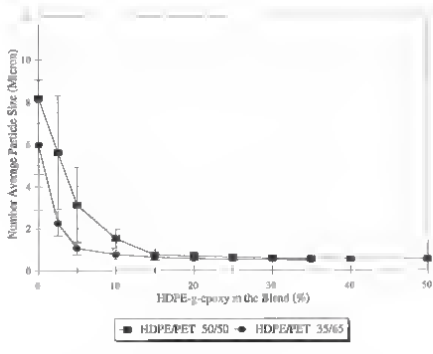

Figure (6-9) The decreasing domain sizes along with the increasing amount of grafted HDPE for HDPE/PET (35/65 and 50/50) blends

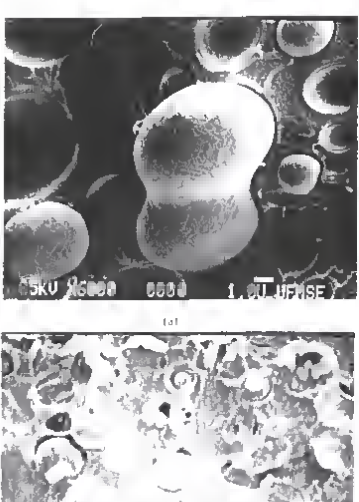

(a)

(b)

Figure (6.10) The comparison of interfacial morphologies of control and compatibilized HDPE/PET (35/65) blends. (a) The uncompatibilized blends(X6000). (b) Compatibilized blends with 5% of grafted HDPE (X10000).

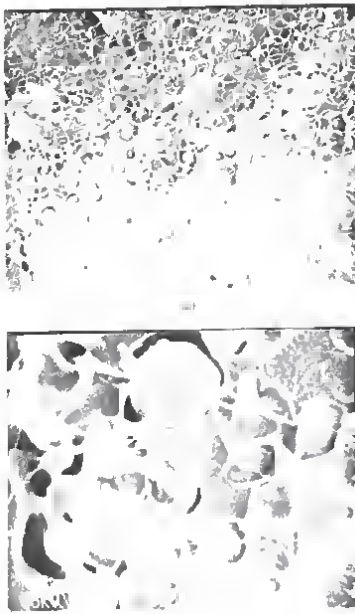

Figure (6-11) (a) The fracture surface of HDPE/grafted HDPE/PET (20/15/65) (X2000) (b) The larger magnification in the same area (X10000)

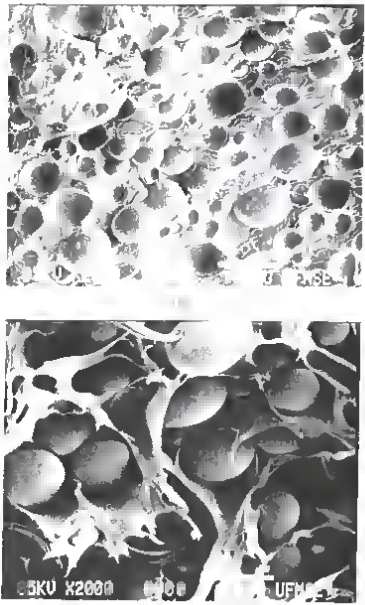

(b)

Figure (6.12) The comparison of morphology stability between HDPE/PET (35/65) blend and HDPE/grafted HDPE/PET (3%/5/65) blend (a) HDPE/PET (35/65) without any annealing (X2000) (b) HDPE/PET (35/65) with 10 min annealing at 260°C (X2000)

(c)

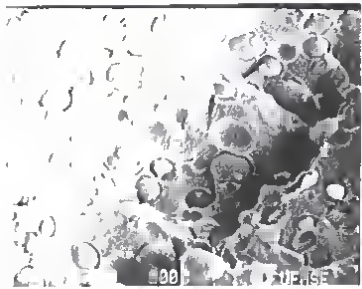

(d)

Figure (6.12 continued) (c) HDPE/grafted HDPE/PET (30/5/65) without any annealing (X6000) (d) HDPE/grafted HDPE/PET (30/5/65) with 10 min annealing at 260°C (X6000)

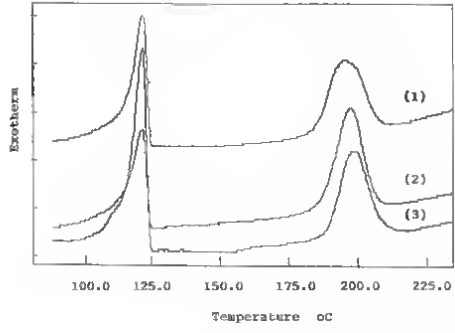

Figure (6 13) DSC spectra of control and compatibilized HDPE/PET (35/65) blends.
(1) HDPE/grafted HDPE/PET (15/20/65), T_c of PET component = 191.6°C
(2) HDPE/grafted HDPE/PET (25/10/65), T_c of PET component = 194.7°C
(3) HDPE/PET (35/65) T_c of PET component = 197.8°C

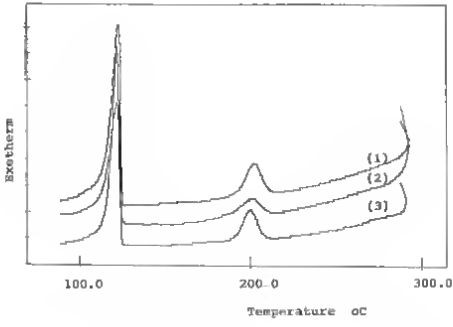

Figure (6-14) The effect of GMA oligomer on the DSC spectra of HDPE/PET (50/50) blends
(1) HDPE/PET/GMA oligomer = 50/50/1, T_c of PET is 205.8 °C
(2) HDPE/PET/GMA oligomer = 50/50/0.5 T_c of PET is 203.9 °C
(3) HDPE/PET = 50/50 T_c of PET is 200.2 °C

Table (6 1) The comparisons of grafted HDPE and pure HDPE

Properties	Pure HDPE	HDPE-g-epoxy with different graft ratios (%)			
		0 8	1 0	1 2	1 9
Gel amount (%)	0	0	0.17	0 24	0.57
T_m (°C)	136 8	137 1	136 9	137 7	138 1
ΔH_m (kJ/kg)	198 6	194 8	189 3	186.5	176 4
T_c (°C)	118 4	121 6	122 4	122.2	123 1
MFI (g/10 mins)	5.2	3 6	3 2	3 3	2 1

Table (6-2) The effects of compatibilization on the crystallization transition of PET component for HDPE/PET (35/65) blends

HDPE-g-epoxy Concentration wt.%	Normalized $\Delta H_{crystallization}$ for PET Component kJ/kg	PET T_c °C
Pure PET	42 6	197 8
5	41.3	195 5
10	38 7	194 7
15	37 2	192 1
20	35 1	191 6
25	34 5	191 7

Table (6-3) The effects of various amounts of compatibilizer on the mechanical properties of HDPE/PET (50/50) blends

Grafted HDPE (%)	STB (Kpsi)	Strain at Break (%)	E.to Failure (lbs/in^2)	STY (Kpsi)	Izod Impact (ft lbs/in)*	Flexural Modulus (Kpsi)
Control	3.57 ±0.12	13.22 ±1.25	334.82 ±103.74	6.41 ±0.11	0.4 ±0.2	241.8 ± 16.4
10	3.64 ±0.34	24.40 ±3.68	549.31 ±138.37	6.53 ±0.21	0.8 ±0.1	252.9 ± 12.8
15	4.28 ±0.38	30.87 ±3.48	943.74 ±129.95	6.47 ±0.25	1.5 ±0.3	254.8 ± 14.3
20	4.54 ±0.23	35.55 ±3.76	1045.27±106.69	6.63 ±0.34	2.3 ±0.4	271.8 ± 11.8
25	4.76 ±0.29	38.17 ±3.50	1428.61±132.12	6.84 ±0.19	3.8 ±0.6	274.6 ± 13.8
30	4.92 ±0.24	32.53 ±4.04	1231.95±189.23	6.98 ±0.17	4.2 ±0.5	284.5 ± 11.5

STB Strength at Break, E to Failure Energy to Failure, STY Strength at Yield,
* The Izod impact property was detected under room temperature with notched specimen.

CHAPTER 7
THE REACTIVE COMPATIBILIZATION OF PVC/POLYOLEFIN BLENDS

7.1 Introduction

In chapter 6 two major components of recycled plastics, PET and HDPE are reactive compatibilized using GMA grafted HDPE (HDPE-g-epoxy).The compatibilization mechanism is based on the interfacial reaction of epoxy group of the HDPE phase with the carboxylic acid or the hydroxyl groups of PET end groups. In this chapter, GMA grafted polyolefins are used to compatibilize two other major components of recycled plastics. Poly(vinyl chloride) (PVC) and polyolefins. PVC and polyolefins constitute about 50% of all polymer waste [101]. Due to the thermodynamic incompatibility of PVC and polyolefins, processing of PVC/polyolefin mixtures is unlikely to yield products with usable mechanical properties. This incompatibility is due to the apolar molecular structure of polyolefins and the highly polar structure of PVC. Early in 1973, Paul [102, 103] used chlorinated PE (CPE) as a compatibilizer to upgrade recycled PE/PVC blends. Later, Nakamura applied the crosslinking technique to form cocrosslinked product at the PE/PVC interface [104]. Francis [101] compared the two most widely used crosslinking techniques, peroxide and irradiation, and found that peroxide is more effective and economical than the other. Further, Xu [105, 106] employed nitrile rubber (NBR) and peroxide trying to form compatibilization-crosslinking synergism in PVC/LDPE blends. Recently, Ajji [107] used methylmethacrylate ethylacrylate

copolymer as a processing aid along with various additives such as ethylene-vinylacetate copolymers, ethylene-methacrylic acid ionomer and peroxide to compatibilize PVC/recycled polyethylene blends. From the wide variety of publications, it is clear that, until now, there was no efficient and cost-effective compatibilizer available which can be applied to PVC/polyolefin blends on a large scale. The copolymers used as compatibilizers are usually extremely expensive due to the high cost synthesizing route. The peroxide can cause dehalogenation of PVC although it may possibly induce graft structures at the interfaces of the blends.

In this part of study, the author attempts to develop compatibilized PVC/polyolefins blends based on GMA grafted polyolefins which are synthesized by melt grafting as illustrated in chapter 4. The reactive epoxy groups can connect the polyolefin backbones with those of other polymers by chemical bonding, by which the copolymer functioning as compatibilizer for the blend could be formed *in situ* during the melt processing. This kind of *in situ* compatibilization has been successfully used for polyolefins/PET blends in Chapter 5. Unlike PET, however, PVC in this blending system has no reactive sites to form direct bonds with the grafted polyolefins. In this study, an indirect bonding between PVC and polyolefins is investigated using carboxylated nitrile rubber (XNBR) as another reactive component. This kind of compatibilization route is named as dual-functional-polymer compatibilization model, which has been successfully developed in our research group. Basically, for this model, the compatibilized blends is composed of four components, like A/A a/B b/B. Here, the A and B are two polymers that need to be compatibilized, A-a and B-b are two functional polymers which are miscible with the A and B components, respectively. The a and b groups are reactive with each other. In the polyolefin/PVC compatibilization, nitrile rubber is

thermodynamically miscible with PVC while the reactive carboxylic acid groups of XNBR can form chemical bonds with the epoxy groups of the grafted polyolefins. In this way, the *in situ* formed compatibilizer, polyolefin-g-XNBR, can be generated during melt processing.

Similar to Chapter 6, the improvement of mechanical properties caused by the compatibilization and the mechanism of compatibilization will be discussed in detail in this chapter. In addition, the interfacial chemical reaction is optimized by mixing sequences.

7.2 Experiment

7.2.1 Materials

The polymers used in this study included PP (Tenite polypropylene PSM2Z-012) offered by Eastman Chemical Company, HDPE acquired from Waste Alternative Co. with a MFI of 5.2 g/10 min, PVC (Geon 87444 transparent pellets 004) generously donated from Geon Company, and carboxylated NBR (XNBR) acquired from Mde Inc. Two kinds of XNBR are used. Krynac X1.46 having an acrylonitrile(AN) unit content of 31-34 wt.% and carboxylic acid content of 1.46 wt. %, and Krynac X7.50 having an acrylonitrile (AN) unit content of 27 wt.% and carboxylic acid content of 7.5 wt. %. The grafted polyolefins HDPE-g-epoxy and PP-g-epoxy were synthesized as described in Chapter 4 and their physical properties are listed in Table (7-1).

7.2.2 Procedures

Polymer blends were prepared by twin screw extrusion (Brabender Plasti-Corder pl2000) at 60 rpm and 180°C. A thermal stabilizer, Irganox B215 (Ciba Geigy, 0.1%), was

used for the PP processing. The weight percents of the blends ranged from XNBR 5%, PVC 20% grafted polyolefins 10-30%, polyolefins 35-65% XNBR was cryogenically crushed to powder before processing. When preparing XNBR coated PVC particles the PVC was ground to a powder first and then XNBR dissolved in methylene chloride. The PVC powder was then coated with the XNBR/methylene chloride solution and then the solvent was vaporized in vacuum oven. After blending the extrudate was water quenched and pelletized. The pelletized blends were dried in air and then transferred to a compression molder to be pressed into tensile specimens at 170°C under 2000 lb for 15 min.

7.2.3 Characterizations

Tensile testing was carried out at room temperature according to ASTM D638 and at a strain rate of 2 in/min. Notched Izod impact tests were conducted according to ASTM D256. All test specimen were injection molded at 3000 psi to a thickness of 6.98 mm. For morphological evaluation, the blends were cryogenically broken in liquid nitrogen and examined by scanning electron microscopy (SEM) after coating with a thin gold film. The melt flow index (MFI) of the blends was measured according to ASTM D 1238 using a Tinius Olsen extrusion plastometer. The torque values used to investigate the interfacial reaction were detected by using a Brabender measuring head driven by a Brabender plasti-corder pl2000. The temperature of the measuring heading was kept at 180°C while the blades rotated at 60 rpm. The torque data were acquired by a PC computer. FTIR was conducted using Magna IR spectrometer 450. The transparent sample film was prepared by compression molding at 180°C.

7.3 Results and Discussion

7.3.1 The GMA Grafted Polyolefins

In this investigation, glycidyl methacryate (GMA) grafted HDPE and PP (HDPE-g epoxy and PP-g-epoxy) are used as grafted polyolefins in the compatibilization. The details of the melt grafting and its advantages are discussed in Chapter 4. Table (7-1) summarizes information about the grafted HDPE and grafted PP used in this study. The peroxide used in grafting results in a small amount of crosslinking in the grafted HDPE and some thermal degradation of the PP resulting in a low or a high MFI value, respectively. The crosslinked PP g-epoxy which was synthesized in Chapter 5 is also used in this study in order to see the effects of the crosslinks of the grafted PP on the compatibilization. The crosslinked PP g epoxy has a lower graft ratio than degraded PP g-epoxy, however, it has superior mechanical and rheological properties as illustrated in Chapter 5.

7.3.2 The Mechanism of Compatibilization

The theoretical base for the design of this compatibilized blending system is that PVC is totally miscible with nitrile butadiene rubber (NBR) if the acrylonitrile content of NBR is higher than 23% [108]. For the carboxylated NBR, although it has small amount of carboxylic unit on its backbone, it does not interfere with this miscibility [109]. Meanwhile, the carboxylic acid groups offer the potential chemically reactive site for the PVC/XNBR phase to form interfacial bonding with the epoxy grafted polyolefin phase by esterification (Figure (7-1)). This reaction results in the binding between the two originally immiscible polymer phases.

There are complicated physical and chemical interactions among the four components (polyolefin, grafted polyolefin, XNBR and PVC) of this blend during melt processing. Besides the chemical bonding formed between the carboxylic acid groups of XNBR and the epoxy groups of grafted polyolefins described above, the other major interactions are classified below:

1 XNBR and PVC (strong specific interaction)

There are numerous publications about the miscibility of NBR and PVC [109-111]. This miscibility increases with increasing acrylonitrile unit content in the rubber. Zakrzewski found that the critical acrylonitrile (AN) content to form a total miscible blending system with PVC is 23% [108]. It has recently been reported [112] that NBR/PVC blends can also be self-crosslinked under higher temperatures and long processing times.

2 XNBR and HDPE (Interaction in crystalline region)

In the past, NBR was believed to be incompatible with polyolefins, especially for NBR with high AN content. However, recently it has been reported that when NBR chains are forcefully dispersed with PE during melt blending, they are not able to separate entirely from the HDPE phase before HDPE crystallizes. The NBR chains become trapped by the crystalline region when the blend is cool [113]. Therefore, the NBR with high AN content used in this study can be confidently assumed to have certain interactions with the HDPE crystalline region.

3 Polyolefin-g-epoxy and PVC (weak specific interaction)

Because of the apolar nature of the polyolefin molecular chain, the specific interactions between PVC and polyolefin phases are very weak compared with the specific interactions between XNBR and PVC. However, melt grafting the polyolefins by GMA can

increase the polarity of the polyolefins facilitating miscibility between the polyolefins and PVC. Also, the number and the length of the grafted GMA chain can greatly affect this interaction.

Benedetti [114] in his investigation on a di-n-butyl-phthalate (DBP) grafted polyolefin/PVC system pointed out that DBP gives rise to interaction with PVC mainly through a hydrogen bond between the carbonyl group of DBP and the methine hydrogen of PVC. It is shown that the dipole-dipole interaction of the type -C=O----Cl-C could also be involved. Since the grafted GMA has a similar ester structure to DBP, it is safe to infer that there should be a similar specific interaction between PVC and the GMA grafted polyolefin. In a very recent publication, D'Alessio [115] studied the interaction between grafted polyester and PVC, and noticed that the high mobility of the grafted ester groups improves the specific interaction. In our case, since the polyolefin-g-epoxy has a grafting structure, the pendent poly(glycidyl methacrylate) may have higher possibilities of forming interactions with the PVC component than the commonly used block or random copolymers. Figure (7.2) shows the proposed mechanism of the interaction for grafted polyolefin and PVC.

7.3.3 The Effects of XNBR on the Compatibilization

As mention before, XNBR offers chemical bonding between polyolefin and PVC/XNBR phases because of its miscibility with PVC and its chemical interactions with polyolefins due to its reactive carboxylic acid group. Besides this, it improves the impact property of the blend. It also increases the melt viscosity during the melt processing, increasing the shear force and making the components well dispersed. Xu [106] used NBR in his PVC/LDPE blending and found that NBR upgrades the phase dispersion and decreases

the domain size of the minor component A similar phenomena is also observed in the improvement of tensile properties for PVC/HDPE blends brought by the addition of XNBR in this study As shown in Figure (7 3), when 5% of XNBR is added tensile strength and elongation at break increases simultaneously which indicates that XNBR can function as a quasi-compatibilizer for the blend Unfortunately XNBR has poor tensile strength after 5% of XNBR is added, any increase in XNBR content decreases tensile strength although the elongation at break increases In this study the amount of XNBR is kept at 5% in order to keep the highest tensile strength

7.3.4 The Improvement of Tensile Properties by Compatibilization

Table (7 2) lists the improved tensile properties for the uncompatibilized control sample and compatibilized blends The HDPE/PVC(50/20)(control 1) blend has rather poor tensile properties especially with respect to its elongational property owing to the incompatibility of the components When 5% XNBR is added without any grafted HDPE (control 2), tensile strength and elongation at break increase to a certain extent, revealing that XNBR can improve interfacial adhesion.

When only 5% epoxy grafted HDPE is added, the tensile properties of the blend increase significantly In this case XNBR connects to HDPE both by the trapping within crystalline regions and by, more efficiently the formation of chemical bonds between carboxylic groups and epoxy groups.

There are improvements in tensile strength but more significant improvements are noted in the strain at break values which directly contribute to increased toughness. As the tensile specimen were prepared by compression molding the factors like zero orientation and

having adequate time for crystallization made the overall values of elongation low However, the differences between the compatibilized and uncompatibilized blends are dramatic

There are also certain improvements of tensile properties for compatibilized PP/PVC, but not so extreme as the HDPE/PVC blends (Table (7-3)) This could be due to the low graft ratio of PP g-epoxy (0.75%) Another possible reason is the low melt viscosity of degraded PP g-epoxy (MFI 67 8 g/10 min) which makes it difficult to disperse into PP or PVC phases Table (7-4) compares the differences of mechanical properties of PP/PVC blends compatibilized by degraded PP-g-epoxy and crosslinked PP g-epoxy There are certain improvements in strength at break (STB), modulus, and strength at yield (STY) especially the elongational properties for the crosslinked PP g-epoxy compatibilized blend Since the graft ratios of the degraded PP-g-epoxy is higher than that of crosslinked PP g-epoxy (as shown in Table (7 1)), the only possible cause of the better tensile properties of blends compatibilized by crosslinked PP-g-epoxy could be their different melt viscosities As it is well known, the viscosity ratio is a controlling parameter in the micromechanics of the melt drop breakup. The viscosity similarity between crosslinked PP-g-epoxy and pure PP facilitated PP-g-epoxy homogeneously disperses into PP phases. For degraded PP-g-epoxy, its much lower melt viscosity makes it agglomerate during its melt blending with pure PP and PVC, and function as a lubricant for PP phase. As the shearing force which affected the PP phase is weak, the phase dispersion of PP phase is insufficient which results in poor compatibilizing effects compared with crosslinked PP g-epoxy with higher melt viscosity

7.3.5 The Confirmation of Interfacial Reaction

As shown in Figure (7-1), the interfacial reaction results in ester bonding and hydroxyl groups· the epoxy groups and carboxylic acid groups are consumed. Unfortunately, both newly formed ester and hydroxyl groups are covered by the original ester groups of the GMA and the hydroxyl groups of the XNBR and cannot be used as a judgement of the reaction. In addition, the epoxy group has no strong absorption in the FTIR spectrum and is difficult to discriminate. However, the consumption of the carboxylic group can be detected by the decreasing absorption of the carbonyl group (1700 cm^{-1}) which is not covered by the carbonyl group from GMA (1730 cm^{-1}). Figure (7-4) shows the FTIR spectra of compatibilized blend (PP/grafted PP/XNBR/PVC(60/15/5/20)) and control blend (PP/XNBR/PVC(75/5/20)). Comparing the control and compatibilized samples, both have a strong absorption around 1731 cm^{-1} corresponding to the carbonyl stretching vibration of the ester structure [116] relating to the ester structure of GMA or those formed by the reaction. For the control spectrum, there is also a small peak at 1700 cm^{-1} corresponding to the carbonyl stretching vibration of R-CO_2H structure [116]. This peak disappears in the spectrum of the compatibilized sample, while the carbonyl stretching peak of the ester structure becomes strong. The disappearance of carbonyl stretching absorption of the R-CO_2H characteristic peak and the intensification of the ester peak indicates that the carboxylic acid group on the XNBR backbone has been consumed by the reaction with epoxy group and a new ester bonding formed during the melt processing. Thus indirectly, FTIR spectra confirms the exist of the reaction.

Torque value detecting of the reactive blending system is another widely used method to qualitatively determine the presence and intensity of interfacial reactions [43, 117]. In this study, it is used to get qualitative information about chemical reactivity and the extent of reaction between the epoxy groups and carboxylic acid groups. In order to excluded the effect from the GMA oligomer formed during grafting, the grafted polyolefins were purified by precipitating from hot toluene in methanol. Figure (7-5 b) shows Brabender torque plots as a function of mixing time for the control and compatibilized PVC/HDPE blends. According to the plot, PVC/XNBR/HDPE (20/5/80) (control sample 2) has a higher torque level than PVC/HDPE (20/80) (control sample 1). Obviously, XNBR efficiently increases the melt viscosity of the blend and consequently increases the shear force during processing. The compatibilized blends demonstrate a substantially higher torque level than both uncompatibilized control 1 and dispersion upgraded control 2. As the torque level of the individual component are much lower than that of the compatibilized blends, this kind of increment is only due to the interfacial chemical reaction which forms HDPE-g-XNBR graft copolymer at the interface functioning as the compatibilizer for the blend. Typically, after 12 min, the torque stabilizes and no further changes occur.

For the control and compatibilized PP/PVC blends (Figure (7-5 c), a similar phenomenon is observed. The compatibilized blends have higher torque levels than both control samples, although PP-g-epoxy added for compatibilization has a much lower torque level than any other component as shown in Figure (7-5 a). Unlike HDPE/PVC blends, the PP/grafted PP/XNBR/PVC results in slightly decreased torque values after long time mixing (>15 min). The likely reason for this is the degradation accelerated by the residual peroxide. When the thermal degradation of PP increases to a certain level, the increased molecular

weight of the blend can no longer compensate for the low molecular weight of degraded PP

The interfacial reaction is confirmed further by the decreasing melt flow index (MFI) values of the blends with the addition of grafted polyolefins (Figure (7-6)), thus indicates that the increasing molecular weight is caused by the esterification reaction and higher interfacial friction.

The effect of compatibilization on morphology is shown in Figures (7-7) and (7-8) The uncompatibilized HDPE/PVC(80/20) blends (control 1) have a much bigger domain size than HDPE/XNBR/PVC (80/5/20) blends (control 2) (Figure(7-7), obviously, the high shear force caused by the addition of XNBR effectively reduces the PVC domain size When 10% of HDPE g-epoxy is added (Figure (7-8 b), PVC domain size is dramatically reduced because of the *in situ* formed compatibilizer Further additions of grafted HDPE to the blend (Figure (7-8 c)) results in smaller, more dispersed particles Another morphological feature of the compatibilized blends is the uniform dispersion and narrow distribution of domain size The smaller domain size, homogenous dispersion and narrow domain size distribution contribute to the improved mechanical properties of the compatibilized blends as illustrated before Theoretically, PVC and XNBR should form one phase because of their miscibility, but during mixing, it is possible that some of the XNBR has no chance to contact the PVC and forms a separated phase. The domains in the SEM pictures might be PVC, XNBR or PVC/XNBR particles, with PVC/XNBR being the majority However, it is clear that the minor components have small domain size and dispersed uniformly in the polyolefin matrix.

7.3.5 Maximizing the Interfacial Reaction by Different Mixing Sequences

The effects of different sequences of component addition on blend compatibilization are studied in some recent publications [118, 119, 92]. It is clear that the *in situ* formation of the compatibilizer and its distribution can be affected by different sequences and modes of component addition [92]. In this study, the prerequisite for the formation of the compatibilizer (polyolefin-g-XNBR) is that the epoxy grafted polyolefins and the XNBR component have enough opportunity to disperse to the interfaces of the polyolefins and the PVC so that they can react with each other. Since both grafted polyolefins and XNBR are minor components, the opportunity for them to contact with each other during melt processing is limited according to the statistics. In order to optimize the phase dispersion and the reaction probability, different mixing sequences and mixing modes are studied as listed below so that the processing times of different components, the initial distribution of the two reactive components, and the dispersion effects can be changed.

Sequence 1: [HDPE + HDPE-g-epoxy + XNBR + PVC] (one-step)

Sequence 2: [HDPE + HDPE-g-epoxy + XNBR] + PVC (two-step)

Sequence 3: [HDPE + HDPE-g-epoxy] + XNBR coated PVC powder (two-step)

Sequence 4: [PVC + XNBR] + HDPE + HDPE-g-epoxy (two-step)

Sequence 5: [HDPE + HDPE-g-epoxy] + [XNBR + PVC] (three-step)

Sequence 6: [HDPE-g-epoxy + XNBR] + HDPE + PVC (two-step)

[A+B] +C +D: A and B are extruded first, then the pellets of A/B are extruded with C and D.

[A + B + C + D]: A, B, C and D are dry mixed first then extruded together.

[A + B] + [C + D] A and B are extruded first, then C and D are extruded. The pellets of A/B and C/D are dry mixed and extruded together

In sequence 1 all of the components are added together in the extruder It is the most convenient and popular method for compounding. Sequence 2, 4, 6 are two-step compounding methods where the four components of the blends are paired up in order to see the best combination. In sequence 3, XNBR is first dissolved in methylene chloride solvent then coated onto PVC powder so that the PVC particles have a XNBR film outside Sequence 6 is designed to provide the maximum probability of the two reactive components to react with each other then the major components are introduced later Sequence 5 is a three-step processing the two major phases are formed during a two-step precompounding then are compounded together in a third step

As the domain size, elongation properties and impact strength directly reflect the degree of compatibilization the comparison among these sequences is carried out by studying these properties. Figure (7 9) shows the SEM morphologies of blends by the different sequences Figure (7 10) shows the comparison of impact properties and elongation properties

Based on these results the most successful compatibilization sequence is sequence 3 To explain this it is very important to understand that the most successful compatibilization system should have the chemical reaction maximized at the interfaces of PVC and HDPE phases, which means the epoxy groups and carboxylic groups should be aggregated at the interfaces Sequence 3 is designed to make apolar HDPE and HDPE-g-epoxy (apolar backbone and polar grafted GMA unit) mixed first so that the polar and reactive GMA units can stretch out to the surface of the apolar HDPE phase. Obviously the grafting structure

facilitates this kind of stretching and makes the reactive groups pendant outside of the HDPE phase. In the second step of compounding, the XNBR has been coated onto the surface of the PVC particles, so that both reactive groups are accumulated at the interface, therefore most of the reaction takes place at the interfaces. Dagli [92], in his recent paper, studied the mixing sequences of HDPE/Ethylene-co-glycidyl methacrylate (EGMA)/PET blends and concluded that precompounding polar EGMA with apolar HDPE component results in a finer morphology and higher mechanical properties compared with other sequences. He attributes this phenomena to the preferred orientation of the polar GMA unit to the HDPE surface. In this study, even though there are four components, the similar phenomena is observed and the same explanation can be applied. This kind of phenomena was also illustrated by Willis and Favis [120] in their polyolefin/polyamide blends with an ionomer as the compatibilizer. They concluded that when one component of the blend is polar and the other is apolar, precompounding the compatibilizer (polar) with the apolar component resulted in a higher degree of compatibilization. As a result, it seems that the surface orientation of the reactive groups caused by the different polarity of reactive groups and its supporter or matrix is crucial in designing the proper mixing sequence.

The second most successful mixing method is sequence 2. In this case, XNBR is mixed with HDPE and grafted HDPE, then recompounded with PVC. The reason for the success of this sequence is quite similar to the explanation given previously. When HDPE, grafted HDPE and XNBR are precompounded, two phases are formed. One is HDPE/grafted HDPE phase with polar GMA units on the surface, the other is XNBR with the polar AN and carboxylic groups oriented toward the interface of the two phases because of the attraction of the polar GMA units on the surface of HDPE phase. Since the two reactive groups

accumulate on the interfaces, during the first compounding, the interfacial reaction is maximized. As the reaction system is diluted by the large amount of HDPE, there is no excessive reaction between the two reactive components, consequently, crosslinking caused by excessive reaction is not a problem for this sequence.

From an economical and simplicity of processing point of view, sequence 1 is the best choice. Surprisingly the overall mechanical properties and domain sizes are fairly good despite its simple procedure. In this case, separated melting or softening of the components could be an explanation. It is well known that HDPE with its high crystallinity melts in a short time period, while the softening of amorphous and rigid PVC would last a longer time in the extruder. When the four components are added to the extruder at the same time, HDPE and grafted HDPE are completely molten first, then XNBR softened and finally PVC softened. This kind of melting and softening sequence causes a very similar situation to sequence 2 where HDPE, grafted HDPE, and XNBR are precompounded then PVC introduced.

From the above sequences, we can see that the success of these compatibilizations can be attributed to the aggregation of reactive groups at the interfaces. The maximizing of epoxy concentration at interface is achieved by the different polarity of the GMA units and the HDPE matrix, while the XNBR concentration at interface is achieved by physical surface coating or the different softening sequence of XNBR and PVC.

Sequence 5 has a inferior morphology and properties than the above three sequences although it is a 3-step sequence. In this sequence PVC and XNBR are deliberately mixed separately in order to have XNBR dispersed well in the PVC phase. However, when PVC(20%) and XNBR(5%) are mixed the butadiene part of XNBR, an apolar segment,

prefers to orient to the surface of the PVC phase while the carboxylic group, which is the polar structure, tends to be enveloped inside the PVC phase instead of stretching out. Although the second compounding makes the GMA unit on the surface of the HDPE phase, it has a lower chance of contacting with the enveloped carboxylic group. This might cause the properties of this sequence to be inferior to the above three sequences. Also, it is a 3-step sequence with two compoundings of PVC and XNBR which may cause crosslinks between PVC and XNBR [112] or in XNBR itself, this could trap the XNBR phase and prevent it from dispersing to the PVC surface. In addition, the dehalogenation of PVC during the long processing time is another serious problem.

At first glance, sequence 6 could easily be regarded as the best design because the two reactive components, grafted HDPE and XNBR, have the most probability of reacting with each other to maximize the reaction. The reaction is do maximized, however, not necessarily at the interface. The more serious problem of this sequence is the difficulty in controlling excessive reactions, which may cause crosslinking and make the formed HDPE g XNBR copolymer difficult to disperse into PVC and HDPE phases because of its high crosslinking density and high melt viscosity. A similar phenomena has been observed in other studies [119, 92]. These results indicates that the esterification reaction should not only be maximized, but also controllable and happening at the interface in order to achieve the optimal compatibilization.

Sequence 4 has the worst mechanical properties and domain size improvements. From the SEM picture (Figure (7.9 d)), it has a relatively large domain size compared with all other sequences. As explained for sequence 5, in precompounding XNBR and PVC, the carboxylic groups tend to be enveloped inside the PVC phase. When HDPE and grafted HDPE are

introduced during the second compounding, the low content of grafted HDPE (15%) reduces the probability of its dispersion to interface and its reaction with the enveloped carboxylic group of XNBR. Consequently, there is not enough *in situ* formed compatibilizer and the blend is almost uncompatibilized

7.3.7 XNBR with High Acrylonitrile and Low Carboxylic Acid Content

In order to achieve a successful compatibilization, XNBR should not only be surface accumulated but also dispersed in and miscible with the PVC phase. Although the critical AN content is 23% for total miscibility with PVC, high AN content can increase the polarity of XNBR and consequently strengthen its specific interaction with epoxy grafted polyolefins and PVC. Also it makes XNBR disperse easily into the PVC phase.

The XNBR used above is Krynac X7.50 (carboxylation: 7.5%, AN content: 27%) which has high carboxylic content and low AN content. As an alternative, we tried X1 46NBR (carboxylation: 1.46%, AN content: 31.34%) which has a much lower carboxylation degree, but a higher AN content making it easier to form a miscible phase with PVC. A comparison of mechanical properties between these blends with two kinds of XNBR, as listed in Table (7-4), X7.50NBR appears to improve the properties more than X1.46NBR for the given blend ratio. X7.50NBR has a higher carboxylic acid content, therefore the higher content of reactive groups leading to a higher probability of interfacial reaction. On the other hand, the higher miscibility of X1.46NBR with PVC does not seems to bring an obvious benefit to the compatibilization compared with the high concentration of reactive groups. In a conclusion, if the AN content of XNBR is higher than the critical content (23%), the high reaction intensity between carboxylic group and epoxy group plays a more critical role than

the high specific interactions between PVC and XNBR or XNBR and grafted GMA unit on the polyolefin backbone.

7. 4 Conclusions

In this chapter, Polyolefin/PVC blends are compatibilized by using epoxy grafted polyolefins and carboxylated nitrile rubber (XNBR) as reactive components, following conclusions are drawn.

1. The *in situ* formed compatibilizer by dual-functional-polymer model, polyolefin-g XNBR, can effectively compatibilize polyolefin and PVC phases resulting in a dramatic improvement of mechanical and morphological properties. For the comparison of mechanical properties, the most dramatic improvements is the elongation property, which directly reflect the success of this compatibilization method.

2. The proposed compatibilization mechanism is the interfacial reaction between the carboxylic acid groups of XNBR and the epoxy group of the grafted GMA unit on the polyolefin backbone. This reaction is confirmed by comparison of FTIR spectra, torque values and melt flow index values of the uncompatibilized control blends and the compatibilized blends.

3. Based on the published studies of different blending systems, the mixing sequences of this system are compared. It turns out that the interfacial reaction can be optimized by selecting proper mixing sequences. The most successful mixing sequence is the one having the reactive groups - epoxy and carboxylic acid group - accumulated on the interfaces of HDPE and PVC, so that the *in situ* compatibilizer can be formed at the interfaces. The different polarities of the two reactive groups and their supporters, or matrices, play an

important role in this surface accumulation.

4. Two kinds of XNBR are used in the compatibilization. Krynac X7.50 with high carboxylic content and low AN content results in better properties than that of low carboxylic content and high AN content Krynac X1.46. It is concluded that if the AN content of XNBR is high enough to keep its miscibility with PVC, the degree of compatibilization of the blends is dependent on the probability of interfacial chemical reaction.

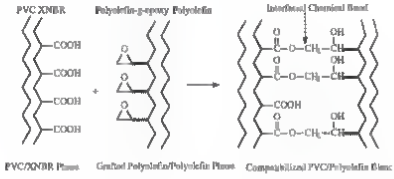

Figure (7-1) The chemical bonding between PVC phase and polyolefin phase

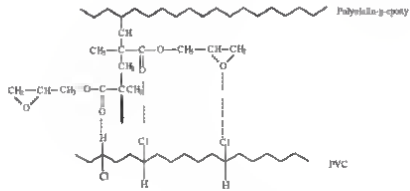

Figure (7-2) The proposed specific interactions between grafted polyolefin and PVC.

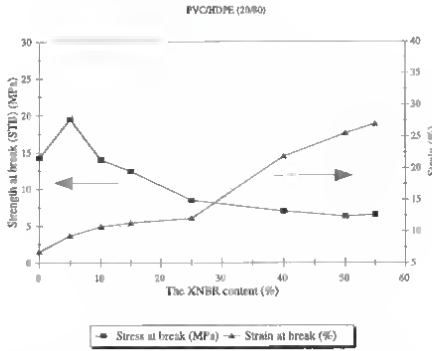

Figure (7.3) The influence of XNBR on the mechanical properties of PVC/HDPE (20/80) blends

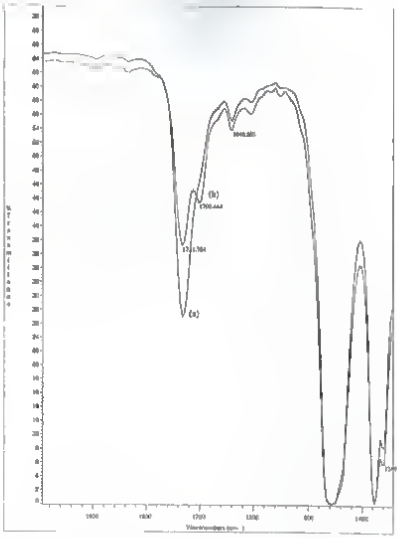

Figure (7-4) The FTIR spectra for
(a) The compatibilized PP/grafted PP/XNBR/PVC(65/15/5/20) blend.
(b) The control PP/XNBR/PVC (75/5/20) blend

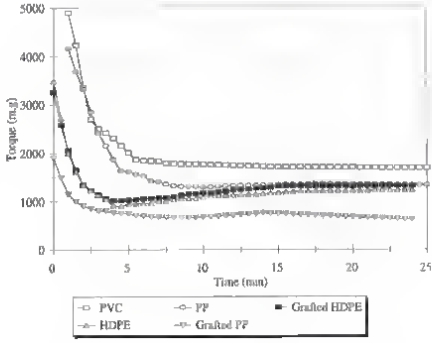

Figure (7-5) The torque measurements for (a) The blending components.

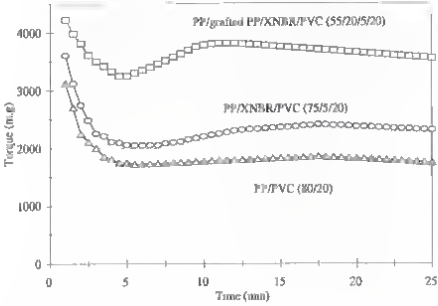

Figure (7-5 continued) The torque measurements for (b) Control and compatibilized PP/PVC blends

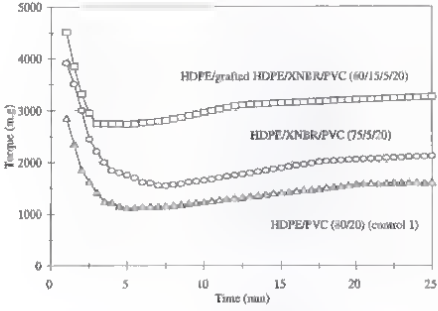

Figure (7-5 continued) The torque measurements for (c) Control and compatibilized HDPE/PVC blends

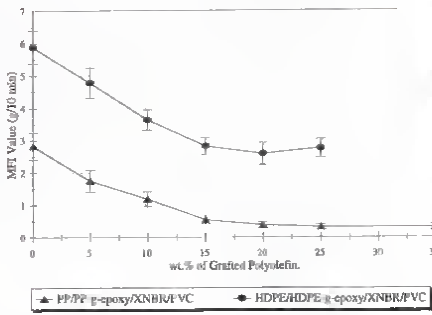

Figure (7-6) Melt flow index values for the compatibilized blends with different blending ratios.

(a)

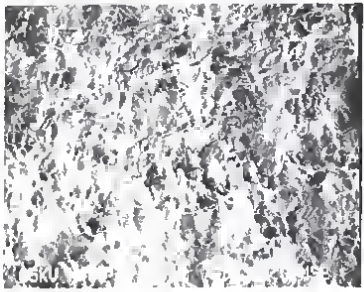

(b)

Figure (7.7) SEM fracture surface (×300)
(a) Blend with composition HDPE/PVC (80/20)
(b) Blend with composition HDPE/ANBR/PVC (80/5/20)

(a)

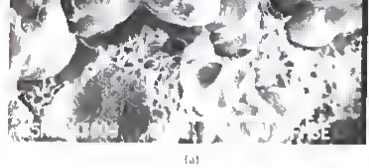

(b)

Figure (7.8) SEM fracture surface (X3000)
(a) Blend with composition HDPE/XNBR/PVC (80/5/20)
(b) Blend with composition HDPE/grafted HDPE/XNBR/PVC (70/10/5/20)

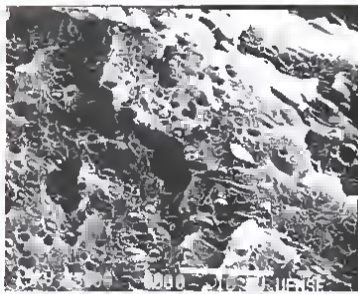

(c)

Figure (7.8 continued) SEM fracture surface (X3000)
(c) Blend with composition HDPE/grafted HDPE/XNBR/PVC (45/35/5/20)

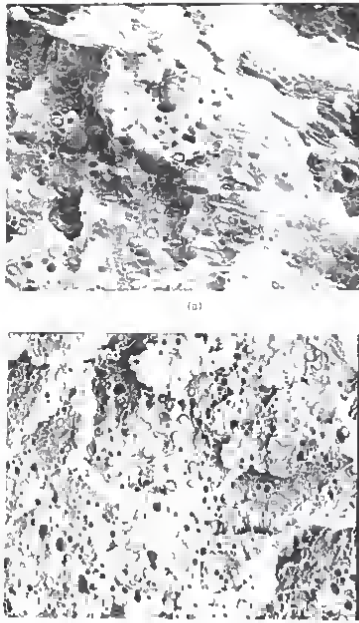

Figure (7.9) SEM fracture surface of HDPE/grafted HDPE/ANBR/PVC (45/35/5/20) blends by different sequences (X3000)
(a) Sequence 1 (b) Sequence 2

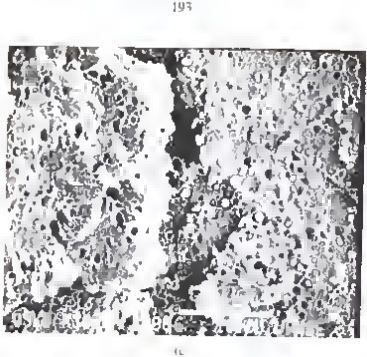

(c)

(d)

Figure (7.9 continued) SEM fracture surface of HDPE/grafted HDPE/XNBR/PVC (45/35/5/20) blends by different sequences (X3000)
(c) Sequence 3 (d) Sequence 4

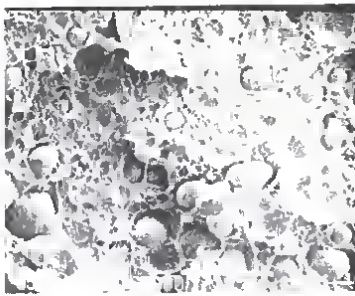

(e)

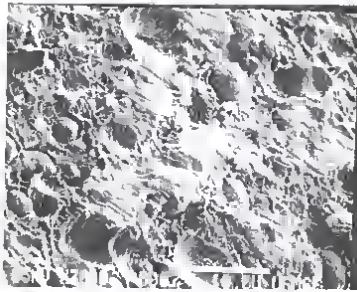

(f)

Figure (7.9 continued) SEM fracture surface of HDPE/grafted HDPE/NBR/PVC (45/35/5/20) blends by different sequences (X3000)
(e) Sequence 5 (f) Sequence 6

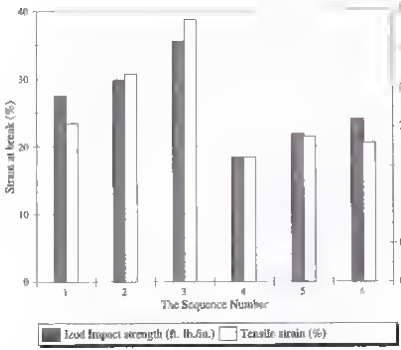

Figure (7-10) The comparison of Izod impact and elongation properties for the blends got from different sequences

Table (7 1) The comparison of the grafted polyolefins and the pure polyolefins

Properties	Pure HDPE	HDPE-g-epoxy	Pure PP	Crosslinked PP-g-epoxy	Degraded PP g-epoxy
Gel amount (%)	0	0 24	0	0 63	0
T_m (°C)	136 8	137 7	165 5	161 4	153 2
ΔH_m (kJ/kg)	198 6	186.5	106 7	101 6	103 5
T_c(°C)	121 4	122.2	112 4	111.5	107 6
Graft ratio (%)	0	1,2	0	0 62	0 78
MFI (g/10 min)	5 2	3,3	2 6	2 7#	67 8

Table (7-2) The Comparison of mechanical properties for the unreactive control samples (HDPE/PVC and HDPE/XNBR/PVC) and reactive compatibilized samples (HDPE/HDPE-g-epoxy/XNBR/PVC)

Table (7-2)	HDPE/HDPE-g-epoxy/XNBR/PVC				
Blend Ratios (%)	STB (Mpa)	Strain (%)	Modulus (Mpa)	E. to Failure (KJ/m^3)	STY (Mpa)
80/0/0/20 (Control 1)	14.26 (±1.35)	6.72 (±1.17)	460.77 (±35.72)	775.52 (±213.12)	16.27 (±2.28)
80/0/5/20 (Control 2)	19.51 (±2.28)	9.27 (±1.51)	438.17 (±51.69)	1255.66 (±380.45)	19.55 (±2.32)
75/5/5/20	20.66 (±2.59)	13.55 (±2.33)	382.59 (±16.61)	2034.2 (±582.52)	21.16 (±2.22)
70/10/5/20	20.99 (±1.84)	16.63 (±3.34)	381.85 (±14.78)	2610.31 (±682.83)	21.72 (±1.19)
65/15/5/20	21.3 (±2.17)	21.9 (±3.29)	400.79 (±29.98)	3868.54 (±691.58)	22.12 (±2.69)
60/20/5/20	23.19 (±2.36)	23.41 (±4.45)	369.73 (±35.67)	4365.18 (±772.22)	23.72 (±2.18)
45/35/5/20	22.6 (±0.93)	23.06 (±7.62)	392.33 (±36.14)	4405.61 (±613.06)	24.13 (±1.06)

STB Stress at break E. to Failure. Energy to failure STY Stress at yield

Table (7.3) The comparison of mechanical properties for the unreactive control samples (PP/PVC and PP/XNBR/PVC) and compatibilized samples (PP/PP g epoxy/XNBR/PVC)

Table (7.3)	PP/PP-g-epoxy/XNBR/PVC				
Blend Ratios (%)	STB (Mpa)	Strain (%)	Modulus (Mpa)	E. to Failure (KJ/m^3)	STY (Mpa)
80/0/0/20 (Control 1)	16.59 (±2.10)	9.58 (±3.21)	414.72 (±72.72)	1248.94 (±228.72)	16.27 (±2.28)
80/0/5/20 (Control 2)	17.29 (±1.69)	13.91 (±1.78)	346.90 (±51.51)	1869.15 (±407.96)	17.61 (±1.64)
75/5/5/20	19.96 (±2.64)	16.27 (±3.76)	327.57 (±51.76)	2483.79 (±652.58)	20.28 (±2.65)
70/10/5/20	19.40 (±2.11)	17.38 (±2.55)	341.54 (±22.84)	2555.44 (±549.96)	19.58 (±1.94)
65/15/5/20	19.62 (±2.02)	19.65 (±2.10)	335.43 (±46.30)	3020.55 (±379.40)	19.79 (±1.40)
60/20/5/20	19.45 (±1.65)	21.35 (±4.33)	327.96 (±28.78)	3433.96 (±953.40)	20.21 (±0.65)
55/25/5/20	21.42 (±0.86)	20.97 (±4.59)	304.94 (±25.71)	3434.44 (±895.34)	21.79 (±0.97)

Table (7-4) The different compatibilization effects of crosslinked and degraded PP g-epoxy

Sample*	STB (Mpa)	Strain (%)	Modulus (Mpa)	E to failure (kJ/m^3)	STY (Mpa)
Blend 1	21 42 ±0.88	20 97 ±4.50	304 94 ±25 71	3434 44 ±895.34	21 79 ±0 97
Blend 2	24 36 ±1 26	34 56 ±2.14	404 07 ±26 71	5261 68 ±287 20	24 85 ±2 10

* Blend 1 PP/PP-g-epoxy/XNBR/PVC (65/15/5/20)
Blend 2 PP/Crosslinked PP g-epoxy/XNBR/PVC (65/15/5/20)

Table (7 5) The comparison of the mechanical properties for the compatibilized blends by using X7.50NBR and X1 46NBR.

Table (7 5)	HDPE/HDPE g-epoxy/XNBR/PVC				
Blend Ratios(%)	STB (Mpa)	Strain (%)	E to Failure (KJ/m^3)	STY (Mpa)	Izod Impact Streng (ft-lb/in)
60/20/5/20 X7 50NBR	23 19± 2.30	23 41± 4.45	4365 18 ±1072.22	23 72 ±2 18	2 244 ± 1.3
60/20/5/20 X1 46NBR	22 85± 2.07	17 76± 5.68	3081 25 ± 1199.59	23 17 ±1 85	1 895 ± 2.7

STB Stress at break E to Failure. Energy to failure, STY Stress at yield

CHAPTER 8
THE REACTIVE COMPATIBILIZATION OF PP/ABS BLENDS

8.1 Introduction

In the study of last two chapters, GMA grafted polyolefins have been successfully used in the reactive compatibilizations of two polyolefins based polymer blends. They could compatibilize PET/HDPE blends based on the interfacial reaction between grafted epoxy groups on the HDPE backbone and the carboxylic acid or hydroxyl end groups of PET. For other polymers with no reactive end groups like PVC, the compatibilization can be carried out by adding a second reactive compatibilizer which is miscible with PVC but has reactive groups to accomplish the interfacial reaction with the polyolefin phase. Chapter 7 illustrates the successful compatibilization of polyolefin/PVC blends by adding two reactive functional polymers simultaneously which are miscible with their intended phases. In the studies of this dissertation, this compatibilization model is named as dual-functional-polymer model.

In this chapter, dual-functional-polymer model is applied in the compatibilization of another major recycled polymer blends, acrylonitrile-butadiene-styrene (ABS)/polypropylene (PP) blends, based on the reactivity of grafted epoxy groups on the grafted polypropylene (PP-g-epoxy) with another functional polymer which is miscible with ABS. ABS and PP are two major plastic components in the automotive industry. During recycling, they usually contaminate each other making it economically infeasible to separate them. Like any other recycled polymers, compatibilization is the only way to upgrade their physical properties and

find their high-value applications Similar to polyolefin/PVC blends, ABS in this blending system, has no reactive groups which can let the epoxy groups of PP-g-epoxy react with in order to form interfacial bonds Therefore it is necessary to find another functional polymer which is not only miscible with ABS but also reactive with PP g-epoxy

Recently ABS is being used as an impact modifier for various semicrystalline or amorphous polymers including PET [121] PBT [122, 123], nylon [124, 125], and PC [126] for improved low temperature impact properties The most common compatibilization strategy employs functional copolymers which are miscible with the styrene-co acrylonitrile (SAN) matrix ABS and have reactive groups to form interfacial bonds with other components Chung and Carter [121] patented a polymer which claims to have excellent low temperature impact properties based on polycarbonate (PC), poly(ethylene terephthalate) (PET), high butadiene content ABS rubber and styrene-acrylonitrile-glycidyl methacrylate (SAG) copolymer The SAG was synthesized by suspension copolymerization of styrene, acrylonitrile, and GMA monomers It is believed that the presence of SAG functions as a precursor of *in situ* compatibilizer between PET or PC and ABS rubber Suzuki and Yamamoto [122] briefly reported SAG as reactive compatibilizer precursor in the polymer blends of poly(butyl terephthalate) (PBT) and ABS Later, Lee, etc [123] reported a extreme upgrading of PBT impact properties by adding SAG SAG was also used to compatibilize nylon/ABS blend based on the reactivity of epoxy with the amine end groups of nylon [124, 125] Again, the high reactivities of epoxy groups with both acids and bases show the advantages of involving GMA monomer in the compatibilization of polyblends

Besides SAG another approach takes advantage of the fact that styrene-co maleic anhydride (SMA) copolymers are miscible with the SAN matrix of ABS within a certain

composition range [126-129]. Paul [126] successfully compatibilized nylon 6/ABS blends by using SMA with similar MA content to the AN content of SAN matrix of ABS. Here, the MA is not only the functional group for interfacial reaction, but also the cause of polarity of SMA for miscibility with SAN. It should be mentioned that SMA can only react with basic groups like amine groups or electrophilic groups like epoxy and oxazoline groups, and therefore could not be used as a compatibilizer for the PET or PBT/ABS blends. Taking the reactivity of SMA into account, it does not have the high versatility of SAG. However, SAG as a kind of functional copolymer, still has not been commercialized, while SMA has the advantage of low cost and commercial availability.

In this study, the PP/ABS blends are compatibilized by using the two functional polymers, SMA and PP-g-epoxy, to form *in situ* compatibilizer during melt blending. The selection of these two functional polymers is based on the considerations of their low cost and high reactivities with each other. As illustrated in previous chapters, PP-g-epoxy could be synthesized by melt grafting in twin screw extruder efficiently, while for SMA, as a well known functional polymer, it has been manufactured widely in polymer industry for years. On the other hand, epoxy functionalized polyolefin has extremely high reactivity with carboxylic acid group based on the reactivity study in Chapter 3. It can be inferred that the reactivity between epoxy and anhydride should be higher. The interfacial reaction between epoxy groups and anhydride groups is shown in Figure (5.1).

Similar to the other blending systems studied, this blending system is studied by comparing its mechanical and morphological properties with uncompatibilized blends. The intensity of interfacial reaction and its effect on the morphology and bulk mechanical properties are investigated.

8.2 Experiment

8.2.1 Materials

Table (8-1) summarizes pertinent information about the materials used in this work. PP-g-epoxy was synthesized by melt grafting according to Chapter 4. An ABS typical of the plastics used in engineering applications (ABS 541) was used. This material is a mass-made product which has a rubber content around 16% by weight in the form of below 0.5 μm particles. Its styrene-co-acrylonitrile (SAN) phase contains about 25% acrylonitrile content.

Table (8-1) The polymers used in this study

Materials	Materials/ Description	Composition	MFI (g/10min) or Molecular weight	Source
ABS	ABS 541	16% rubber 25% AN in SAN	M_n = 59,000 M_w = 140,000	Dow Chemical
PP	Tenite PP		MFI = 3.2	Eastman Chemical
SMA 25	styrene/maleic anhydride copolymer	25% MA	viscosity = 4.73[a]	Monsanto Chemical
PP-g-epoxy	GMA grafted PP (chain recoupled)	1.2% GMA	MFI = 3.4	Home made[b]
SAN	Styrene/acrylonitrile copolymer	25% AN	M_n = 77,000[c] M_w = 152,000	Dow Chemical

[a] Viscosity at 25°C, in mPa s of 10% solution in methyl ethyl ketone
[b] The synthesis and recoupling is illustrated in Chapter 4 and Chapter 5
[c] From GPC using polystyrene standards. For ABS materials the information shown is for soluble SAN

8.2.2 Melt Blending and Characterizations

The blends were mixed in a Brabender Plasti-Corder PI 2000 twin screw extruder (diameter =2.5 cm , L/D = 30) at 205°C. Since the processing temperature in this case is much higher than the normal processing temperature of PP, a novel thermal stabilizer based a mixture of three stabilizers, Doverphos S-9228/Irganox B215/P-2 (50/25/25), was added during the extrusion. The stabilizing ability of this stabilizer is illustrated in Appendix C. A single strand was extruded, cooled in a water bath, and pelletized. The pellets were compression molded into standard test specimens with the temperature at 205°C and the pressure at 30,000 lb. Standard Izod impact (ASTM - D256), tensile (ASTM-D638), and lap shear adhesion (ASTM D3165) tests were carried out at ambient conditions. FTIR measurement and SEM characterizations were carried out following the same methods illustrated in Chapter 6 and 7.

For lap shear adhesion measurements, void free plaques (20 cm x 20 cm x 0.318 cm) of PP (PP/PP-g-epoxy (80/20)) were prepared by compression molding using a frame mold. PP and PP g-epoxy were premixed at 180°C. ABS sheets (ABS/SMA with changing ratio) were prepared by similar molding at 200°C using a 0.5 mm thick frame mold. Similarly ABS and SMA were premixed in the extruder with the temperature kept at 215°C. A sandwich of two PP outer layers with the sheet in between were laminated in a frame mold at 200°C under a pressure of 250 psi for 10 min followed by cooling to room temperature by circulating water in the platens of the mold. These laminates were cut and notched to form specimens conforming to ASTM D3165 with dimensions shown in Figure (8.2). Samples with any visible defect were not tested. The specimens were pulled with a MTS at 2 inch/min until

failure, and the results reported as failure load divided by crossectional area. For all mechanical tests, at least seven specimens were examined and the averages are reported

8.3 Results and Discussion

8.3.1 The Miscibility of SMA in SAN Matrix of ABS

As illustrated before, the interfacial reaction of this system is based on the epoxy group reacting with the anhydride group generating an ester structure. The prerequisite for the interfacial reaction, however is that SMA be miscible in the SAN matrix of ABS. ABS has a phase separated structure with the polar SAN matrix and SB rubber domains. The high polarity of the MA unit in SMA facilitates the specific interaction between SMA and SAN matrix. If the specific interaction between these two components is large enough, they become miscible with each other. It has been widely published that SMA and the SAN matrix of ABS are miscible within a certain copolymer composition range [128 132]. Hall [130] found that the two copolymers are miscible, as evidenced by a single glass transition temperature, if the SAN and SMA contain approximately equal amounts of styrene (in wt.%). Recently Paul [126] reported that a weak exothermic interaction exist between the MA and AN units. Several authors have also reported that cyclic anhydrides are good solvents for the polyacrylonitrile [133 134]. Many authors have mapped the regions of MA and AN contents for which SMA and SAN copolymers form miscible or immiscible blends. Figure (8.3) summarizes all the available data of miscibility between SMA and SAN copolymers with the changing of component ratio based on the collected references. The area within the two drawn lines represents the miscible zone. It can be seen that the wt % of MA

in SMA should be between 20% to 35% for the two phases to be miscible if the AN content in SAN is around 25%. Since the SMA used in this study contains 25% MA component, it should be miscible with SAN based on the published data.

In order to reconfirm this miscibility, DSC measurements for the glass transition temperature (T_g) of blends of SAN (25% AN) and SMA (25% MA) as a function of blending ratios are carried out (Figure (8-4) and (8-5)). For all ratios, only one T_g appears, and the dependence of the T_g on the blend ratio can be approximated by the Fox Equation

$$\frac{1}{T_g} = \frac{M_1}{T_{g_1}} + \frac{M_2}{T_{g_2}}$$

M_i: Mass (weight) fraction of the components

Based on that, we confirm that SAN (25% AN)/SMA (25% MA) blend is miscible with no phase separation and consequently the SMA should be miscible with the SAN matrix of ABS.

8.3.2 The Interfacial Reaction and Characterization of Copolymer Formation

The reactivity of epoxy with carboxylic acid has been studied in Chapter 3. It was found that the carboxylic group is reactively similar to amine group but reactively higher than hydroxyl or second amine group in the melt. It can be inferred safely that the reactivity of a anhydride with an epoxy group will be higher than a carboxylic acid. To study the intensity of this reaction in the current system, FTIR spectroscopy was employed to detect the decreasing amount of reacting groups and the increasing amount of generated groups. Figure (8-6) shows the FTIR spectra of unreacted and reacted SMA/PP-g-epoxy (50/50) blends. The

unreacted sample was prepared by dissolving PP-g-epoxy and SMA in hot toluene solvent then dropping the solution onto a KBr disk and vaporizing the toluene solvent in a vacuum oven. For the unreacted sample the two strong peaks at 1777 cm^{-1} and 1868 cm^{-1} correspond to the antisymmetric and symmetric $(C=O)_2$ stretching of the anhydride structure, respectively. The strong absorption of the blends at 1730 cm^{-1} is related to the carbonyl group of ester structure from the grafted GMA monomer. After melt blending it is clear that the carbonyl absorption increases dramatically while the peaks corresponding to the anhydride group are suppressed. This means the reaction consumes anhydride groups and generates ester structures conforming to the proposed interfacial reaction as shown in Figure (8-7).

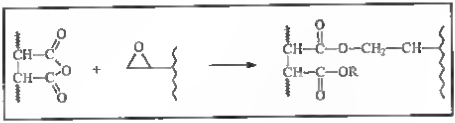

Figure (8-7) The interfacial reaction

8.3.3 Interfacial Adhesion

In the study of Chapter 6 and Chapter 7, both FTIR and torque measurements were used to detect the presence of chemical bonds across the interface. In this study, lap shear adhesion measurement of laminates is used as another technique to test the interfacial adhesion. Using the standardized procedure described above, it is found that the average shear stress for interfacial debonding of PP/ABS/PP laminates is about 330 kPa, which is in the range for typical immiscible polymer pairs. Replacement of PP with PP-g-epoxy/ABS/PP

g-epoxy blends gives a value of 720 kPa, evidently reflecting the more favorable interaction with ABS caused by the polar epoxy units in PP

Similar measurements were made using mixtures of SMA in ABS as the interlayer (PP/(PP-g-epoxy))/(SMA+ABS)/(PP/(PP g-epoxy)). The results are shown in Figure (8 8) Each point is the average of up to 10 determinations. For this system each specimen failed by interfacial debonding The adhesion is increased several fold by the reaction of PP g epoxy with SMA The response, however, is not proportional to the amount of PP-g epoxy, probably because at some point there is an over abundance of reactive MA units and the extent of reaction at the interfaces is limited by the availability of the reactive groups in the PP phase

8.3.4 Characterization the Distribution of Generated Copolymer

In Chapter 7, it was found that the interfacial reaction could be maximized by employing different mixing sequences. As a continuous study, in this chapter, the distribution of the *in situ* formed copolymer by the interfacial reaction is investigated It has been widely accepted that the copolymer formed during the interfacial reaction should exist mainly at the interface of the two phases. Recently however, it has been reported that the reacted copolymers are not exclusively distributed along the interface, some may distribute in both phases [125] To study the distribution of the generated copolymer in the SAN phase of ABS and PP phases, the solvent fractionation method (Soxhlet extraction with methyl ethyl ketone (MEK) (bp 80°C)) was used to separated the unreacted SMA or SMA-PP copolymer from the PP/PP g-epoxy/SMA/SAN (25/25/25/25) blends The mixing conditions of the blend was the same as other blends illustrated in the Experiment section. The blend was first ground to

powder to facilitate the extraction, then extracted over night. FTIR spectra of the MEK-extracted solution (after solvent removal) from the blend essentially have no characteristic peaks of PP (Figure (8-9 b)), only SAN and SMA peaks are present. This means that the copolymer PP-SMA, if formed, does not distribute into the SAN phase. On the other hand, the extracted residue contains SMA characteristic peaks as shown in Figure (8-9 c) which means that the copolymer will tend to remain in the PP phase. After repeated extractions, 12.87 g of residue from 20.00 g of the PP/PP g-epoxy/SMA/ABS (25/25/25/25) blend was obtained. Therefore, a maximum of 2.87 g of SMA has been converted into SMA-PP copolymer by the reaction between the grafted epoxy functionality and the anhydride groups in a typical extruder mixing. The conversion is larger than 10%. Thus means there is a significant fraction of SMA reacting with PP g-epoxy and quite possibly a certain amount of SMA distributed into PP phase instead of remaining at the interface of the two phases, in the form of PP-g-SMA or SMA phase itself. The effect of the distribution of copolymer into the PP phase on the bulk properties of the blends is still not clear; the possible influence on the toughness will be discussed later.

8.3.3 Morphological Study

Figure (8-10 b) shows the micrographs of the blends of PP/PP-g-epoxy/SMA/ABS (75/5/5/25) compared with the control blend of PP/ABS (75/25) (Figure (8-10 a)). Since ABS is the minor component in this case, the dispersed domain should be ABS. 5% of PP-g-epoxy and SMA can reduce the domain size dramatically, while the presence of 7.5% SMA and 5% of PP-g-epoxy results in a blurring of the phases and even more decrease of the domain sizes (Figure (8-10 e)). The presence of additional SMA or PP-g-epoxy both resulted in a finer

domain. Figure (8-10 b to c) shows the decreasing domain size with the increasing amount of SMA at constant PP g-epoxy. Figure (8-10 d to g) shows the morphologies with a increasing amount of FP-g epoxy and a constant amount of SMA, the same phenomena of decreasing domain size is observed. The presence of the two functional polymers cannot only result in fine domains but also the uniform domain size. The decreasing rate of domain size, however, is not proportional to the amount the compatibilizers added. Based on the SEM pictures, it can be seen that domain size is more sensitive to the initial amount of added functional polymers, later the addition of more functional polymers could not effectively reduce the domain size. This phenomena has been observed and discussed in the compatibilization study of HDPE/PET (Chapter 6). This might be due to the same reason as the leveling down of lap shear adhesion value illustrated above. The extent of the interfacial reaction is limited by the availability of both reactive group. Over abundance of one reactive group could totally consume the other group and leave the reaction saturated. As a result, maximizing the interfacial reaction by keeping proper ratio of the two reactive functional polymers is very crucial for the dual-functional-polymer model.

8.3.6 Impact and Tensile Properties

Mechanical properties of compatibilized and uncompatibilized blends are shown in Table (8-2). It is clear that for compatibilized blends, the impact and tensile properties are significantly improved compared with the control samples. Nevertheless, the overall properties of compatibilized blends increased with the increasing amount of functional polymers added. Figure (8-11) to (8-12) show the improvement of elongation and tensile strength properties of PP/ABS (75/25) with increasing amounts of SMA at constant PP-g

epoxy content (20% in PP phase). Obviously, the compatibilization can upgrade the toughness of the blends at all blending ratios. Increasing the amount of PP-g-epoxy at constant SMA has a similar effect on the bulk properties of the blends (Table (8-2)). The effect of PP-g-epoxy on the toughness (elongation and impact properties) and domain size are compared in this case (shown in Figure (8-13)). Notice that the maximum toughness is achieved when the content of PP g-epoxy is 10%, after which, the addition of more PP-g epoxy caused a detrimental effect on the toughness properties. Surprisingly, the domain size of ABS keeps decreasing after the maximal strain value has been reached. As we know, the finer domain size usually represents higher interfacial adhesion and better dispersity, corresponding to higher toughness. In this case, however, it seems that more improvements of adhesion and dispersity in the immiscible polyblend do not guarantee an improvement of its toughness.

The reasonable interpretation of this might lie in two factors. First, as discussed in the HDPE/PET study, a high content of PP g-epoxy reacted with SMA, which has high content of MA units could result in certain crosslinking and it could have a negative effect on the toughness of the blends. Second, we have to look at the effect of the compatibilizer copolymer distribution and its subsequent influence on matrix properties. As shown in Table (8-2), SMA is a very brittle polymer with an elongation at break of only 3.21%. Blending ABS or PP with equal amount of SMA will result in a detrimental toughness loss in the case of PP, but not so significant in the case of ABS. If SMA was a nonreactive copolymer, it most likely would stay in the SAN phase of ABS (due to their polarity and specific interaction), with little or no change in interfacial adhesion. However, since the presence of interfacial reaction, the copolymers will be formed and SMA could distribute to the PP phase

in the form of SMA PP copolymer The more copolymer is formed the higher concentration of brittle SMA in the PP phase. Figure (8-14) shows the proposed model for compatibilizer distribution in the ABS and PP phase. The toughness improvements due to adhesion increase and better dispersity appear to be compensating for the toughness loss due to the higher concentration of brittle SMA in PP phase. Compared with the case of low PP-g-epoxy content, obviously, more copolymer is formed in the case of high PP-g-epoxy content and, consequently exhibits a higher concentration of SMA in the PP phase. Therefore, the addition of a brittle compatibilizer to blends with ductile components does not assure a dramatic improvement in toughness This point of view has been virtually neglected in the literature, probably because not many examples have been discovered. In the study of Chapter 6 and 7, none of the functional polymers added are so brittle as SMA, as a result, these phenomena were not observed then, even though the *in situ* formed compatibilizers are still distributed in both phases

In conclusion, the added functional polymers affect not only the morphology and adhesion but also the inherent toughness of the other two components. If the functional polymers (having high toughness) improves or at least does little damage to the two components individually the improvement of interfacial adhesion and better phase dispersity certainly results in a toughness increase, and this is what most literature and our previous study have reported. When the added functional polymer has a detrimental affect on either or both blend components, the resultant toughness is determined by the competition between these two factors

8.4 Conclusions

In this study, two major components of polymer waste from the automotive industry, ABS and PP, are reactively compatibilized by employing PP g-epoxy and SMA as functional polymers to form an *in situ* compatibilizer during melt blending. The major conclusions from the study of this chapter are summarized as follows:

1. It is confirmed that the interfacial reaction between PP-g-epoxy and SMA in SAN phase of ABS exists according to FTIR and lap shear adhesion measurements. The overall morphological and mechanical properties of compatibilized ABS/PP with various ratios are significantly improved compared to the control samples.

2. The solvent extract study (Soxhlet extraction) reveals that PP-SMA is formed but may not reside exclusively along the interface, a certain fraction of PP-SMA may distribute into the PP phase. The reasons for the different solubility of PP-SMA in the different phases are still not clear; it could depend on several factors such as chemical structure, processing method, molecular weight, type of copolymer, and many more.

3. The compatibilizer distributed in the blend components will certainly alter the inherent toughness of these components. The presence of large amounts of PP-SMA in the PP phase may cause a detrimental effect on the final mechanical properties of the blends although the interfacial adhesion and dispersity of components improves. This study confirms that a good compatibilizer in a multi-components blend does not assure a dramatic improvement in its toughness.

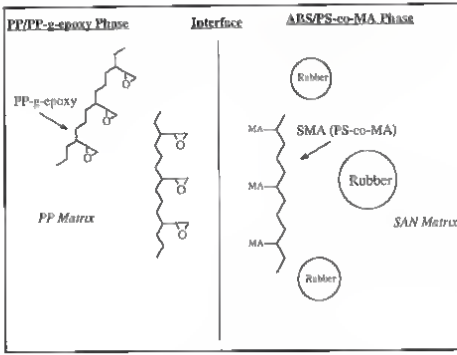

Figure (8-1) The interfacial reaction between PP phase and SAN matrix of ABS

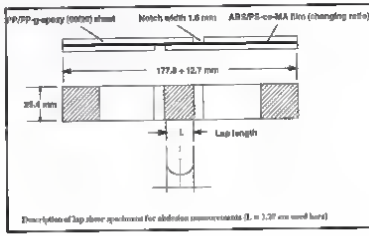

Figure (8-2) The geometry description of lap shear specimens

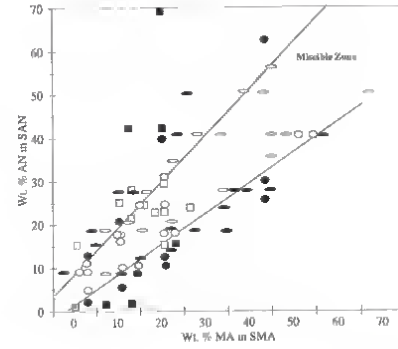

Figure (#3) Miscibility map for SMA SAN blends Open points indicate completely miscible blends grey points correspond to partial miscibility, and solid points denote immiscibility Circles identify results from Paul *et al* [126], whereas squares represent data from Hall *et al* [127] Ellipses indentify the result from Kamruer *et al* [128]

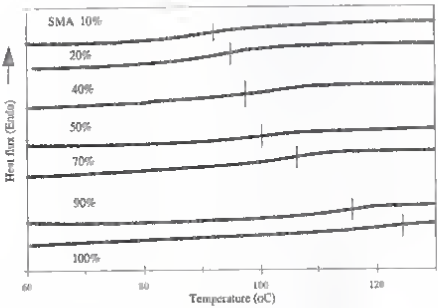

Figure (8-4) The DSC measurements of glass transition temperatures (T_g) of the blends of SAN (25% AN) and SMA (25% MA)

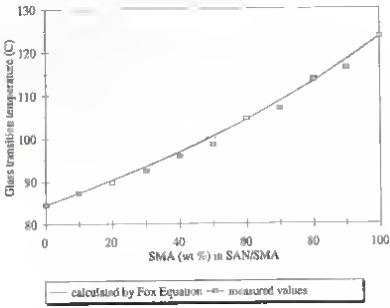

Figure (8-5) The dependence of the glass transition temperature (T_g) on the blend ratio for SAN/SMA blends

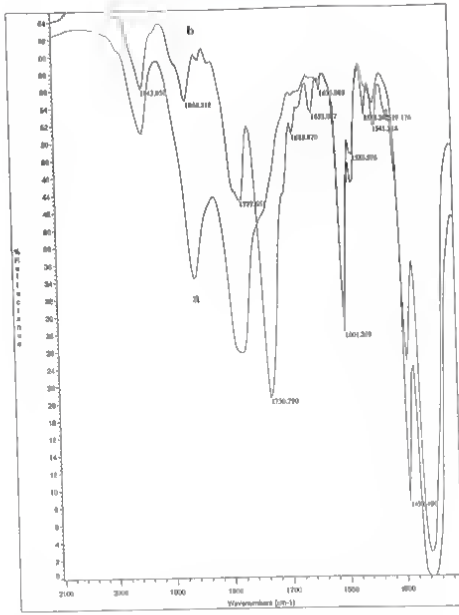

Figure (8-6) FTIR spectra of (a) Unreacted, and (b) Reacted SMA/PP g-epoxy (50/50) blends

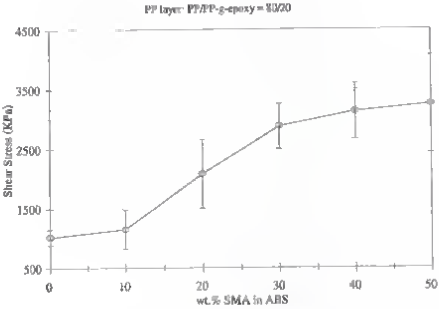

Figure (8-8) Lap shear adhesion strength between PP/PP-g epoxy (80/20) and ABS/SMA laminates bonded at 200°C for 10 min

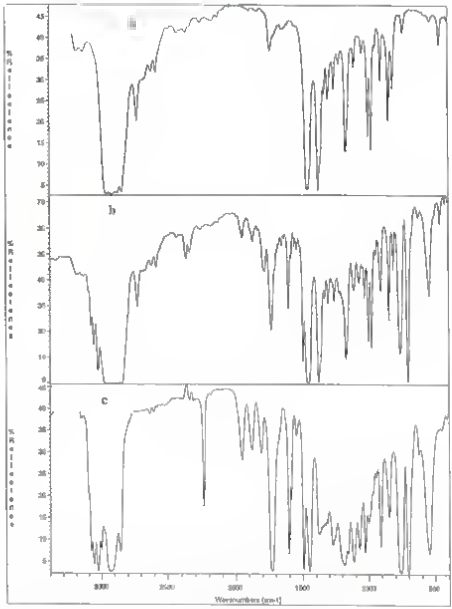

Figure (8 9) FTIR spectra of (a) Pure PP g-epoxy; (b) Extracted residue of PP/PP-g epoxy/SMA/SAN (25/25/25/25) blends Notice the SMA characteristic peaks at 1730 1600 1777 cm^{-1} (c) Extracted components No PP peaks

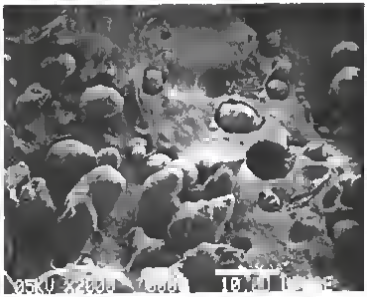

(a)

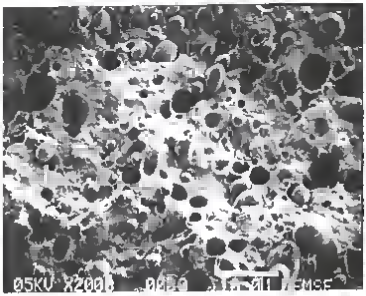

(b)

Figure (8.10) Morphologies of immiscible polymer blends and compatibilized PP/ABS blends
(a) Uncompatibilized PP/ABS 75/25 (X2000)
(b) PP/PP-g-(PP/SMA) ABS 75/5/5/75 (X2000)

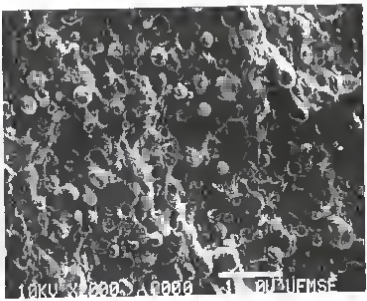

(c)

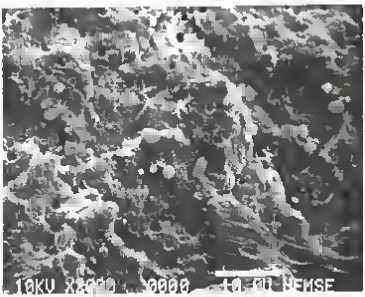

(d)

Figure (8-10 continued) (c) HDPE/PP/Epoxy/SMA/ABS 75/5/7.5/2.5 (X2000)
(d) HDPE/PP/Epoxy/SMA/ABS 75/7.5/7.5/2.5 (X2000)

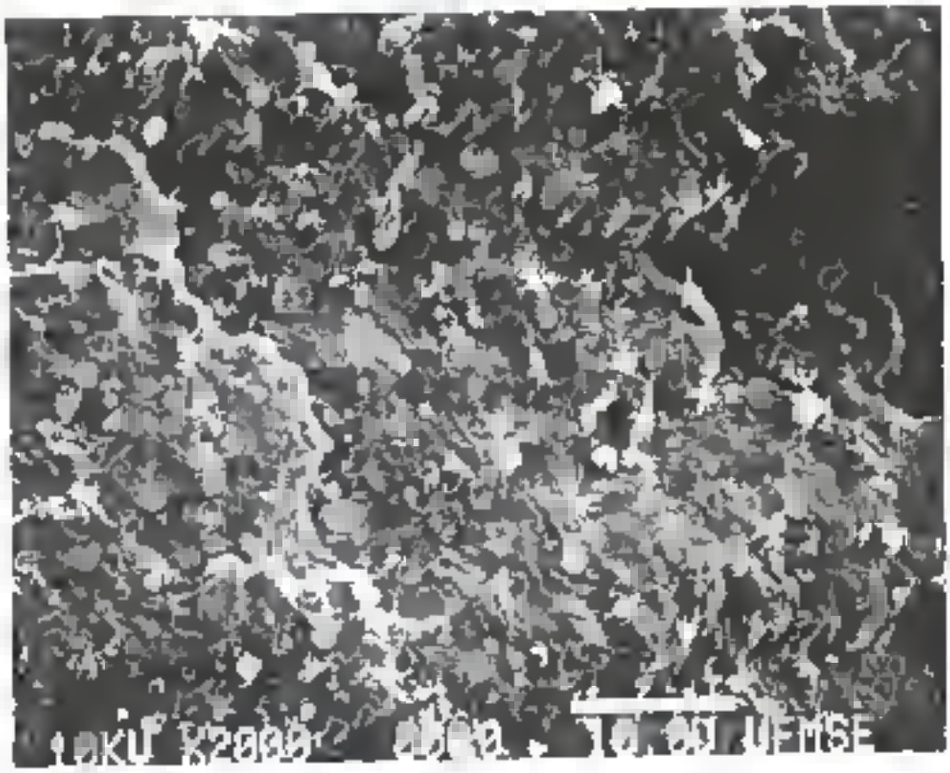

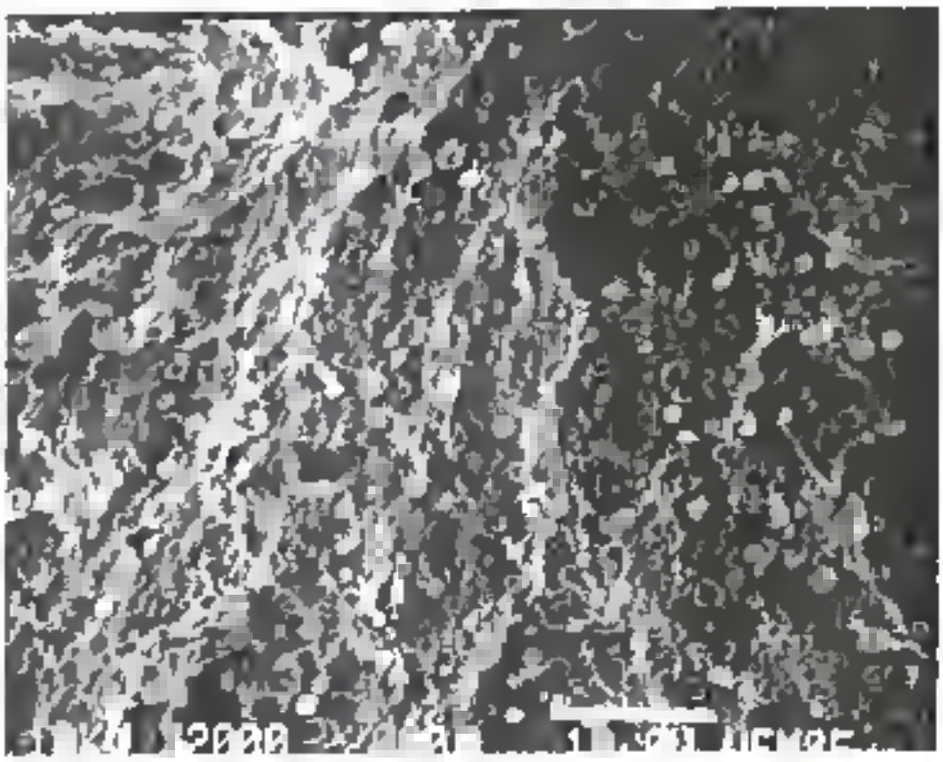

Figure (8-B) continued) [illegible] PE/PP g-epoxy/SMA/ABS [illegible] X400
[illegible] PE/PP g-epoxy/SMA/ABS [illegible] X400

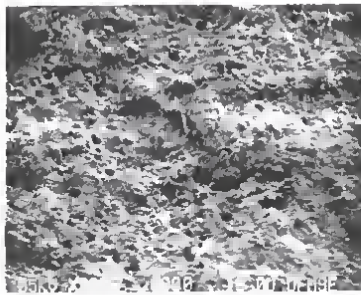

Figure (8-10 continued) (c) PP/PP-g-epoxy/SMA/ABS 75/0/0/7.5/25 (X2000)

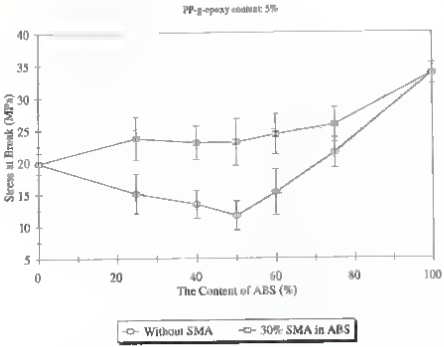

Figure (8.11) The effect of compatibilization on stress at break of the blends

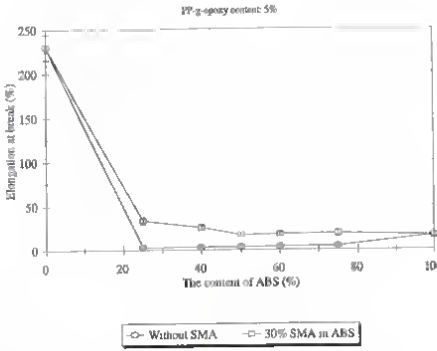

Figure (8-12) Effect of compatibilization on elongation at break of the blends

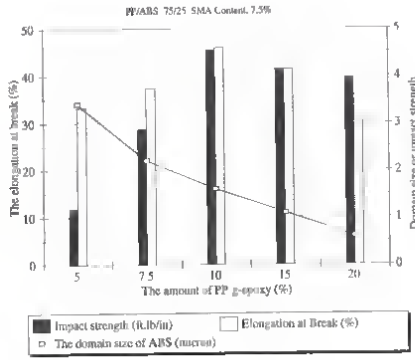

Figure (8-13) The effects of compatibilization on toughness and domain size with SMA content at 7.5%

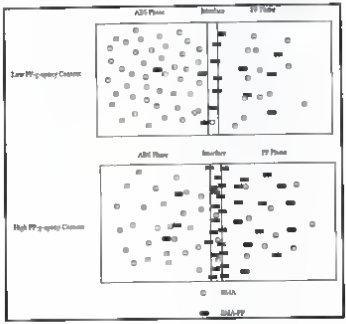

Figure (8-14) The proposed model for compatibilizer distributed in ABS and PP phases

Table (8-2) Some Data of the Mechanical Properties of the Components and Blends

Composition by Weight	Impact† (ft.lb/in)	Y str (Mpa)	Elong. (%)	Modulus (Mpa)
ABS	7.244 ± 0.813	33.58*± 2.24	16.16 ± 1.43	712.43±34.62
PP	3.693 ± 0.434	32.83 ± 1.38	230.32±20.86	450.55±27.86
SMA	0.573 ± 0.124	43.25*± 1.05	3.21 ± 0.28	756.35±42.54
ABS/SMA. 70/30	7.058 ± 0.656	35.76 ± 1.26	15.86 ± 0.89	723.53±31.52
PP/SMA. 70/30	0.827 ± 0.116	21.51*± 2.36	13.87 ± 1.27	512.38±18.53
PP/ABS 75/25	0.899 ± 0.246	15.08*± 3.06	3.32 ± 0.21	543.25±22.57
PP/grafted PP/SMA/ABS 75/5/5/25	1.057 ± 0.412	23.96 ± 1.16	24.68 ± 3.81	581.63±43.28
75/5/7.5/75	1.174 ± 0.221	26.79 ± 2.76	33.19 ± 4.22	572.84±18.76
75/7.5/7.5/25	2.865 ± 0.428	28.24 ± 0.56	37.35 ± 2.54	589.45±38.72
75/10/7.5/25	4.545 ± 1.078	28.95 ± 0.67	45.84 ± 3.36	583.65±22.24
75/15/7.5/75	4.140 ± 1.049	29.12 ± 2.34	41.35 ± 2.38	596.38±33.29
75/20/7.5/75	3.985 ± 0.564	28.46 ± 1.53	31.18 ± 1.17	586.67±12.49
PP/ABS 50/50	1.028 ± 0.171	10.61*± 2.28	3.52 ± 0.51	592.76±18.59
PP/grafted PP/SMA/ABS 50/5/5/50	1.136 ± 0.268	23.82 ± 3.63	10.55±1.81	535.76±29.57
50/5/10/50	1.691±0.295	26.99 ± 4.26	14.21±3.64	520.00±14.38
50/5/15/50	2.614 ± 0.438	28.92 ± 2.57	17.33±2.51	546.97±32.18
PP/ABS 25/75	1.105 ± 0.202	21.38*± 2.34	4.25±1.12	606.98±22.75
PP/grafted PP/SMA/ABS 25/5/7.5/75	1.245 ± 0.138	25.71*± 2.64	9.41±0.44	705.97±12.28
25/5/15/75	2.967 ± 0.389	28.82 ± 3.14	13.48±2.23	682.42±35.85
25/5/22.5/75	3.248 ± 0.245	32.27 ± 2.14	18.61±3.42	643.83±52.39

* Ultimate breaking stress, no yielding

† The Izod impact properties were detected under room temperature with notched specimen.

CHAPTER 9
SUMMARY AND SUGGESTED FUTURE WORK

9.1 Summary and Conclusions

The studies presented in this dissertation are part of the ongoing research in this laboratory Polymers Processing and Properties Center at the University of Florida. One of the major goals of our current research is to develop high efficiency functional polymers for the reactive compatibilization of various recycled polymers. The functional polymers should meet the requirements of low cost, high efficiency and versatility Epoxy grafted polyolefins synthesized by melt grafting are a promising family of functional polymers which could be used in the compatibilization of various polymer blends The major conclusions from this study are summarized as follows

1 Polyolefins including polyethylene and polypropylene can be grafted by several monomers, including maleic anhydride (MA) (containing anhydride groups) glycidyl methacrylate(GMA) (containing epoxy groups) and 2 isopropenyl-2 oxazoline (IPOZ) (containing oxazoline groups), via. melt grafting solid-state grafting, and solution grafting Based on the consideration of grafting time, graft ratio and efficiency and side reactions, it is concluded that GMA grafted polyolefins can be synthesized successfully by melt grafting

2 Among the three functional monomers grafted polyolefins, GMA and oxazoline grafted polyolefins have high reactivities with both acidic end groups of polyesters (hydroxyl and carboxylic acid), and basic groups of nylon (amine). In order to make comparisons of

their reactivities in the melt, small molecule model was employed to carried out the reactivity study It is found that an epoxy grafted polyolefin has higher or equivalent reactivities with acidic or basic groups compared with oxazoline grafted polyolefin. Since oxazoline grafted polyolefin can only be synthesized by solution grafting GMA grafted polyolefin has the advantages of high reactivity, versatility, and low synthesizing over oxazoline grafted polyolefins which makes GMA grafted polyolefins the best choice for the future reactive compatibilization.

3 The grafting of LLDPE, HDPE, PP with GMA monomer is accomplished via reactive twin-screw extrusion. By employing proper initiator, extrusion parameters, and procedures, all of these three polyolefins could be grafted by GMA monomer with high graft ratios

4. Thermal degradation of polypropylene accelerated by peroxide is one of the major problems for the melt grafting of PP In this study a mulufunctional monomer (TMPTA) is used to form certain amounts of chain recoupling and crosslinking in order to compensate for the chain scission of PP during melt grafting The chain recoupling restores the mechanical and rheological properties of the grafted PP close to pure PP

5 GMA grafted HDPE (HDPE-g-epoxy) could be used as a precursor of compatibilizer in the compatibilization of HDPE/PET blends The compatibilizing effects of HDPE-g-epoxy are manifested by a dramatic improvement of processability, mechanical and morphological properties of the blends The proposed interfacial reaction could be observed by torque and MFI measurements

6. GMA grafted polyolefins (including HDPE and PP) can be used as precursors of compatibilizers for polyolefin/PVC blends By using carboxylated nitrile rubber (XNBR) as another precursor, the compatibilizer HDPE-g-XNBR or PP g XNBR was formed *in situ*

during compounding. The proposed compatibilization mechanism is further confirmed by the studies of mechanical, morphological, and rheological properties. The success of this compatibilization indicated that not only those blending components possessing reactive groups could be *in situ* compatibilized, polymers with no reactive groups can also be compatibilized by using two functional polymers as compatibilizer precursors. This compatibilization model is named as dual-functional polymer model in the studies of this dissertation.

7. Dual-functional polymer model is applied successfully in the compatibilization of another blend, PP/ABS. Two functional polymers, poly(styrene-co maleic anhydride) (SMA) and PP g-epoxy, are used to form *in situ* compatibilizer PP-g-SMA. It was found that adding functional polymers affect not only the morphology and adhesion but also the inherent toughness of the mixing components. A deep compatibilization does not assure a dramatic improvement in its toughness.

9.2 The Future Work

The future work for this project could be oriented into several directions:

1. Upgrade the graft ratio and graft efficiency of the melt grafting by optimizing the screw configuration of the reactive twin-screw extruder. The screw configuration could be modified to bring in proper residence time, finer dispersion of monomers in the polymer melt, and higher shear forces, by which the graft ratio and efficiency could be significantly improved.

2. Study the feasibility of completing melt grafting and subsequent compatibilization in one twin screw extruder. Currently, polyolefins are grafted as a separate extrusion step, and the grafted polyolefins are then blended with other polymers in a second extrusion step.

If both the grafting and blending steps are executed in the same extrusion step, it will be more economical for industry consideration. For example grafting polyolefins can be carried out in the first part of the extruder followed by subsequent interfacial reaction between other polymers and the grafted polyolefins.

3 Modify various METALLECENE™ polyolefins with GMA monomer Among all kinds of polyolefins, METALLECENE™ polyolefins, a kind of thermal plastic elastomer, have absorbed more and more attention. Besides the normal applications of elastomers they could be used as impact modifiers for various polyesters according to our initial study [78]. The advantage of this kind of thermal plastic elastomer (TPE) over traditional elastomers is its completely saturated structure with high UV stability Fortunately, they could also be efficiently grafted by GMA monomer by melt grafting according to our initial work [66] These grafted METALLECENE™ polyolefins are ready to form interfacial interactions with the end group of polyesters and make the two phases compatibilized

4 Apply the GMA grafted polyolefins in other polymer blends, including PS/polyolefins PMMA/polyolefins, nylon/polyolefins and polyolefins/wood fiber or glass fiber, etc

APPENDIX A
THE SYNTHESIS OF 2-ISO-PROPENYL-2 OXAZOLINE

A. 1 Introduction

Two synthesis routes for 2-iso-propenyl 2-oxazoline (IPOZ) have been reported in reference. Kagiya *et al.* synthesized IPOZ by the isomerization reaction of N-methacryloyl ethyleneimine, prepared from ethyleneimine and methacryloyl chloride with the use of sodium iodide catalyst [135] and purified by several distillations under reduced pressure (bp 50 5-51 5°C/17 Torr). Another synthesis route was reported by Liu and Baker in their recent publication [136] based on 2-ethyl-2-oxazoline as initial compound. In this study, the second synthesis route is employed.

A. 2 Materials

Analytical grade of 2-ethyl 2-oxazoline and paraformaldehyde were bought from Aldrich Chemical Corporation.

A 3 Mechanism

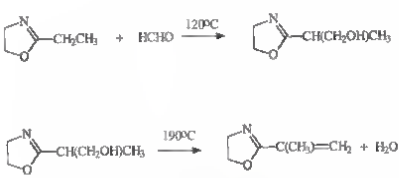

A 4 Experiment

500 g of analytical grade 2-ethyl-2-oxazoline is mixed with 160 g of analytical grade paraformaldehyde with molar ratio of 1/1 05 in a 1 L flask equipped with a condenser and a thermometer In the first step of synthesis the mixture is heated up to 120°C with a silicon oil bath. The reaction is exothermic and finished with the temperature rising to around 170°C. The reaction mixture should be cooled down to maintain a temperature of 120°C for 5 h with stirring

In the second step, the flask is converted to a distillation device and the temperature of the reaction mixture raised to 190°C at which point dehydration occurs to give 2 iso-propenyl-2-oxazoline.

The final mixture of products are distillated and the distillates between 110°C and 145°C are collected and dried twice with solid sodium and filtered. The overall yield is around 45%

APPENDIX B
THE FTIR CALIBRATION CURVES FOR THE DETECTION OF GRAFT RATIO

B.1 Methods

The graft ratio of maleic anhydride (MA), and 2-iso-propenyl 2-oxazoline (IPOZ) grafted HDPE can be calculated by measuring the absorbance of the characteristic peaks of MA (1706 cm^{-1}) or IPOZ (1637 cm^{-1}) in FTIR spectra. A calibration curve is needed to correlate the peak height with the absolute graft ratio

Since the absorbances of these two peaks are also influenced by the thickness of specimen and instrumental factors, the characteristic peak of methyl group of polyethylene (1376 cm^{-1}) is used as internal reference peak. The ratios of peak height of MA or IPOZ characteristic peaks to the peak height of internal reference (methyl group of PE) are used to correlate with the absolute graft ratios.

The absolute graft is obtained by employing a F002 Heraeus CHN-O-Rapid Elemental Analyzer. Since polyethylene has no oxygen elemental composition, the detected oxygen amount in the purified grafted polyethylene should come from the grafted MA or IPOZ monomer. Based on the amount of oxygen, the absolute graft ratio can be calculated.

B. 2 The Calibration Curves for MA Grafted and IPOZ Grafted HDPE

Table (B-1) and (B-2) list the correlation between peak ratios and graft ratios for purified MA and IPOZ grafted HDPE. Figure (B-1) and (B-2) are the two calibration curves for the calculation of graft ratios based on the ratios of peak heights.

Table (B-1) The correlation between the ratios of peak heights and graft ratios of MA grafted HDPE.

ν CO/δ CH_2	Oxygen (%)	Graft ratio (%)
0	0	0
0.41	0.34	0.69
0.72	0.58	1.18
0.81	0.73	1.49
1.59	1.31	2.68
2.05	1.69	3.46
2.72	2.24	4.58
2.85	2.56	5.24

Table (B-2) The correlation between the ratios of peak height and graft ratios of IPOZ grafted HDPE.

ν Oxazoline ring/δ CH_2	Oxygen (%)	Graft ratio (%)
0	0	0
0.08	0.05	0.63
0.37	0.23	1.62
0.52	0.32	2.25
0.65	0.40	2.76
0.78	0.48	3.34
1.04	0.64	4.45

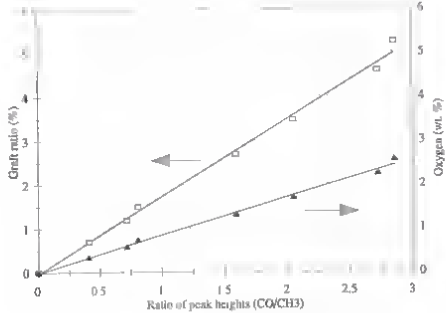

Figure (B 1) The calibration curve for the calculation of graft ratio of MA grafted HDPE

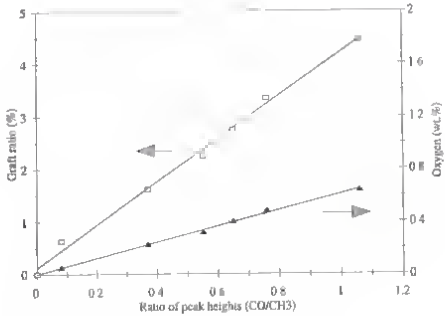

Figure (B-2) The calibration curve for the calculation of graft ratio of IPOZ grafted HDPE

APPENDIX C
THE STABILIZERS FOR POLYPROPYLENE PROCESSED UNDER HIGH TEMPERATURE

C. 1 Introduction

The thermal degradation and crosslinking of polyolefins is a potential problem in their melt processing especially for the recycled polyolefins which have been processed repeatedly Worse than crosslinking thermal degradation cause chain scission which greatly reduce the mechanical properties of polyolefins For PE, both chain scission and crosslinking occur during the thermal processing, while PP mainly suffers from chain scission. In the study of the compatibilization of PP/ABS blends of this dissertation, the processing temperature is above 205°C, which is higher than the normal PP processing temperature. It is believed that the thermal degradation caused by high processing temperature should exist Besides this residual peroxide remained in the PP g-epoxy could accelerate the degradation for during the processing which could be fatal to the bulk properties of the blends In this appendix various commercially available thermal stabilizers are compared and modified in order to prohibit the thermal degradation of PP during grafting The major detecting tool for the rate of thermal degradation is melt flow index (MFI) measurement

C. 2 Materials and Mechanisms

There are various commercially available thermal stabilizers, most of which are one of the two kinds of antioxidant. primary antioxidants (for example, phenolic-type and amine type) secondary antioxidants (for example, sulfate and phosphite) The radical scavenging mechanism of these two kinds of antioxidants are shown below

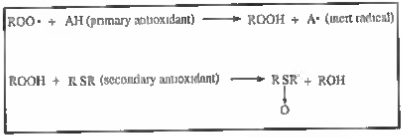

In this study four kinds of different stabilizers or mixture of stabilizers (as shown in the Table (C-1)) are compared The choosing of the following stabilizers is based on their high vaporing points. The mixing of the stabilizers is for the synergistic effect

C. 3 Experiment

PP (MFI. 2 6 g/10 min Tenite) was extruded with or without stabilizer under 230°C and 100 rpm in Brabender Plasti Corder PI 2000 The amount of stabilizer added was kept at 0 1% 0.01% of peroxide was added to imitate the residual peroxide remained in the PP-g epoxy when it is used as functional polymer for the compatibilization.

C. 4 Results and Discussion

Figure (C 1) shows the effects of all the stabilizers below on the MFI values along with the times of extrusion. Without any antioxidant, the thermal degradation of PP is very obvious. P-2 shows poor antioxidation ability partially because of its relatively low vaporing point. Doverphos S-9228 has a quite similar molecular structure as P 2, but the phenyl structure stabilizes the whole molecule and makes it stable at higher temperatures.

Table (C 1) The list of stabilizers compared

Name	Chemical Composition	Manufacture
P 2	Distearyl pentaerythritol diphosphite	Borg Warner Chemicals Inc
Doverphos S-9228	Bis (2, 4 dicumyl phenoxy) pentaerythritol diphosphite	Dover Chemical Corporation
Irganox B215	One part of primary antioxidant (hindered phenol) and two parts of secondary antioxidant (phosphite)	Ciba-Geigy Corporation
Doverphos S-9228/ Irganox B215/P 2 (50/25/25)	Mixture of three the stabilizers	Home made

Compared with all of these stabilizers in Figure (C 1), the binary and ternary stabilizers (Irganox B215 and the ternary mixture of Doverphos, Irganox, and P 2) show excellent thermal stabilizing effect that could be due to the synergistic effect of different stabilizing mechanisms. In conclusion, ternary stabilizer will be selected for PP stabilization under high processing temperatures.

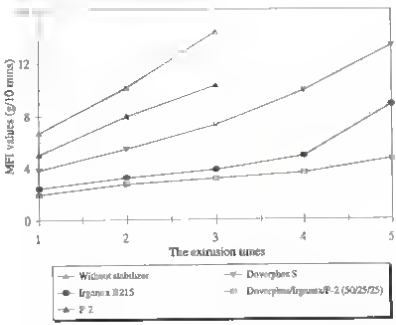

Figure (C 1) The effect of stabilizers on MFI values The stabilizers 0.1%

LIST OF REFERENCES

1 J A Manson and L. H. Sperling, *Polymer Blends and Composites* Plenum Press, New York, 1967

2 D R. Paul and S Newman *Polymer Blends*, Academic Press, New York, 1978

3 O Olabisi, L. M. Robeson, and M T Shaw, *Polymer-Polymer Miscibility*, Academic Press, New York, 1979

4 D R. Paul and J W Barlow, and H Keskkula, in *Encyclopedium of Polymer Science and Engineering*, Plenum Press New York 2nd Edn, Vol. 12, p 399, 1988

5 D R Paul in *Functional Polymers* (Eds D E. Bergbreiter and C E. Martin), Plenum Press, New York, p 1, 1989

6 L M Robeson *Polym. Eng Sci*, **24** 587 (1984)

7 Mitsui Petrochemical Industries, Ltd., Jpn Kokai Tokkyo Koho JP 59, **149** 939 (1984)

8 J W Barlow and D R. Paul, *Polym. Eng Sci*, **24** 525 (1984)

9 L. D'Orazio R Greco C. Mancarella, E Martascelli, G Regosta, and C Silvestre, *Polym. Eng Sci*, **22** 536 (1982)

10 P G Andersen U S Patent, 4,476,283 (1984)

11 T D Traugott J W Barlow, and D R. Paul, *J Appl Polym. Sci*, **28**, 2974 (1983)

12 L. D'Orazio R Greco E Martascelli, and G Regosta, *Polym. Eng Sci*, **23**, 489 (1983)

13 R. Fayt, R. Jerome and P Teyssie, *Polym. Eng Sci* **27**, 328 (1984)

14 D K. Yoshumura and W D Richards, *SPE ANTEC Tech. Papers* **32**, 688 (1986)

15 E M Woo, J W Barlow, and D R. Paul, *Polymer*, **26**, 763 (1983)

16 M. Hajian, C Sadrmohaghegh and G Scott, *Eur Polym. J*, **20**, 135 (1984)

17 F Ide and A. Nasegwe, *J Appl. Polym. Sci.*, **8**, 963 (1974)

18 B N Epstein, U S Patent 4,174,358 (1979)

19 B N Epstein, U S Patent 4,172,859 (1979)

20 F H Owens and J J Clonis, U S Patent 3,668,274 (1972)

21 C F Hanne and H. K. Sinclair U S Patent 3,972,961 (1976)

22. Dow Chemical U S A. Literature on Reactive Polystyrene (RPS), Midland MI (1985)

23 P M. Subramanian and V Mehra, *Polym. Eng Sci*, **27**,663 (1987)

24 I Park, J W Barlow and D R. Paul *J of Polym. Sci*., **30** 1021 (1989)

25 R. E Lavengood, A. F Harris, and A. R. Padwa, Eur Pat Appl. EP 202, 214 (1986)

26 J C Woodbrey and M V Moncur, U S Patent 4,320,214 (1982)

27 K. F Lin and F C Chang, *Polym. Networks Blends*, **4 (2)** 51-59 (1994)

28 C. T Mau and F C Chang *J Appl Polym. Sci*, **49** 913 (1993)

29 J Y Chung and R. P Carter U S Patent 4,554,315 (1985)

30 M K. Akkapeddi B VanBuskirk *Polym. Mater Sci Eng*. **67**, 317 (1992)

31 M. K. Akkapeddi, B VanBuskirk and C D Mason, *Polym Prepr* **34(2)**, 848 (1993)

32 F C Chang and C Y Hwu *Polym. Eng Sci* **31**, 1509 (1991)

33 D Y Chang and F C Chang *Polym. Networks Blends* **4 (2)** 157 (1994)

34 S H Chen and F C Chang *J Appl. Polym. Sci.* **51**, 955 (1994)

35 H H Chang, J S Wu and F C. Chang *Polym. J* 12 345 (1995)

36 B S Chang and F C Chang, *Proceedings of the 15th ROC Polymer Symposium Taiwan*, 425 (1992)

37 W B Liu and F C Chang, *Eur Polym. J.* in press.

38 D H Fan, J S Wu, and F C Chang, *Proceedings of the 16th ROC Polymer Symposium Taiwan* 303 (1993)

39 R. Clark, *ANTEC'94*, 1352 (1994).

40 A. Simmons and W E Baker *Polym. Eng Sci.* **29**, 1117 (1989)

41 Z. Song and W E Baker, *Polymer*, **33**, 3266 (1992)

42 W E Baker and M Saleem, *Polym. Eng Sci* , **27**, 1634 (1987)

43 C E Scott and C W Macosko, *Polym. Eng Sci.* **35**, 1939 (1995)

44 D Braun and U Essenlohr, *Angew. Makromol Chem* , **55**, 43 (1976)

45 N C. Liu, W E Baker, and K. E Russell *J Appl. Polym. Sci.* **41**, 2285 (1990)

46 N G. Gaylord R. Mehta, and V Kumar Am Chem. Soc Prepr Org. Coat *Appl Polym. Sci.* **46**, 87 (1982)

47 N G Gaylord and R. Mehta, *J Polym. Sci., Polym. Chem. Ed.* **26**, 1189 (1987)

48 V Khunova, *Plasty a kaucuk*, **31**, 372 (1994)

49 V Khunova and Z. Zamorsky *Polym.-Plast Technol. Eng* , **32 (4)** 289 (1993)

50 V Khynova, M. M Sain and I Sunek, *Polym. Plast. Technol. Eng* , **32 (4)**, 299 (1993)

51 G D Iones R. M Nowak, US Patent 3,177,270 (1965)

52 S Porejdo *J Polym. Sci* A 1, **5** 1539 (1967), S Porejko, *J Polym. Sci* A-1, **7**, 617 (1969)

53 R. L McCollell, US Patent 3 658 948 (1975)

54 R. A. Stenkamp and T J Grail, US Patent 3,862 265 (1975)

55 Z. Song and W. E Baker *Angew Makromol. Chem.* **181** 1 (1990)

56. K. E. Oliphant, K. E. Russell and W. E. Baker, *Polymer*, **36**, 1597 (1995)

57. T. Alfrey, Jr., and C. C. Price, *J. Polym. Sci.*, **2**, 101 (1947).

58. J. Brandrup and E. H. Immergut, *Polymer Handbook*, 3rd ed., John Wiley & Sons, New York (1989)

59. W. Regel and C. Schneider, *Makromol. Chem.*, **182**, 237 (1981)

60. R. Backai, *J. Polym. Sci. Polym. Chem. Ed.*, **14**, 1797 (1976)

61. K. J. Kim and B. K. Kim, *J. Appl. Polym. Sci.*, **48**, 981 (1993)

62. N. Cardi, R. Po, G. Giannotta, E. Occhiello, F. Garbassi, and G. Messina, *J. Appl. Polym. Sci.*, **50**, 1501 (1993)

63. V. J. Tracca, S. Zane, J. W. Barlow, H. Keskkula and D. R. Paul, *Polymer*, **32**, 1401 (1991)

64. A. Doshi and A. Fradet, *J. Polym. Sci., Poly. Chem. Ed.*, **33**, 691 (1995)

65. A. W. Birley, B. Haworth, and J. Batchelor, *Physics of Plastics*, Hanser Publishers, Munich (1991)

66. G.L. Yao and C.L. Beatty, Nov., *1996 PPS Annual Meeting*, Chicago. Preprint (in press)

67. J. A. Radosta, *SPE Antec Tech. Papers*, **30**, 145 (1984)

68. I. Shun, SPE *Antec Tech. Papers*, **30**, 132 (1984)

69. E. M. Fettes, *Chemical Reactions of Polymers*, Wiley Int., New York (1964)

70. E. Ceresa, *Block and Graft Copolymers*, Butterworths, London (1962)

71. M. Lambla, *Polym. Proc. Eng.*, **5**, 297 (1988)

72. J. Tarranco, O. Laguna, E. P. Collar, *J. Polym. Eng.*, **11**, 335 (1992)

73. A. Hogt, *ANTEC'88*, 1478 (1988)

74. G. H. Hu, J. J. Flat, and M. Lambla, *ANTEC'94*, 2775 (1994).

75. Y. J. Sun, G. H. Hu, and M. Lambla, *Die Angew. Makromol. Chem.*, **229**, 1 (1995)

76 P K. Dhal, *J Macromol. Sci Chem.*, **A23** 181 (1986)

77 S Wu, *Polymer* **26**, 1855 (1985)

78 G L. Yao and C. L Beatty, Nov , *1996 MRS Annual Meeting*, Boston, Preprint (in press)

79 B K. Kim and K. J Kim *Advances in Polymer Technology*, **12 (3)** 263 (1993)

80 L K. Yoon, C H Choi, and B K. Kim *J Appl Polym. Sci.* **56** 239 (1995)

81 F Yoshu, K. Makuuchi, S Kikukawa, T Tanaka, J Saitoh, and K. Koyama, *J Appl Polym. Sci.*, **60**, 617 (1996)

82 C H Wu and A. C Su, *Polym. Eng Sci* **31**, 1629 (1991)

83 B J Kim and J L. White, *Intern. Polymer Processing* **3**, 213 (1995)

84 L. A. Utracki, in *Multiphase Polymers Blends and Ionomers*, L. A. Utracki and R A. Weiss eds., Amer. Chem. Soc , Washington, D C p 235, ch.7, 1989

85 A. W Birley, B Haworth and J Batchelor, *Physics of Plastics*, Hansec Publishers, Munich (1991)

86 N G Gaylord, M Mehta, and R Mehta, *J Polym. Sci* , **33** 2549 (1987)

87 P Sambaru and S A. Jabarin, *Polym. Eng Sci* , **33**, 827 (1993)

88 S A. Jabarin E. A. Lofgren and S. B Shah, in *Emerging Technologies in Plastics Recycling*, G D.Andrews and P M Subramanian, eds , American Chemical Society Washington, D C p 342, ch. 17 1992

89 P Chandran and S Jabarin *Adv of Polym. Technol.*, **12 (2)** 119 (1993)

90 M E Stewart, A. J Cox and S E George, *5th Intern. Conf Alloys & Blends*, Ann Arbor Mich. (1992)

91 M K. Akkapeddi, B Van Buskirk and X Swamikannu, Am. Chem. Soc , *Polym. Mater Sci & Eng* **67**, 317 (1992)

92 S S Dagli and K. M Kamdar, *Polym. Eng Sci* , **23**, 1709 (1994)

93 *Modern Plastics* Sept (1996)

94 M Xanthos and S S Dagli, *Polym. Eng Sci.*, **31**, 929 (1991)

95 C T Mas and F C Chang, *J Appl. Polym. Sci.* **49**, 913 (1993)

96 M Xanthos, M W Young and J A. Biesenberger, *Polym. Eng Sci.*, **30**, 355 (1990)

97 Z. L. Luo and F C Chang *J Appl Polym. Sci.* **52**, 1115 (1994)

98 S Danesi and R. S Porter, *Polymer*, **19** 448 (1978)

99 J J Elmendorp and A. K. Van der Vegt, *Polym. Eng Sci*, **16**, 1331 (1986).

100 B D Favis, *J Appl. Polym. Sci.* **39**, 285 (1990).

101 J Francis and K. E George, *J Elastom. and Plastics* **24-April**, 151 166 (1992)

102. D R Paul, C. E. Locke and C E Vinson, *Polym. Eng Sci.* **13**, 202 (1973).

103 C. E. Locke and D R Paul, *Polym. Eng Sci* **13**, 308 (1973)

104 Y Nakamura, A. Watanabe K. Tamura and H Miyazaki, *J Polym. Sci.* Part C **25**, 127(1987)

105 C Xu, M. Zhong, S. Ge, *China Plastics* **17(2)**, 15 (1988), C A.**109** 191302b (1988)

106 C Xu Z. Fang and J Zhong *Die Angewandte Makromolekulare Chemie* **212** 45 (1993)

107 A. Ajji, *Polym. Eng Sci* **35** 64 (1995)

108 G A Zakrzewski, *Polymer* **14** 347 (1973)

109 P Ramesh and S K. De *Polymer Communications* **31**, 466 (1990)

110 L. Chandler and E Collins *Appl Polym. Sci* **13**, 1385 (1969).

111 R. Erro Zozaya and M Buso, *J Vinyl Technology* **15**, 132 (1993)

112 P Ramesh and S K. De, *J Appl. Polym. Sci* **50**, 1369 (1993)

113 Z. Fang, S Eno X Shan C Xu, *Preprints of 1992 Symposium on Polymers* Changchun, China 1111 (1992)

114. E. Benedetti F Posar A. D Alessio P Vergamini, G Pezzin and M Pozzoli, *J Polym. Sci., Polym. Phys Ed.* **23**, 1187 (1985)

115 G Ruggeri, R. Bertani, M Aglietto, M Pracella, E. Benedetti and A. D'Alessio *Polym. Networks & Blends*, **2** (3) 167-71 (1992)

116 *The Infrared Spectra Atlas of Monomers and Polymers*, Sadtler Research Lab. Division of Bio Rad Laboratories, Inc (1980)

117 C. E Scott and C. W Macosko *Intern. Polymer Processing*, **1**, 36 (1995)

118 S Cimmino, F Coppola, L. D'Orazio, R. Greco, G Maglio, E Malinconico, C Mancarella, E Martuscelli and G Ragosta, *Polymer*, **27**, 1874 (1986)

119 K. M Kamdar and S S Dagli 1249, *ANTEC '93*

120 J M. Willis and B D. Favis, *Polym. Eng. Sci.* **28**, 1416 (1988)

121. J Y. J. Chung and R. P Carter, US Patent 4,554,315 (1985)

122. S Suzuki and T Yamamoto, *Plastics* (Jpn) **41 (6)** 116 (1990)

123 P C. Lee, W F Kuo, and F C Chang *Polymer*, **36**, 5641 (1994)

124 H H Chang, J S Wu and F C. Chang, Polym. J in press

125 V J Triacca, S Ziaee, J W Barlow, H Keskkula and D R. Paul, *Polymer*, **32**, 1401 (1991)

126 H. J Kim, J W Barlow, and D R. Paul, *J Polym. Sci Polym. Phys Ed.* **27**, 233 (1989)

127 W J Hall, R C Kruse, R. A. Mendelson, and Q A. Trementozzi. *ACS Symp Ser* **229**, 49 (1983)

128 J Kressler H W. Kammer, G Schmidt Naake, and K. Herzog, *Polymer*, **29**, 686 (1988)

129 Y Aoki, *Macromolecules* **21** 1277 (1988)

130. W J Hall. R. L. Kruse, R A. Mendelson, and Q A. Trementozzi, Am. Chem Soc Div Org Chem *Plast. Prepr* **47** 298 (1982)

131 T Kato N Kobayashi, and A Takahashi, *Kobunshi Kobonshu* **40**, 661 (1983)

132. Y Aoki, *Polym. J* (Tokyo) **16**, 431 (1984)

133 J V Flanagan US Patent 260 751 (1952)

134 M. K. Phibbs, *J. Phys. Chem.* **59** 346 (1955)

135 T. Kagiya, T. Matsuda, and K. Zushi, *J. Macromol. Sci. Chem.*, **A6 (7)** 1349 (1972)

136. N. C. Lin and W. E. Baker, *Polymer* **35 (5)**, 988 (1994)

BIOGRAPHICAL SKETCH

Li Yao was born in Zhejiang, China.

He graduated from Shanghai Jiaotong University Shanghai, China, in 1989 with a Bachelor of Engineering degree in applied chemistry specializing in polymeric materials. He then continued his graduate study in the same department and university. In February 1992, he received his Master of science degree in polymeric materials. After getting his master degree, he was first hired as research engineer in Shanghai Rubber Products Co., then employed as a developing engineer at DuPont Far East Chemical Co. in March 1992.

In August 1992 he entered the graduate program in the Chemistry Department of Florida State University and got his second master's degree in analytical chemistry in May 1994. Since August 1994, he has been studying in the Ph.D program of polymeric materials in the Department of Materials Science and Engineering at the University of Florida.

While working toward the degree of Doctor of Philosophy in materials science he served as a research assistant in the Department of Materials Science and Engineering. He is a member of the Society of Plastics Engineers and American Chemical Society

I certify that I have read this study and that in my opinion it conforms to acceptable standards of scholarly presentation and is fully adequate in scope and quality as a dissertation for the degree of Doctor of Philosophy

Charles L. Beatty, Chairman
Professor of Materials Science and Engineering

I certify that I have read this study and that in my opinion it conforms to acceptable standards of scholarly presentation and is fully adequate, in scope and quality as a dissertation for the degree of Doctor of Philosophy

James H. Adair
Associate Professor of Materials Science and Engineering

I certify that I have read this study and that in my opinion it conforms to acceptable standards of scholarly presentation and is fully adequate in scope andquality, as a dissertation for the degree of Doctor of Philosophy

Stanley R. Bates
Associate Professor of Materials Science and Engineering

I certify that I have read this study and that in my opinion it conforms to acceptable standards of scholarly presentation and is fully adequate, in scope and quality as a dissertation for the degree of Doctor of Philosophy

Christopher D. Batich
Professor of Materials Science and Engineering

I certify that I have read this study and that in my opinion it conforms to acceptable standards of scholarly presentation and is fully adequate in scope and quality as a dissertation for the degree of Doctor of Philosophy

Arthur L. Fricke
Professor of Chemical Engineering

This dissertation was submitted to the Graduate Faculty of the College of Engineering and to the Graduate School and was accepted as partial fulfillment of the requirements for the degree of Doctor of Philosophy

December, 1996

Winfred M. Phillips
Dean, College of Engineering

Karen A. Holbrook
Dean, Graduate School